DECEMBER 2018 M.Sc.in Mechanical Engineering MÜSLÜME KÖŞKER

UNIVERSITY OF GAZİANTEP

GRADUATE SCHOOL OF

NATURAL & APPLIED SCIENCES

EFFECT OF CURVED AND REVERSE CURVED CROSS SECTIONAL TWISTED TAPES ON HEAT TRANSFER ENHANCEMENT

M. Sc THESIS

IN

MECHANICAL ENGINEERING

BY

MÜSLÜME KÖŞKER

DECEMBER 2018

Effect of Curved and Reverse Curved Cross Sectional Twisted Tapes on Heat Transfer Enhancement

M. Sc. Thesis

In

Mechanical Engineering

University of Gaziantep

Supervisor

Assist. Prof. Dr. Fuat YILMAZ

by

Müslüme KÖŞKER

December 2018

REPUBLIC OF TURKEY
UNIVERSITY OF GAZİANTEP
GRADUATE SCHOOL OF NATURAL&APPLIED SCIENCES
MECHANICAL ENGINEERING

Name of the thesis: Effect of Curved and Reverse Curved Cross Sectional Twisted Tapes on Heat Transfer Enhancement

Name of student: Müslüme KÖŞKER

Exam Date: 14 December 2018

Approval of the Graduate School of Natural and Applied Sciences

Prof. Dr. Ahmet Necmeddin YAZICI
Director

I certify that this thesis satisfies all the requirements as a thesis for the degree of Master of Science.

Prof. Dr. M. Sait SÖYLEMEZ
Head of Department

This is to certify that we have read this thesis and that in our opinion it is fully adequate, in scope and quality, as a thesis for the degree of Master of Science.

Assist. Prof. Dr. Fuat YILMAZ
Supervisor

Examining Committee Members:	Signature
Prof. Dr. M. Yaşar GÜNDOĞDU	……..
Assoc. Prof. Dr. Önder ALBAYRAK	……..
Assist. Prof. Dr. Fuat YILMAZ	……..

I hereby that all information in this document has been obtained and presented in accordance with academic rules and ethical conduct. I also declare that, as required by these rules and conduct, I have fully cited and referenced all material and results that are not original to this work.

Müslüme KÖŞKER

ABSTRACT
EFFECT OF CURVED AND REVERSE CURVED CROSS SECTIONAL TWISTED TAPES ON HEAT TRANSFER ENHANCEMENT

KÖŞKER, Müslüme

M.Sc. in Mechanical Engineering

Supervisor: Assist. Prof. Dr. Fuat YILMAZ

December 2018

82 pages

Present study investigated the effects of the curved and reverse curved cross sectional twisted tapes on heat transfer enhancement in a circular pipe by means at computational fluid dynamics at Reynolds numbers ranging from 5800 to 31000. Twelve different geometries such as three curved and three reverse curved twisted tapes with two different twist ratios (3 and 4) were analysed. The diameter ratios of curved tape to pipe were changed as 1.761, 2.252, and 3.271. The diameter ratios of reverse curved tape to pipe were changed as 0.554, 0.647 and 0.872. The changes of the heat transfer, friction, and performance evaluation criteria were found out.

Several concluding remarks are evaluated for the curved cross sectional twisted tapes. The Nusselt numbers are higher than the smooth pipe approximately in the region of 31 to 89 % for all curved twisted types. The highest Nusselt number is obtained at the highest Re for was around 112 and obtained from the C1TR3 model, which has the highest curve ratio and the lowest twist ratio. The maximum friction factor is obtained around 0.11 at lowest twisted ratio and Re. The curve ratio effect on friction is negligible. The friction factors are higher than the smooth pipe approximately 122 to 206%. The maximum performance evaluation factor is calculated around 1.3 at Reynolds number 5800 for C1TR3 and C1TR4 cases due to the best mixing and high swirl. Better performance evaluation factors are observed in the lower Reynolds number.

Some of the important conclusions are evaluated for reverse curved cross sectional twisted tapes. The highest Nusselt number is calculated the lowest twist ratio and the highest curve ratio for the case R1TR3. The Nusselt number is higher than the smooth pipe approximately 0 to 85 %. The curve diameter is the less effective than twist ratio on the friction factor. The friction factor of reverse curved cross sectional twisted tapes is higher than the smooth pipe in the region of 124 to 238 %. The maximum value of PEC for the reverse curved cross sectional twisted tape is calculated around 1.22 at Reynolds number 5849 for R1TR3 and R1TR4.

Key Words: Twisted Tape, Heat Transfer Enhancement, Reynolds Number, Nusselt Number, Friction Factor.

ÖZET
KAVİSLİ VE TERS KAVİSLİ KESİT ALANINA SAHİP BÜKÜLMÜŞ BANTLARIN ISI TRANSFERİNİN ARTIRILMASI ÜZERİNE ETKİSİ

KÖŞKER, Müslüme

Yüksek Lisans, Makina Mühendisliği

Tez Yöneticisi: Dr. Öğr. Üyesi Fuat YILMAZ

Aralık 2018

82 sayfa

Bu çalışmada, kavisli ve ters kavisli kesite sahip bükülmüş bantların dairesel bir boruda ısı aktarımının geliştirilmesi üzerine etkileri, 5800'den 31000'e kadar Reynolds sayı aralığında hesaplamalı akışkanlar dinamiği kullanılarak araştırılmıştır. İki farklı büküm oranına (3 ve 4) sahip üç kavisli ve üç ters kavisli kesite sahip bükülmüş bantların kullanıldığı on iki farklı geometri analiz edildi. Kavisli kesite sahip bükülmüş bantlarda, kavisin çapının boru çapına oranları 1.761, 2.252 ve 3.271'dir. Ters kavisli kesite sahip bükülmüş bantlarda, ters kavisin çapının boru çapına oranları 0.554, 0.647 ve 0.872'dir. Isı transferinin değişim, sürtünme ve performans değerlendirme kriterleri araştırıldı.

Kavisli kesite sahip bükülmüş bantlar için elde edilen sonuçlara göre Nusselt sayısı yaklaşık % 31 ila % 89 arasında düz borudan daha yüksek bulunmuştur. En yüksek Nusselt sayısı en yüksek Re sayısında 112 civarında en yüksek çap oranına ve en düşük büküm oranına sahip olan C1TR3 modelinden elde edildi. Maksimum sürtünme faktörü en düşük büküm oranında ve en düşük Re sayısında yaklaşık 0.11 civarında elde edildi. Çap oranının sürtünme üzerindeki etkisi ihmal edilebilir olduğu gözlemlendi. Sürtünme faktörü, düz borudan yaklaşık % 122 ila 206 daha yüksek olarak elde edildi. Maksimum performans değerlendirme faktörü, en iyi karıştırma ve yüksek girdap nedeniyle C1TR3 ve C1TR4 için Reynolds sayısı 5800'de 1.3 civarında hesaplanmıştır. Düşük Re sayısında daha iyi performans değerlendirme faktörü gözlenmiştir.

Ters kavisli kesite sahip bükülmüş bantlar için önemli sonuçlardan bazıları aşağıda çıkarılmıştır. En yüksek Nusselt sayısı, en düşük büküm oranı ve en yüksek çap oranına sahip olan R1TR3 modeli için hesaplanmıştır. Nusselt sayısı yaklaşık % 0 ila 85 arasında düz borudan daha yüksektir. Çap oranı, sürtünme faktörü üzerindeki büküm oranından daha az etkilidir. Ters kavisli kesite sahip bükülmüş bantlarının sürtünme faktörü, 124 ila 238% aralığında düz borudan daha yüksektir. Ters kavisli kesite sahip bükülmüş bantlar için performans değerlendirme faktörünün maksimum değeri, R1TR3 ve R1TR4 için Reynolds sayısı 5849'da yaklaşık 1.22 olarak hesaplanmıştır.

Anahtar Kelimeler: Bükülmüş Bant, Isı Transferi Geliştirme, Reynolds Sayısı, Nusselt Sayısı, Sürtünme Faktörü

to my father Mehmet and mother Mediha…

ACKNOWLEDGEMENTS

First of all, I would like to thanks to my education advisor, faculty member Assist. Prof. Dr. Fuat YILMAZ who is patiently shares his knowledge and experience and spends of time during this thesis study. Also, I would like to thanks to Prof Dr. Yaşar GÜNDOĞDU for his spiritual support and thanks to University Scientific Research Projects Governing Unit (BAP) for their financially support on my thesis (MF.YLT.17.12). Finally, I would like to give my grateful to my husband Ersin, my daughters Ayşenaz and Berra for their goodwill, trust and patient to me during the study.

TABLE CONTENTS

Page

LIST OF FIGURES

Page

LIST OF TABLES

Page

LIST OF SYMBOLS

A	Area, m^2
Cp	Secific heat, J/kg K
D	Tube diameter, m
f	Friction factor
h	Heat transfer coefficient, W/m2 K
k	Thermal conductivity, W/m K
l	Pitch length based on 180°, m
L	Tube length, m
m	Mass flow rate, kg/s
Nu	Nusselt number
Pr	Prandtl number
q	Heat transfer rate, W
Re	Reynolds Number
T	Temperature, °K
U	Velocity, m/s
w	Tape width, m
TR	Twist ratio, (l/D)
$\frac{D_c}{D_p}$	Curve ratio
δ	Twisted tape thickness, m
ρ	Density, kg/m3
μ	Dynamic viscosity, kg/m-s
PEC	Performance evaluation criteria
P	Pumping power,W
Q	Heat transfer rate,W
a	air
b	bulk temperature
i	inle

m	mean temperature
out	outlet
t	tube
p	plain tube
w	wall

CHAPTER 1

INTRODUCTION

Everyday life needs more and more energy sources due to increasing population, urbanization, industrialization, technological development, and raising standards of living. So the most important topic of our day is the efficient use of natural resources. At this point, the most accurate selected way to regenerate natural resources and produce energy with minimal damage to the environment are considered important.

Energy resources are divided into two groups as renewable and non-renewable. Renewable resources are solar energy, water energy, wind energy, geothermal and bioenergies. Non-renewable sources are coal, oil, natural gas and nuclear energy sources. These energy sources are also called primary energy sources, which can be used directly. A primary energy consumption rate distribution in the world is composed of 33.1% petroleum, 30.3% coal, and 23.7% natural gas [1]. All non-renewable resources will be removed from underground and consumed one day. Therefore, non-renewable energy becomes important. According to researches, primary energy consumption in the world between 2010 and 2040 will increase by 56% [2]. The cost and the limitation of non-renewable resources in addition to the increasing demand make energy efficiency as important as renewable-energy sources. Energy efficiency is the decrease of the amount of energy consumed without lowering the quantity and quality of production by protecting economic development and social welfare. It is necessary to avoid losses during energy consumption, provide recycling and reduce consumption with technological innovations by increasing efficiency. Energy efficiency can be supported by energy saving. Energy saving means sensible use of energy without any loss at home, in production, in comfort of life and in labour, in other words, it means avoiding unnecessary energy consumption. Increasing energy efficiency and energy saving are contributing to reduce the external dependency of energy resources in terms of our country. As a

result of the so fast rising energy request in Turkey, the dependency on energy imports is increased especially oil and natural gas. Turkey imports 64 %, 95% and 99% of its coal, oil and natural-gas needs respectively [2].

The main problem of the energy sector in Turkey is that the increasing the energy production does not the response to energy request at the same time. While approximately 25% of the total energy demand of our country is supplied by our sources, this suggests us how to produce our energy and how important it is to use our energy efficiently [3].

The 47.6% of total energy was used by industry at Turkey in 2015 [4]. Energy-efficient and saving must be increased, and the most efficient devices and technologies should be used in the industry. Energy recovery systems to reduce energy costs are favourite techniques in recent years. This involves the heat-transfer improvements.

1.2 HEAT TRANSFER ENHANCEMENT TECHNIQUES

Besides the efficient energy usages, the efficient heat transfer system is one of the important things in the energy consumption sector. The enhancement of heat transfer provides to increase of high heat flux. Furthermore, enhancement in heat transfer rate also supplies to minimize of elements size and drop the process temperature. The minimize size of element is important for financial case, also reduction of temperature is important to increase efficiency and decrease of entropy generation, which means that minimum energy destruction in a process. For improving the efficiency of heat transfer, it is necessary to increase the thermal contact surfaces and to decrease the using pumping power. Because of these reasons, it is essential to use the different methods for improvement of the heat-transfer enhancement [5-7].

The heat transfer improvement techniques are usually used many sectors such as heating, cooling, chemistry process, auto sector, etc. This technique is basically classified as active, passive and compound methods. The active methods need external energy by extra equipment. However, the passive methods do not need any external energy. Passive technique is more used compared to other techniques

because of the easy usage. The heat transfer improvement is gotten by surface geometry modify and fluid movements. Additionally, both passive and active techniques are used together, which is called as compound method [5].

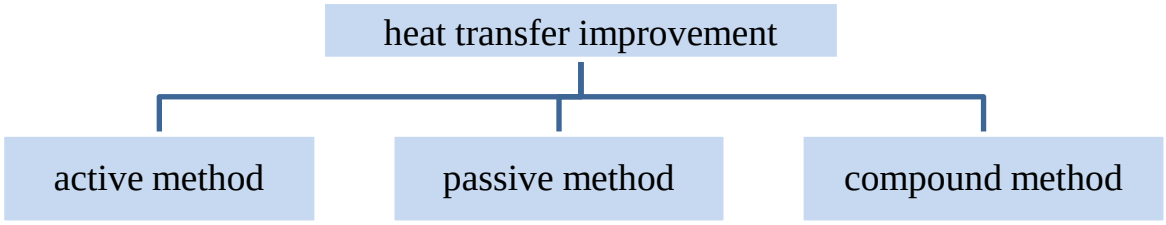

Figure 1.1 Methods of heat transfer improvement

1.2.1 ACTIVE METHODS

There are many kinds of active method;

1.2.1.1 Flow and Surface Pulsation: It has been used in single phase flows. Boundary layer is broken by the frequency producing motor [6, 8].

1.2.1.2 Mechanical Aids: Heat transfer enhancement is made by turning the surface and mixing the fluid which is generally used in the chemical sector [6, 8].

1.2.1.3 Fluid Vibration: Heat transfer is made by surface pulsation that is used for single phase flows [6, 8].

1.2.1.4 Injection and Suction: Gas is injected into the flow in single phase fluids, while it can be use both two and single phase for heat transfer enhancement [6, 8].

1.2.1.5 Jet Collision: The heat transfer enhancement is gotten with crashing the fluid to the surface by using jet [6, 8].

1.2.1.6 Electrostatic surfaces: This method is used insulator fluids in a process [6, 8].

1.2.2 PASSIVE METHODS

1.2.2.1 Process Surfaces: The surface is covered with material for improving the heat transfer. These are used essentially for phase conversion [6, 8].

1.2.2.2 Rough Surfaces: Principle of the method is to increase the turbulence in the fluid by using roughness of the surface. By this way, the heat transfer can be increasing by irritating the boundary layer at a tube wall [6, 8].

1.2.2.3 Augmented Surfaces: It is based on augmented of the surface using inserts. Renewal of the boundary layer is principal for this method [6, 8].

1.2.2.4 Whirl Flow Instruments: It makes whirl flow and increases the turbulence, which is made good the heat transfer; however, pressure drop increases. It creates a secondary flow for single or multi-phase flows by using inserts such as rings, fins, and coiled wires [6, 8].

1.2.2.5 Surface Tension Instruments: It consists of vacuum or grooved surfaces, which are used for phase conversion [6, 8].

1.2.2.6 Additional Ingredients: the addition of solid, liquid or gas is added on the single phase flow due to the drop the surface tension of the fluid [6, 8].

1.2.3 COMPOUND METHOD: Combination of the two methods together, for examples coiled wires with a twisted tape, or extended surface with fluid pulsation, electrostatic areas with twisted tapes [6, 8].

1.3 TWISTED TAPES

They are metal tape, which is the different geometries and size for the better performance. Twisted tape inserts are the most preferred technique for heat transfer augmentation, owing to inexpensive and easily using according to other methods [6, 8].

Twisted tape inserts in a tube are able to make the convective heat transfer irrigated the boundary layer at the tube wall, and helping the best mixing due to the changing

the surface geometry, thus the better heat transfer can be supplied. However, the pressure drop may be increased unfortunately inside the tube.

There are important parameters for twisted tape inserts such as the half-pitch (y), twist ratio (TR), the number of revolutions (N), and clearances [7].

The half pitch: y is represented as the axial distance of 180 degree rotation of point on the twisted tape in the pipe [9].

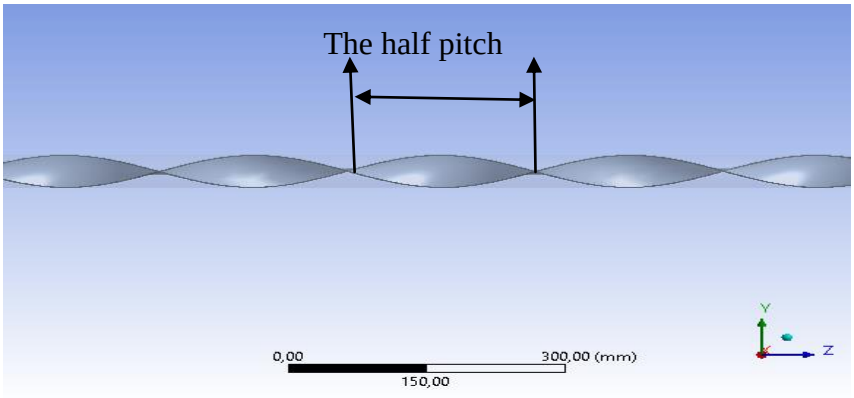

Figure 1.2 Twisted tape

The twist ratio: TR is represented as the ratio of the axial distance of 180 degree rotation to the inner diameter of a tube [9].

It is calculated by

$$TR = y/D_{in} \qquad (1.1)$$

The number of revolutions: N is explained as the number of 360 degrees rotation of same point on the twisted tape [9].

Clearance is the distance between twisted tape and tube wall. Clearances can produce turbulence in the flow between twisted tape and tube wall, which makes to heat transfer and undesirable pressure drop. Tape inserts cause resistance against flow direction, which is the secondary flow. In addition to this, flow velocity also

increases a little. The secondary flow produces turbulence and mixing, which improve temperature rate [6, 7, 9].

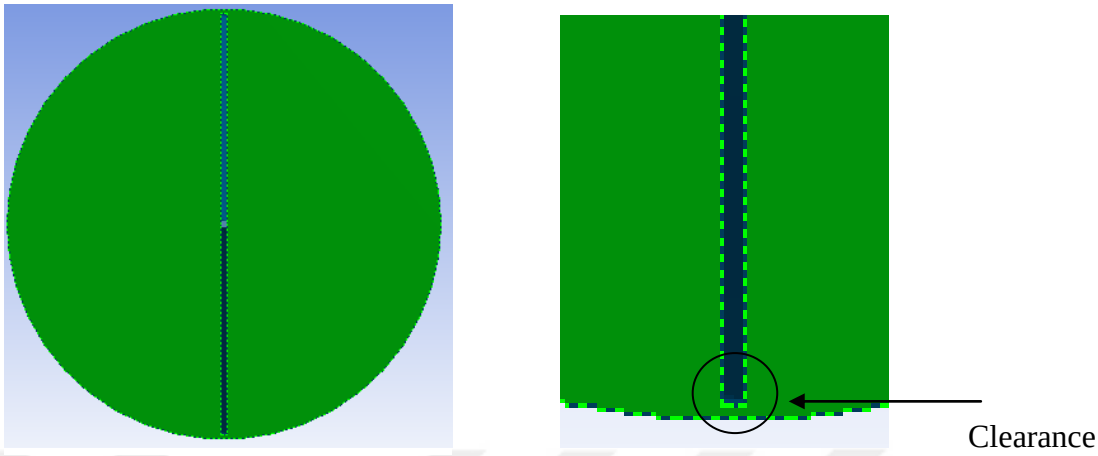

Figure 1.3 Clearance between twisted tube walls

1.4 PURPOSE OF THE THESIS

According to the literature, heat transfer enhancement by the twisted tape inserts is extremely dependent on geometry and layout of the inserts in the tube or channel due to the strong turbulence and perfect fluid mixing. There are many studies in the literature to deal with heat transfer enhancement. However, this study includes curved and reverse curved cross sectional twisted tapes using in a circular tube which are different from others. The computational fluid dynamics (CFD) technique is used for analyzing in this study, which is made the opportunity to analyses the geometry with a lot of data without setting up the experiment rig. Thus, it was decided to use the CFD technique to analyses the enhancement of heat transfer by these new geometries.

CHAPTER 2

LITERATURE SURVEY

2.1 INTRODUCTION

A lot of research has been done on heat transfer enhancement. Heat transfer enhancement has become more important in recent years due to the limited energy sources. As a result, a large literature on this subject has been established.

2.2 STUDIES ON ENHANCEMENT OF HEAT TRANSFER WITH TWISTED TAPE

Especially energy usage and also related to economic situation heat transfer enhancement is an important subject for researchers. The use of passive instruments like whirl flow inserts, twisted tapes or wire coils, rough surfaces and enhancement surfaces, etc. are advantageous methods of heat transfer enhancement. A lot of studies on different types of passive technique, especially twisted tape geometries to increase the heat transfer rate have been done.

2.2.1 EXPERIMENTAL INVESTIGATIONS

The effect of non-Newtonian nano fluids on a heat transfer in a circular tube was studied experimentally by Hojjat et al. [10]. Three different nanofluids were used with base fluid as carboxymethyl cellulose. Fluid regime was turbulent with the range of The Reynolds number 8000-33000. Wall temperature was constant. At the end of the study, they observed that the enhancement of the heat-transfer coefficient of nano fluids was higher than those of the base fluids if the nanoparticle concentration was increased the heat transfer increased. Furthermore, the heat-transfer coefficient increased with a Peclet number. Peclet number was generally

used for liquid metal fluid defined as the ratio of the heat transfer by convection to thermal conduction.

Liao and Xin [11] reported a result of the experimental study on the heat transfer and friction factor characteristics for mixing of the water, ethylene glycol, and ISO VG46 turbine oil with Reynolds number between 80 and 50000 inside four different size tubes with three-dimensional internal extended surfaces. Prandtl number region was from 5.5 to 590. The experimental resulted show that the heat transfer was increased a little, although the friction factor was increased considerably for in turbulent and transitional flow regions, whereas the three-dimensional internal extended surface tube with twisted-tape inserts was suitable for the heat transfer for laminar flow.

Saha et al. [12] experimentally investigated heat transfer and pressure drop characteristics in a circular tube with regularly spaced twisted-tape elements. Flow was laminar and viscous. The swirl was generated by regularly spaced twisted-tape inserts with different tape-width, different diameters circular rods and different phase angles. Constant wall heat flux and isothermal friction factor data were recorded. At the end of the study, both the decreasing tape-width and the increasing phase angle were not effective according to the heat transfer.

Rahimi et al. [13] reported an experimental and computational fluid dynamics (CFD) study; the rig was formed with bent tube and cubic shape bath. Cold water with a temperature of 16 °C was used. The effect of the classic, perforated, notched, and jagged twisted tape inserts on the friction factor, Nusselt number and thermal hydraulic performance of a tube were calculated by using CFD. The Reynolds number was in the range from 2950 to 11800. At the end of study, they observed that the Nusselt number and performance of the jagged insert were higher than other. Moreover, the higher turbulence intensity of the fluid close to the tube wall has been observed.

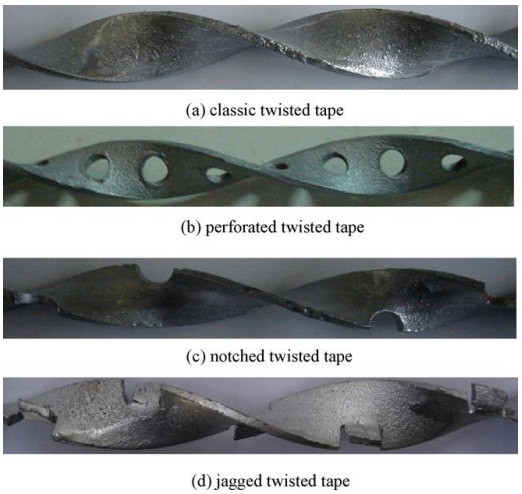

Figure 2.1 The different twisted tape tested by Rahimi et al. [13]

Experimental investigations of the heat transfer and friction factor in a double pipe with spaced twisted tape elements were done by Eiamsa-ard et al. [14]. They were inserted in the tube with two different conditions. It was typically twisted tape with different twist ratio (TR=6 and 8) and four different space ratios. Working fluid was water and the Reynolds number was between 2000 and 11000. They reported that Nusselt number increased with Reynolds number and the heat transfer rate was better than a plain tube due to the strong swirl flow through the tube with twisted tape. In addition, it was observed that the heat-transfer coefficient increased with the increased the twist ratio and increasing the space ratio affected to improvement the heat-transfer coefficient and friction factor.

Another experimental and numeric analysis was done with air in a circular tube with different inserts by Chiu and Jang [15]. Twisted-tape inserts and longitudinal strip inserts with and without holes with three different twisted angles were investigated. Three different inlet velocities were used from 3 to 18 m/s for air. Flow was turbulent with Reynolds number between 7000 and 50000. They observed that the heat transfer coefficient and the pressure drop in the tubes with the longitudinal strip inserts (without hole) were 7–16% and 100–170% greater than those of plain tubes without inserts, respectively. However, the heat transfer coefficient and the pressure drop were 13–28% and 140–220% for the longitudinal strip inserts with holes, respectively, higher than for plain tubes. This result was higher than without holes.

The effects of twisted tapes, taper angle and twist ratio on thermal performance factor characteristics were studied by Piriyarungrod et al. [16]. The tapered twisted tapes with four different taper angles ($\theta=0.0^0$, 0.30^0, 0.60^0, 0.90^0) were using in experiment. The tapered twisted tapes with three different twist ratios were analysed for each taper angle. Air was working fluid. Flow regime was the turbulent flow from 6000 to 20000 Reynolds numbers. At the end of the experiment, heat transfer and friction loss were increased with decreasing taper angle and twist ratio of tape. It could be said that heat transfer enhancement and friction loss depend on decreasing taper angle and twist ratio. It was observed that thermal performance factor increase with increasing taper angle and decreasing twist ratio of tape.

Eiamsa-Ard et al. [17] studied alternate axes twisted tapes with at different lengths. The flow was under the turbulent with Reynolds number from 5000 to 21500. Constant heat flux was applied to the heating wall. Working fluid was water. As a result of study, both uniform and non-uniform alternate lengths gave a higher Nusselt number and friction factor than the twisted tape. The Nusselt number and the friction factor were increased with reducing the alternate length. Moreover, it was observed that heat transfer and friction factor by the non-uniform alternate lengths were directly depended on the alternate length rather than the variation of the length.

In another study, Eiamsa-Ard et al. [18] reported that the influences of circular-ring tabulators and twisted tape on the heat-transfer enhancement, pressure drop and thermal performance factor characteristics. Three different pitch ratios of the circular-ring tabulators and three different twist ratios were used. The experiments' fluid was air under a uniform heat flux condition and turbulent with the Reynolds number from 6000 to 20000. The use of circular-ring tabulators and twisted tape together was more efficient for the heat transfer rate, friction factor and thermal performance factor than circular-ring tabulators alone. The performance factors were greater than one for all enhancement inserts. They observed that while the performance factor decreases the Reynolds number increase. The performance factor increases as the reduction of the pitch ratio and twist ratio.

Bhuiya et al. [19] examined the effect of the perforated twisted tape inserts in a round tube with four different holes (hole diameter=3, 5, 7 and 9 mm) on Nusselt

number, friction factor and thermal performance factor. Air flow was under a turbulent flow regime for Reynolds number ranging from 7200 to 49800 with a uniform heat flux. At the end of the study, it was declared that heat transfer rate, friction factor and thermal performance factor with using perforated twisted tapes were higher than the plain tube. Nusselt number, friction factor and thermal performance factor for the tube with perforated twisted tape inserts were calculated to be 110–340, 110–360 and 28–59% higher than the plain tube values, respectively.

Bharadwaj et al. [20] studied experimentally pressure drop and heat transfer features of flow in a grooved tube with twisted tape insert under constant heat flux. Flow was laminar to fully turbulent at Reynolds number between 100 and 10000. Working fluid was water. Twisted tapes having twist ratios of 10.15, 7.95 and 3.4 with grooved were used in this experiment. Results showed that the twist direction (clockwise and counter-clockwise) effected thermo hydraulic performances. Therefore, it could be said that the heat transfer increased in the laminar and turbulent regions with spirally grooved tube with and without twisted tape according to smooth tube.

Garcia et al. [21] experimentally studied helical wire coil inserts. Fluid was water and water–propylene glycol mixture with Reynolds number from 80 to 90000, flow was in laminar, transition and turbulent region. Prandtl number was from 2.8 to 150. Six different wire coils were used at different temperatures. At the end of the study was shown that pressure drop increased up to nine times and heat transfer up to four times in turbulent flow wire coils compared to the plain tube. Furthermore, it was observed that wire coils used in a transition region increased heat transfer rate about 200%. The wire coil was useful, especially in the transition region because of its advantages other inserts.

Man et al. [22] experimentally studied on the heat transfer and friction factor features in a tube with a new geometry of twisted tape insert. Four twisted tapes with different lengths as 2400, 1800, 1200 and 600 mm were used. Water was used in the Reynolds number between 11000 and 27000. At the end of the study, it was seen that length of twisted tape did not advantage remarkable for plain tube. Besides that, they declared that twisted tape was more suitable for laminar and low turbulent flow

conditions due to the performance evaluation criteria (PEC) for the length ratio at the experiment.

The effect of the clearance between tube wall and the tape on heat transfer was investigated by Al-Fahed and Chakroun [23]. Working fluid was chilled water under the fully developed condition in an isothermal tube with fifteen different tapes having three different twist ratios each five different width. At the end of the tested, it was confirmed that small twist ratio and tight-fit tape were more desirable for designer for high-heat transfer enhancement. So the results of heat transfer for all tapes and twist ratios with tight-fit were a good according to the plain tube.

Ujhidy et al. [24] experimentally studied the secondary flow in a circular cross section pipe with helical static elements. They studied to illustrate the contours of axial and transversal velocities with the coils and twisted tapes under the laminar flow conditions with water as a working fluid. Results of the experiment confirmed that there was secondary flow between the tube wall and the surface of the helical strip. They displayed the secondary flow with using the laser technique.

Yilmaz et al. [25] experimentally tried to understand the heat transfer and pressure drop characteristic of a pipe having radial guide vane swirl generators. Three different configurations of a swirl generator with conical, spherical deflecting element, and without deflecting element for different vane angle were used in experiment with air as working fluid under the constant heat flux boundary conditions Flow was turbulent within the range of Reynolds number 35000-111000. At the end of the experiment, the Nusselt numbers increased within the range of 4-99%, 12-119% and 9-148%, whereas, friction factor increased within the range of 244-1442%, 261-1351% and 236-1699% for the swirl generator with conical, spherical deflecting element and without deflecting elements, respectively. The vane angle increased with the Reynolds number increased like Nusselt number increased. The swirl generator with no deflecting element was more advantageous than the other configurations according to performance evaluation and energy consumption.

Heat transfer and pressure drop were investigated in the horizontal double pipes with and without inserts such as twisted tape by Naphon [26]. Aluminium strip with 1 mm

thickness and 2000 mm length was inserted in a pipe with 8.1 mm inner and 9.54 mm outer diameter. Working fluid was water as cold water between 15 and 20°C, hot water between 40 and 45°C. The results of the experiment confirm that the twisted tape insert lead to the increase the heat transfer and unwanted increase in friction factor.

The effect of the helical screw inserts in a circular cross section under the laminar flow conditions on heat transfer and friction factor was investigated experimentally by Sivashanmugam and Suresh [27]. Working fluid was water within the range of 200-3000 Reynolds number. Four Different twist ratios were tested to compare the plain tube. The heat-transfer coefficient increased with the twist ratio increasing also friction factor increasing.

Chang et al. [28] studied broken twisted tape inserts in the circular cross section pipe. They researched the effect of the broken twisted tape with four different twist ratio on the heat transfer and pressure drop characteristics in the range of 1000-40000 Reynolds number. Working fluid was air. They reported that local Nusselt number and fanning friction factors increased with the twist ratio decreased. Heat transfer coefficient, mean fanning friction factors, and thermal performance factors were 1.28-2.4, 2-4.7, and 0.99-1.8 times greater than the plain tube results, respectively.

Eiamsa-ard et al. [29] studied the effects of peripherally-cut twisted tape insert on heat transfer, friction loss, and thermal performance factor characteristics in a round tube. Nine different peripherally-cut twisted tapes with a constant twist ratio (3), and three tape depth ratios (0.11, 0.22, and 0.33), each with three different tape width ratios (0.11, 0.22 and 0.33) were used in experiment. Water was as working fluid under uniform heat flux but pressure loss was measured under isothermal condition in a range of Reynolds number from 1000 to 20000. At the end of the experiment, results show that heat transfer rate and friction factor for the tube with the peripherally-cut twisted tapes were higher than especially in the laminar flow regime. The higher turbulence intensity was seen in the round of the tube wall produced by the peripherally-cut twisted tape. This result has been encouraged by the typical twisted tape. It was also shown that heat transfer increased when the depth ratio increased, and the width ratio decreased.

Promvonge and Eiamsa-Ard [30] investigated the effect of the conical ring with twisted tape insert on heat transfer, friction factor and thermal performance. Constant heat flux was applied on the tube wall. Air was used within the range of the Reynolds number 6000-26000. Two different twist ratios (3.75 and 7.5) are used. The results of conical ring with twisted tape showed Nusselt number of 4-10% and thermal performance of 4-8% higher than conical ring without twisted tape. The maximum heat transfer and thermal performance were observed for the combined conical ring and twisted tape having 3.75 twist ratio. They reported that the thermal performance decreased with increasing the Reynolds number up to 16000 Reynolds number. However, thermal performance remained the constant value after 16000 Re.

Gül and Evin [31] investigated the effect of the helical swirl generator on the heat transfer characteristic fitted at the inlet of the circular cross section tube. Working fluid was water in the range of 5000-30000 Reynolds number. Three different helical tapes with three different helical angles were used. They reported at the end of the tested that using the helical tape increased the heat transfer rate than the unused the insert.

2.2.2 NUMERICAL INVESTIGATIONS

The effect of four different twist ratio (2, 3, 4 and 5) on thermal characteristics in the range of the Reynolds number 800-2000 was investigated numerically by Savekar et al. [32]. Fluent v13 was used as the commercial software by selecting k-ω turbulence model, second order upwind scheme, pressure field, and the pressure-velocity coupling algorithm SIMPLE. The intensity of 10%, convergence criteria of 10^{-5} for continuity and 10^{-6} for energy were selected. At the end of the analyses, the best result was taken for the smallest twist ratio. They reported that the heat transfer increased with decreasing twist ratio and increasing Reynolds number as well.

Shabanian et al. [33] experimentally and numerically studied on heat transfer, friction factor and thermal performance of three kinds of twisted tape inserts such as classic, jagged and butterfly in three inclined angles of between the butterfly and the rod. Three different twist ratios were used. Working fluid was air under the turbulent flow in the range of the Reynolds number 3000-17000. Fluent 6.2 was used to

simulate the test rig. End of the study, the maximum thermal performance factor was measured for the butterfly insert with 90^{o} inclined angle. Additionally, the heat transfer rate difference between different inserts reduces by reducing the twist ratio.

Yadav and Padalkar [34] studied the heat-transfer characteristics of half-length upstream and half-length downstream twisted tape in a circular cross section pipe. Four different combinations (the half-length upstream, half-length downstream, full length, plain tube) with three different twist ratios were tested. Working fluid was air under the turbulent regime conditions. Results were obtained 3D numerical analysis. They reported that if the Reynolds number increased, heat transfer coefficient also increased. This value was greater 29-86% for full-length twisted tape, 8-37 % for half-length upstream, 9-47 % for half-length downstream than plain tubes at the same condition. Pressure drop decreased with an increased the Reynolds number. It was higher 203-623 % for full-length twisted tape, 36-107% for half-length upstream twisted tape, 31-144% for half-length downstream twisted tape than the plain tube. Moreover, they reported that the thermal performance factor gone to decrease with the Reynolds number increased.

Geyer et al. [35] studied to identity the heat-transfer characteristic in a repeated trapezoidal channel of a semi-circular cross-section like a zig-zag pathway for fully laminar flow by computational fluid dynamics. Prandtl number was 6.13. They observed that if the Reynolds number was increased, the high swirl flow formed in a tube, it caused to fluid mixing and high-heat transfer coefficient.

Salman et al. [36] numerically studied heat transfer and friction factor characteristics in swirling flow conditions using FLUENT v6.3.26. Three-dimensional models for circular tube fitted with typical and quadrant-cut twisted tape inserts (Figure 2.3) with three different twist ratio (TR=2.93, 3.91 and 4.89) and different cut depths (cut depth=0.5, 1.0 and 1.5 cm) were created for the analysis. Fluid was water under laminar condition. At the end of the studies showed that when heat transfer coefficient and friction factor in the tube fitted with quadrant-cut and twisted tape was increasing with decreasing of twist ratio and cut depth. The form of quadrant-cut twisted tape insert with a 2.93 twist ratio and a 0.5 cm cut depth made higher heat transfer rate and friction factor than other twist ratios and cut depths.

Figure 2.2 Geometry of quadrant-cut twisted tape inserts by Salman et al [36]

Another study about twisted tape by Salman et al. [37] researched the effect of V-cut twisted tape in a circular cross section tube on heat transfer and pressure drop using Fluent 6.3.26. V-cut twisted tape having cut depths 0.5, 1 and 1.5 cm with twist ratios 2.93, 3.91, and 4.89. Results were compared by the result obtained by the classical twisted tape at the same condition. Working fluid was water under the laminar flow condition. Constant heat flux boundary condition was applied on the tube wall. The result showed that The Nusselt number increased for both the classical and V-cut twisted tape inserts when the Reynolds Number increases and twist ratio decreasing. Moreover, it showed that V-cut twisted tape having 2.93 twist ratio and 0.5 cm cut depth presented the best heat transfer rate whereas remarkable increasing the friction factor. They reported that new design of twisted tape got 107% of maximum heat transfer.

Three-dimensional simulation of flow in converging-diverging tubes and converging-diverging tubes equipped with twin counter-swirling twisted tapes in turbulent were studied numerically by Yuxiang et al. [38]. Gambit v2.2.30 and Fluent v6.3.26 software was used for the creating mesh and numerical simulation. The effects of Reynolds number, two different pitch lengths (11.25 and 22.5 mm), three different rib height (0.5, 0.8 and 1.1 mm), three different pitch ratio (1:8, 5:4, 8:1) and three different clearance distance (0.5, 4.5 and 8.5) between the twin twisted tapes, and the tape number on Nusselt number, friction factor, and thermal enhancement factor were searched. The fluid was water under uniform heat flux. The fluid was in turbulent flow with Reynolds number between 10000 and 20000. Finally, the converging-diverging insert with 11.25 pitch length, 0.5 rib height and 8 pitch ratio gave the best thermal performance according to the other cases. Moreover, converging-diverging tubes equipped with twin counter-swirling twisted insert with 11.25 pitch length, 0.5 rib height, 8 pitch ratio, and 8.5 gap distance gave the best thermal performance according to the other cases. In addition, it was shown that all geometric parameters had important influences on the thermal performance of converging-diverging tubes and converging-diverging with twin counter-swirling

twisted tapes. Both converging-diverging tubes and converging-diverging with twin counter-swirling twisted tapes had better thermal performance compared to plain tube.

Deshmukh et al. [39] studied numerical modelling for the heat-transfer enhancement in a round tube set with and without helical tape inserts in a heat exchanger in turbulent flow using ANSYS Fluent v14. For numeric simulation analysis, different inserts were used a circular tube, and hot air and cold water are used as a test fluid. Thermal-hydraulic behaviours were examined. The ranges of Reynolds number were between 2300 and 8800. The full-length helical tape with or without a centered-rod of a concentric tube heat exchanger were used. At the end of the result, the helical tape with and without rod caused turbulence in the flow due to the good mixture of the fluid. Heat transfer was increased compared to plain tubes. If between the full-length helical tapes with and without a centered-rod were compared that the heat-transfer values of the helical tape with rod were higher than without rod.

Eiamsa-Ard et al. [40] numerically studied the vortex flow in a tube induced by loose-fit twisted tape insertion. This study included a research on the effects of the four clearance ratio (0.1, 0.2, 0.3, and no clearance) on Nusselt Number, friction factor and thermal performance factor for twisted tapes at two different twist ratios (2.5 and 5.0). The fluid was under constant wall temperature in the turbulent flow in the Reynolds number between 3000 and 10000. The results showed that the mean heat transfer rates of twisted tape insert with 2.5 twist ratio and all each testing clearance ratios were higher than the plain tube. The clearance ratios importantly affected the thermal performance factor of the twisted tape, and the best thermal performance factor was obtained for the close fit twisted tape.

Wang et al. [41] analysed the thermal hydraulic performance of regularly spaced short-length twisted tape in a circular cross section pipe with air under the turbulent flow condition by computational fluid dynamics. Three different space ratios, eight different twist ratios ranging from 2.5 to 8.0 and three rotated angles (180°, 270°, and 360°) were tested to compare the thermal performance of each other. They reported that the twist ratio was an important parameter due to the flow resistance. The smaller twist ratio was given the best performance according to the others, both

Nusselt number and friction factor increased with increasing the rotated angle. The larger free space ratio has a little effect on heat transfer and pressure drop.

Rao and Kumar [42] numerically and experimentally studied the heat transfer with helical and twisted tape inserts in a circular cross section pipe. Working fluid was water. Three different twist ratios under the turbulent flow condition were used. They reported that Nusselt number and friction factor decreased with decreasing the twist ratio.

2.3 SUMMARY OF LITERATURE

According to the literature, the using and changing of inserts, clearance, twist ratio, pitch ratio, cut depth, shapes of inserts, and also fluid significantly affected on heat transfer performance. This is due to the increasing the heat-transfer area, and the generation of second vortex flow.

All these studies encourage further study on this subject by trying the new geometry.

There are many studies in the literature to deal with heat transfer enhancement, but this study includes curved and reverse curved twisted tapes using in a tube. They are different geometries from literatures. The computational fluid dynamics (CFD) technique is used for analyzing in this study, which is made the opportunity to analyze the geometry with a lot of data without setting up the experiment a rig. Thus, it was decided to use the CFD technique to improve heat transfer over a new geometry.

2.4 STUDY SCHEDULE

The aim of the study is to analyze the heat-transfer behaviour of air in a horizontal circular pipe with twelve different types of twisted tape (three curved, and three reverse curved twisted tapes) and two different twist ratios under turbulent flow with uniform heat flux by using ANSYS FLUENT v18 commercial CFD software.

The study schedule of the thesis is to identify the effects of the new geometry and the twist ratio on the Nusselt number (Nu), friction factor (f) by using ANSYS FLUENT v18 commercial CFD software and also calculated the performance evaluation factor (PEC). The numerical study is divided into three steps. Firstly, the numerical study will be checked with the results in the literature for the validation. Results of the new geometries at second step will be calculated with the same calculation method. Finally, the results of curved twisted tape and reverse curved twisted tape will be discussed.

CHAPTER 3

VALIDATION OF NUMERICAL ANALYSIS ON HEAT TRANSFER ENHANCEMENT

3.1 INTRODUCTION

The aim of this thesis is to understand the effects of the curved and reverse curved twisted tape inserts with two different twist ratios on heat transfer enhancement in a circular tube under the uniform heat flux with working fluid as air.

3.2 NUMERICAL CALCULATIONS

The surface friction coefficient and heat transfer depend on the regime of boundary layer, whether laminar or turbulent. If the flow lines are moving along a line and parallel to each other, which is called laminar flow. If the flow lines are moving randomly and irregularly, this is called turbulent flow (Figure 3.1). In the laminar flow, the fluid motion is very uniform with low velocity. On the other hand, fluid motion in turbulent flow is disorder and suddenly velocity changing in the flow. These irregularities increase momentum, energy and mass transfer, and hence viscous friction coefficient. The description of a flow, whether is laminar or turbulent, depends on Reynolds Number. If the Reynolds Number is less than 2300, the flow is called laminar flow. If it is bigger than 4000; the flow is the turbulent flow. Also, if the Reynolds number is between 2300 and 4000, the flow is in the transition regime. In this present work, the flow is turbulent, and Reynolds number is between 5300 and 31000.

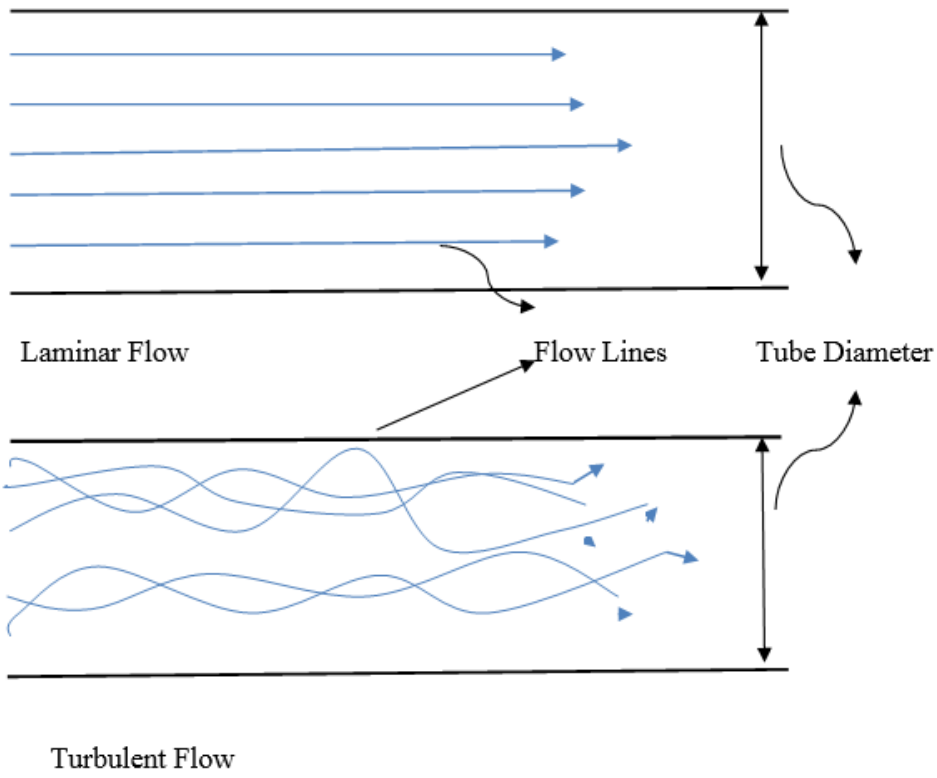

Figure 3.1 Fluid domain in a circular tube

Four parameters are important for this study. These are the friction factor, Nusselt number, Reynolds number, and thermal performance factor. Numerical calculations were done with following equations;

The flow regime can be described from the Reynolds number:

$$\mathrm{Re} = \frac{\rho\, u\, D}{\mu} \qquad (3.1)$$

Heat transfer coefficient in terms of constant heat flux calculation can be obtained by the following equation:

$$\mathrm{h} = \frac{\mathrm{q}}{\mathrm{Tw}-\mathrm{Tb}} \qquad (3.2)$$

T_w is the wall temperature, and T_b is the mean bulk flow temperature:

$$T_b = \frac{Ti+To}{2} \qquad (3.3)$$

Air is used for fluid. All the air thermo-physical properties are determined based on the bulk temperature, T_b.

The average Nusselt Number is calculated from the following equation:

$$\mathrm{Nu} = \frac{h\,D}{k} \tag{3.4}$$

The friction factor in terms of pressure drop (ΔP) can be expressed by

$$f = \frac{2\,\Delta P\,D}{L\,\rho\,u^2} \tag{3.5}$$

When the twisted tape is using in the pipe, the pressure drop will also increase. This increase in the pressure drop will be required more energy as expected. Therefore, it is necessary to compare heat transfer and pressure drop characteristics of an modified inserts with a reference inserts without any inserts [43]. The performance evaluation factor (PEC) is briefly expressed as the ratio of the heat transfer rate to the pressure drop by using Nusselt number and friction factor at the same pumping power. It is way of derived equation of the performance evaluation factor as; the ratios of Nusselt number and friction factor between a modified inserts surface and reference one are gotten at the same Reynolds number with adopted same assumptions as same pumping power, same heat transfer surface, same thermo physical properties of working fluid, and same temperature differences [44,45,46].

At the same Reynolds number, the ratios of Nusselt number and friction factor of modified inserts are given as

$$\left(\frac{f_{tt}}{f_p}\right)_{Re} = \frac{f_{tt}\,(Re)}{f_p\,(Re_p)} = \left(\frac{f_{tt}}{f_p}\right)_{Re}\left(\frac{Re}{Re_p}\right) \tag{3.6}$$

$$\left(\frac{Nu_{tt}}{Nu_p}\right)_{Re} = \frac{Nu_{tt}\,(Re)}{Nu_p\,(Re_p)} = \left(\frac{Nu_{tt}}{Nu_p}\right)_{Re}\left(\frac{Re}{Re_p}\right) \tag{3.7}$$

The ratio of power consumption of modified inserts and plain tube in definitions of pressure drop can be presented as;

$$\frac{P_{tt}}{P_p} = \frac{(A_c \ .V.\Delta p)_{tt}}{(A_c \ .V.\Delta p)_p} = \frac{(A_c \ .V.f.L.\rho.V^2)_{tt}}{(A_c \ .V.f.L.\rho.V^2)_p} \quad (3.8)$$

The ratio of heat transfer rate of the modified inserts and plain tube in terms of Nusselt number can be written as;

$$\frac{Q_{tt}}{Q_p} = \frac{(h.A.\Delta T_m)_{tt}}{(h.A.\Delta T_m)_p} = \frac{(Nu.\frac{k}{D}.A.\Delta T_b)_{tt}}{(Nu.\frac{k}{D}.A.\Delta T_b)_p} \quad (3.9)$$

According to the accepted assumption as same heat transfer surface, same thermo physical properties of working fluid, and same temperature differences, equations (3.8) and (3.9) become as

$$\frac{P_{tt}}{P_p} = \frac{(f.V^3)_{tt}}{(f.V^3)_p} = \frac{f_{tt}.Re^3}{f_p.Re_p^3} = \frac{f_{tt}\ (Re)}{f_p\ (Re_p)}\left(\frac{Re}{Re_p}\right)^3 \quad (3.10)$$

$$\frac{Q_{tt}}{Q_p} = \frac{(Nu)_{tt}}{(Nu)_p} \quad (3.11)$$

From Eq.(3.10) for the same power consumption, the ratio of the friction factor of modify insert and plain tube at different Reynolds number can be written as follows;

$$\frac{f_{tt}\ (Re)}{f_p\ (Re_p)} = \left(\frac{Re}{Re_p}\right)^{-3} \quad (3.12)$$

So;

$$\frac{Re}{Re_p} = \left(\frac{f_{tt}}{f_p}\right)_{Re}^{-1/3} \quad (3.13)$$

Lastly, Performance evaluation factor is derived in terms of Nusselt number and friction factor from Eq. (3.7), Eq. (3.11) and Eq. (3.13) by following formula;

$$\text{PEC} = \frac{\frac{Nu}{Nu_p}}{(\frac{f}{f_p})^{1/3}} \quad (3.14)$$

Where Nu is the Nusselt number of the tube with twisted tape, Nu_p is the Nusselt number in the plain tube, f is the friction factor of the tube with twisted tape, and f_p is the friction factor for the plain tube.

3.3 VALIDATION

It is important to start with validating the solution method. So the results can show the reliability of the thesis' results, it is necessary to verify with the previous studies' results in the literature before starting a new geometry analysis.

3.3.1 VALIDATION FOR TWISTED TAPE USING THE RESULTS OF CHOKPHOEMPHUN ET AL.

ANSYS Fluent Release v18.1 program was used to mesh and solve the governing equations. Tetrahedrons mesh is used with inflation having minimum three layers. Inflation is most important due to the accurately capturing the complex wall-bounded effects on pressure drop and heat transfer on the wall regions of pipe and twisted tape inserts. Mesh is completed by considering quality values such as Y+, skewness, and orthogonal quality.

The study of Chokphoemphun et al. [47] was used for validation for twisted tape inserts. Experimental setup parameters such as fluid domain dimensions and boundary conditions of typically twisted tape can be shown in Table 3.1 for the study.

Table 3.1 Fluid domain dimensions and boundary conditions of typically twisted tape for the study of Chokphoemphun et al. [47]

PARAMETERS / UNITS	VALUE
Diameter of tube / m	0.0508
Length of whole tube / m	3
Length of test section tube / m	1
Twist Ratio	4
Length of the twisted tape / m	1.2
Width of the twisted tape / m	0.042
Thickness of twisted tape / m	0.0008
Twist lengths / m	0.168
Inlet temperature / K	298.15
Heat flux / W/m^2	500
Working fluid	Air
Range of Reynolds number	5300-24000

The geometry of validation study was created by ANSYS v18.1 as shown in Figure 3.2 and Figure 3.3.

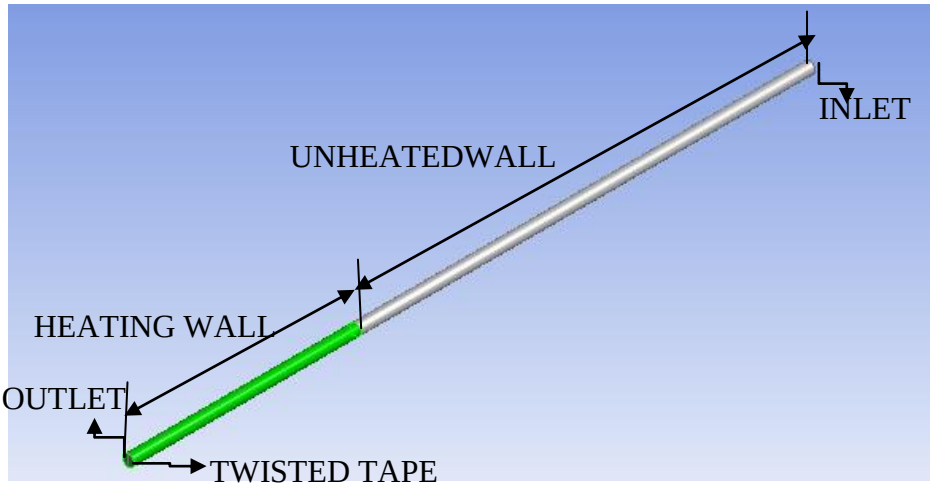

Figure 3.2 Fluid domain

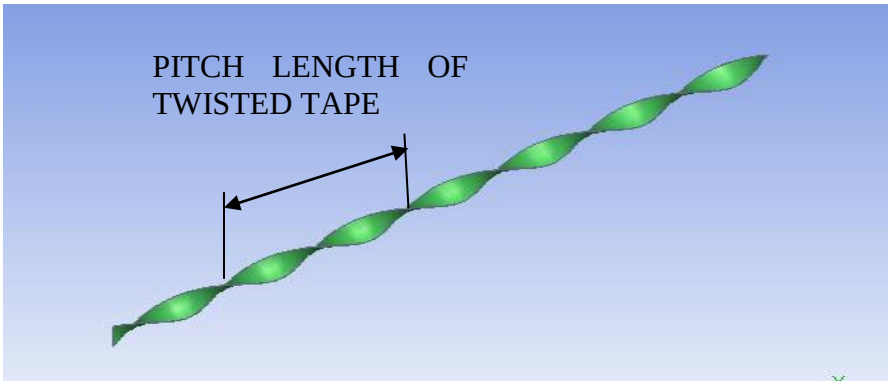

Figure 3.3 Geometry of twisted tape

The best suitable mesh size is selected by mesh independency method according to mesh quality parameters were kept on maximum skewness < 0.95 and minimum orthogonal > 0.1. The 3243239 mesh was selected due to the minimum deviation between the other mesh sizes as shown in Table 3.2. It is expected to reduce run time by choosing the lowest mesh size at minimum deviation. Figure 3.4 and Figure 3.5 show the longitudinal section mesh and outlet mesh for the validation study of Chokphoemphun et al. [47].

Table 3.2 Mesh independency test result for typically twisted tape

Mesh Size	Re	Nu	f
3243239	20867	57.01	0.03737
4193895	20905	57.19	0.03811
5505248	20950	58.15	0.03889
6297857	20966	58.53	0.03922

As well as required quality parameters, inflation, and Y+ are most important parameters to get good and reliable results. Y+ was kept around one at all applied meshes for the study.

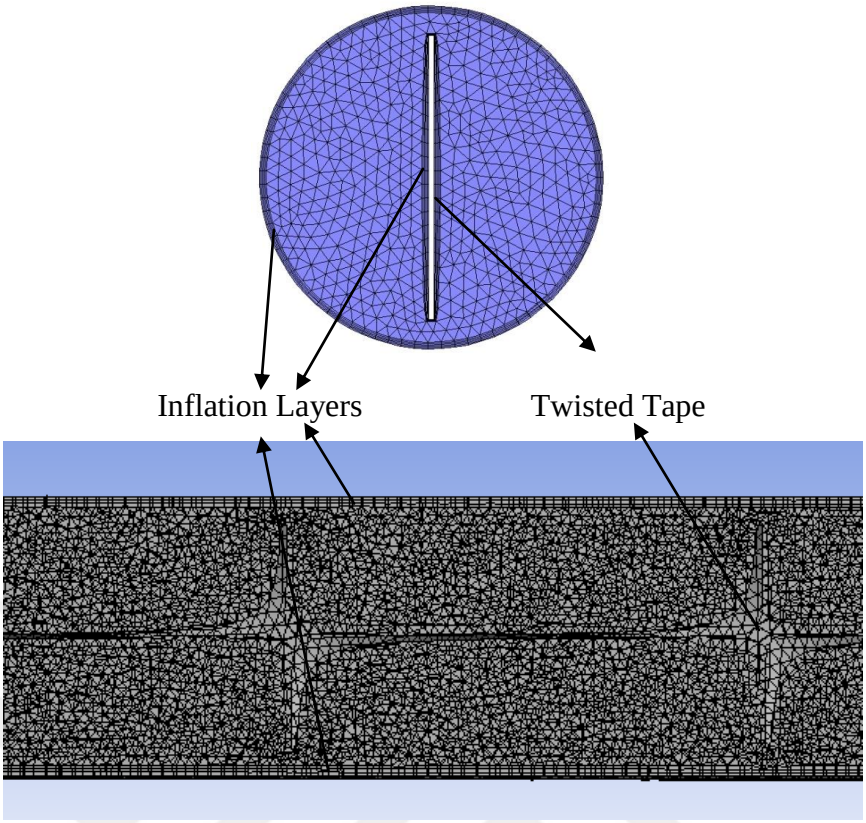

Figure 3.4 Typically twisted tape meshes with the inflation layers at the outlet and longitudinal side

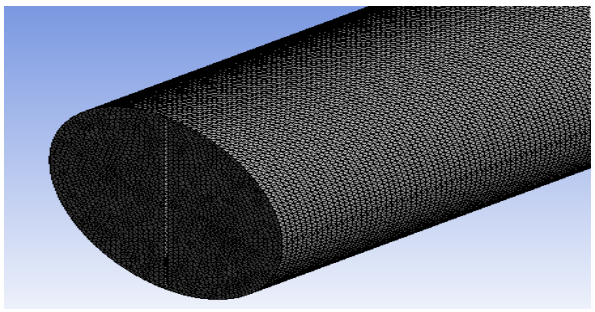

Figure 3.5 Outer mesh view of typically twisted tape

ANSYS Fluent Release 18.1 program was used to solve the governing equations with a pressure-based solver under steady condition. Standard k-epsilon model and standard wall functions were selected for solution. The convergence absolute criteria of the numerical simulations were set to 10^{-6} for energy, and 10^{-3} for momentum, continuity, k, and ε. The Simple algorithm for the pressure-velocity coupling, second order methods for momentum, and energy equations first order methods for other

spatial discretization were selected to solve. The 500 watt constant heat flux was applied, and inlet temperature was set to 298.15 K. Intensity, and hydraulic diameter was calculated by below equations, which were needed for run in numeric calculation. Table 3.3 shows the calculated and used values at run by ANSYS Fluent Release 18.1 program.

The turbulence intensity can be calculated by

$$I = 0.16 * Re^{(-1/8)} \quad (3.15)$$

The hydraulic diameter can be calculated by

$$D_{hydraulic} = \frac{4 * A}{P_{wet}} \quad (3.16)$$

Table 3.3 Turbulent intensities for validation

Velocity	Turbulent Intensity
1.53723	5.517581186
2.30584	5.244901358
3.07443	5.059644256
3.84307	4.920465953
4.61169	4.809595751
5.3803	4.71780761
6.14892	4.63971424
7.68615	4.512087173

Air was using as the working fluid that thermo physical properties and Prandtl number were calculated at bulk temperature by using equation of my thesis advisor. These were density, specific heat, and thermal conductivity, viscosity, and Prandtl number;

$$\boldsymbol{\rho}=5.274314-(0.03205889 *T_b) + (0.0001014443 * T_b^{\,2}) - (1.763213e\text{-}07 * T_b^{\,3}) + (1.597239e\text{-}10 * T_b^{\,4}) - (5.896955e\text{-}14 * T_b^{\,5}) \quad (3.17)$$

$$C_p =567.1317 + (5.42172 *T_b) - (0.02581261 * T_b^{\,2}) + (5.875834e\text{-}05 * T_b^{\,3}) - (6.357366e\text{-}8 * T_b^{\,4}) + (2.662107e\text{-}11 * T_b^{\,5}) \quad (3.18)$$

$$k =0.01122162 - (2.409008e\text{-}05 *T_b) + (4.689012e\text{-}07 * T_b^{\,2}) - (1.048907e\text{-}09* T_b^{\,3}) + (1.088226e\text{-}12 * T_b^{\,4}) - (4.401109e\text{-}16 * T_b^{\,5}) \quad (3.19)$$

$$\mu = (-1.88637e\text{-}06) + (1.048807e\text{-}07 *T_b) - (1.920276e\text{-}10 * T_b^{\,2}) + (3.065498e\text{-}13* T_b^{\,3}) - (2.781028e\text{-}16 * T_b^{\,4}) + (1.049564e\text{-}19 * T_b^{\,5}) \quad (3.20)$$

$$Pr = 0.53988791+ (0.0031265297 * T_b) – (1.6264787e\text{-}5 * T_b^{\,2}) + (3.6645885e\text{-}8 * T_b^{\,3}) - (3.8582455e\text{-}11* T_b^{\,4}) + (1.5660501e\text{-}14 * T_b^{\,5}) \quad (3.21)$$

Raw data was obtained from ANSYS Fluent v18.1 software. Nusselt number, friction factor, and performance evaluation criteria were calculated by using equations of (3.4), (3.5), and (3.14).

The Reynolds number was between 5300 and 24000 in the study of Chokphoemphun et al. [47]. All parameters were calculated according to the bulk temperature, and the variation of the friction coefficient and the Nusselt number relative to the Reynolds number were plotted on Figure 3.6 and Figure 3.7. These figures showed that result of the numerical validation of Chokphoemphun et al. [47] with using twisted tape inserts. The graphics show that maximum deviation between numerical result and the data of Chokphoemphun et al. [47] for Nusselt number and friction factor are about 7% and 12%, respectively.

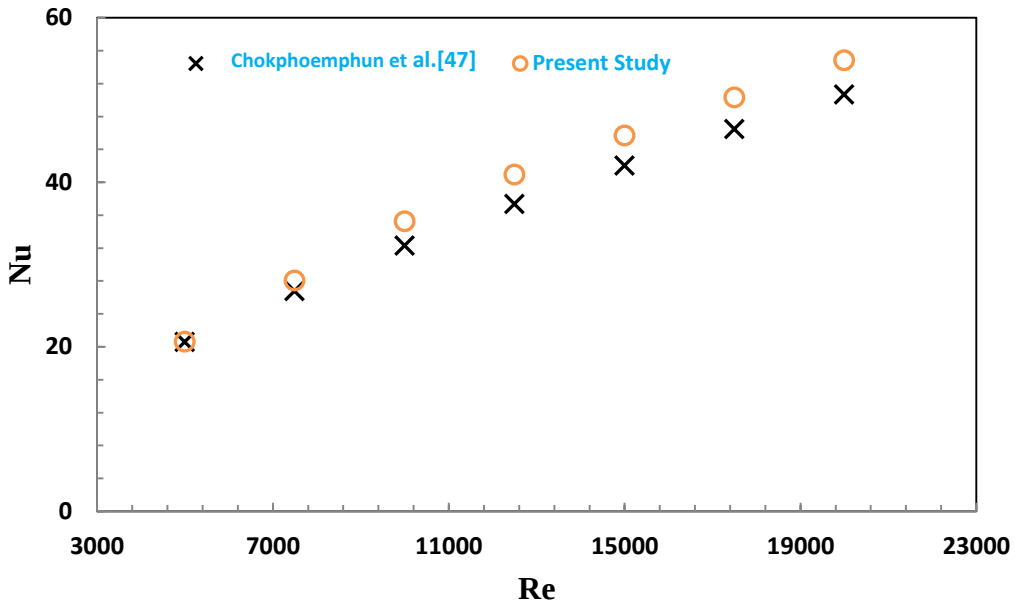

Figure 3.6 Reynolds number versus Nusselt number graphic of numerical results and literature results of Chokphoemphun et al. [47] for twisted tape

According to Figure 3.6, when the Reynolds number was increased, deviation was increased. The most important reason for deviations from experimental and numeric studies was that the method and location of the data were different from each other. In the experiment, the wall temperature was taken with 24 probes in the experimental setup, and average of this data was used in the calculations. This was not done in numerical calculations; surface average temperature was used read from the ANSYS Fluent Release 18.1 in numeric calculation.

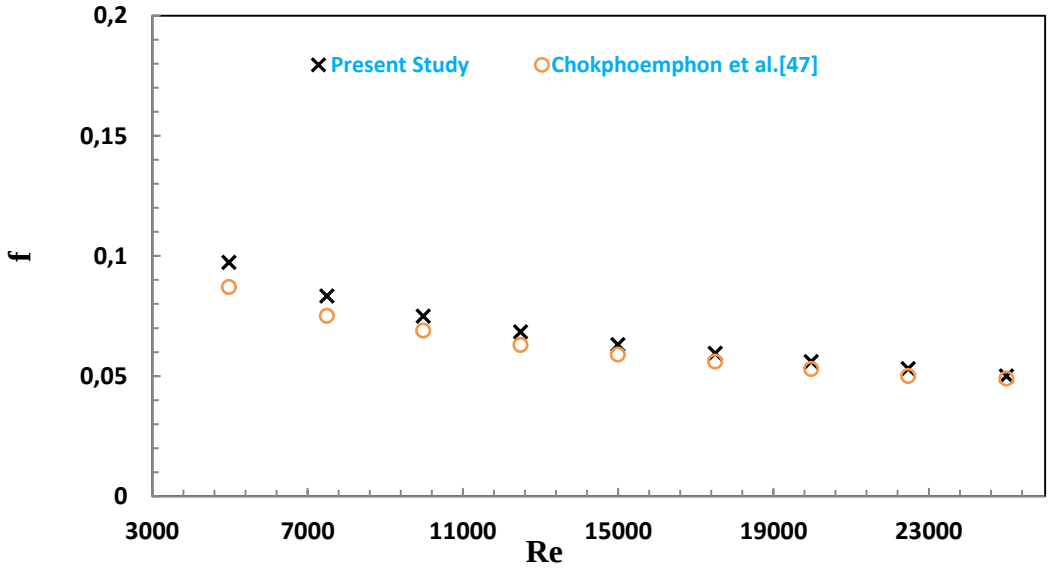

Figure 3.7 Reynolds number versus friction factor graphic of numerical results and literature results of Chokhoemphun et al. [47] for twısted tape

3.3.2 VALIDATION FOR TWISTED TAPE INSERTS USING THE RESULTS OF EIAMSA-ARD AND PROMVONGE

As well as using the results of Chokphoemphun et al. [47] for validation, study of Eiamsa-Ard and Promvonge [46] was also selected for validation for twisted tape before the starting new geometry analysis. Numerical solution results for twisted tape were also compared with Eiamsa-Ard and Promvonge [46].

The test tube has a length of 1250 mm, thickness of 1.5 mm, and inner diameter of 47 mm. The uniform heat flux was applied on the whole the test tube. Also, twisted tape was also 1250 mm long, 0.8 mm thickness, and inserted into the test tube. The inlet temperature is 298.15 K. This fluid domain was created by using ANSYS Fluent v18.1.

Table 3.4 Fluid domain dimensions and boundary conditions of typically twisted tape for the study of Eiamsa-Ard and Promvonge [46]

PARAMETERS / UNITS	VALUE
Diameter of tube / m	0.047
Length of whole tube / m	1.25
Twist Ratio	4
Length of the twist tape / m	1.25
Width of the twist tape / m	0.046
Thick of twist tape / m	0.0008
Inlet temperature / K	298.15
Heat Flux / W/m^2	2000
Working Fluid	Air
Range of Reynolds Numbers	4000-20000

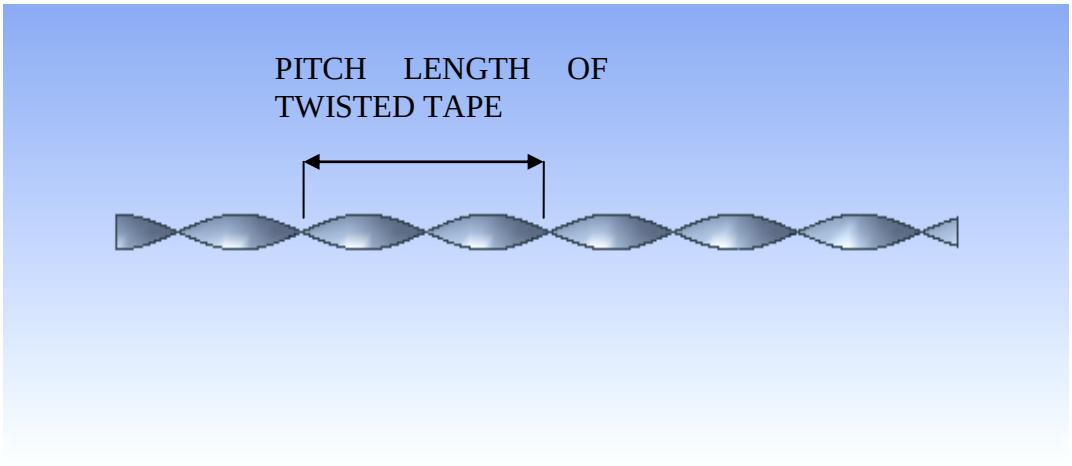

Figure 3.8 Geometry of twisted tape

In the case, firstly, mesh was created by using the Ansys v18.1. In fact, the accuracy of the mesh was important for the correct analysis. Right mesh was selected by looking forward to meshing independency and mesh quality, which were skewness and orthogonal. That was kept on maximum skewness < 0.95 and minimum orthogonal > 0.1. The number of mesh was determined by looking at Nusselt number and friction factor variables among the meshes constructed within these parameters. According to this method, two different mesh sizes are tried to select right mesh size for a reliable result. The 4214375 mesh sizes were preferred due to the close Nusselt Number and friction factor at same The Reynolds number as understanding from Table 3.5.

Table 3.5 Mesh independency for typically twisted tape

Mesh Size	Re	Nu	f
3219930	20132	55.514	0.057681763
4214375	20132	54.975	0.05519035

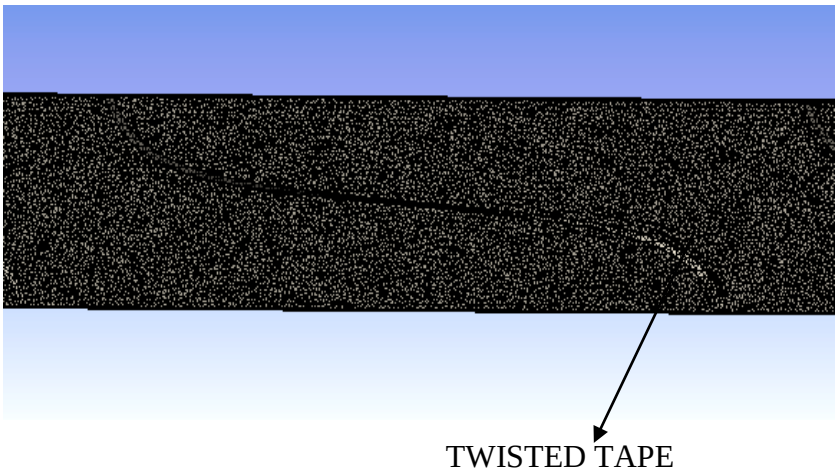

Figure 3.9 Longitudinal front mesh with the inflation layer of Eimsa-ard and Promvonge[46]

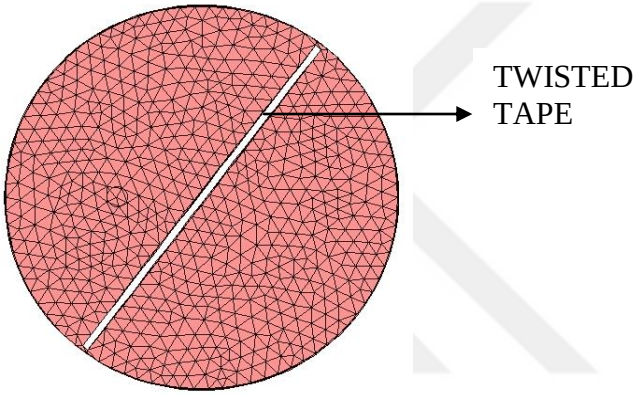

Figure 3.10 Figure 3.10 Inlet mesh with the inflation layer of Eimsa-ard and Promvonge [46]

Table 3.6 Turbulent intensity values

Velocity	Turbulent Intensity
1.386255	5.906364334
2.151085	5.590728707
2.868113	5.39325651
3.346132	5.290329566
4.302169	5.126720829
4.780188	5.059644256
5.258207	4.999722462
6.214245	4.896401966

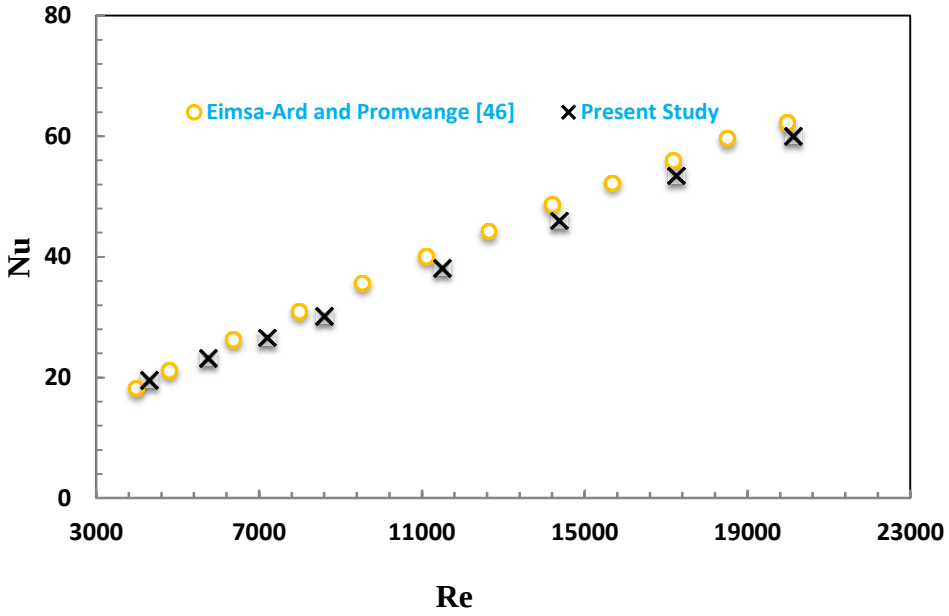

Figure 3.11 Reynolds number versus Nusselt number graphic of numerical results and literature results of Eimsa-ard and Promvonge [46] for twisted tape

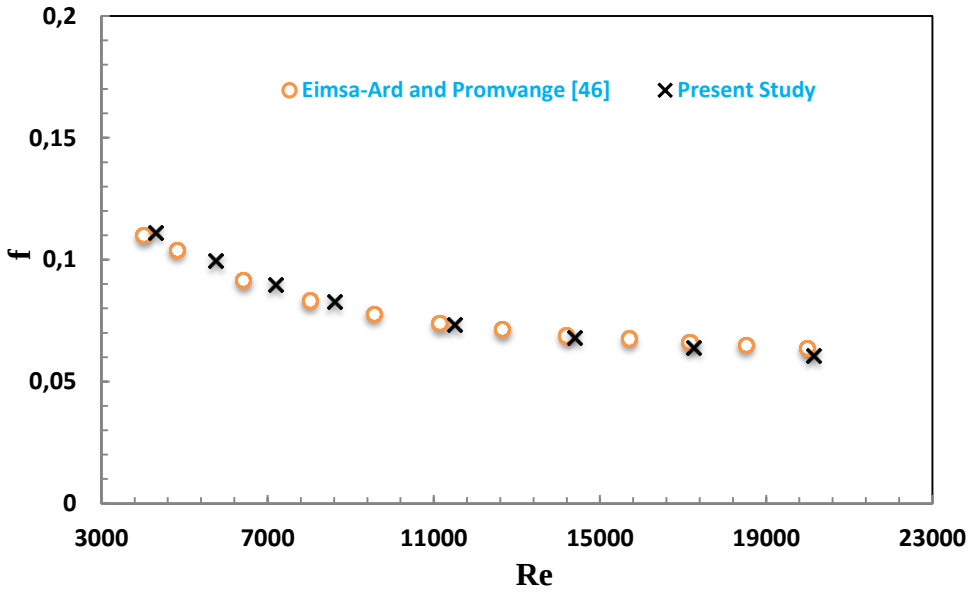

Figure 3.12 Figure 3.12 Reynolds number versus friction factor graphic of numerical results and literature results of Eimsa-ard and Promvonge [46] for twisted tape

Results shown in Figure 3.11 and 3.12 were compared to the results of Eiamsa-Ard and Promvonge [46], and maximum deviation was calculated around 6% and 7% for Nusselt number and friction factor, respectively. Results were harmony with the literature.

CHAPTER 4

NUMERICAL SIMULATION OF THE CURVED CROSS SECTIONAL TWISTED TAPES

4.1 NUMERICAL SOLUTION

To analyse the flow through a pipe with the curved cross sectional twisted tape under the constant heat flux and turbulent flow conditions, Navier-Stokes equations, energy equation, continuity, and turbulence model must be used together for this study. In addition, the curved and reverse curved geometry made the analysis more complex. For this reason, numerical solutions methods can be better to analyses this geometry. ANSYS Fluent Release 18.1 program was used to solve the governing equations with a pressure-based solver under steady condition. Standard k-epsilon model and enhanced wall treatment were selected for solution. The convergence absolute criteria of 10^{-3} for k and ε, and energy, and 10^{-6} for momentum, continuity, energy and x-y-z velocities were selected. The conservation equations for mass, momentum, and energy were given below.

Mass conservation:

$$\frac{\partial \rho}{\partial t} + \nabla . (\rho \, \vec{u}) = 0 \qquad (4.1)$$

Momentum conservation:

$$\frac{\partial (\rho \, \vec{u})}{\Delta t} + \nabla (\rho \, \vec{u} \, \vec{u} \,) = \rho g - \Delta P + \nabla . (\bar{\tau}) \qquad (4.2)$$

Energy conservation

$$\frac{\partial (\rho e)}{\Delta t} + \nabla . \left(\vec{u} (\rho e + P) \right) = \nabla . (Keff \, . \nabla T + (\vec{\tau} eff \, . \ \vec{u} \,)) \qquad (4.3)$$

4.2 COMPARISON OF TRIANGULAR AND POLYGONAL MESH ELEMENTS

The aim of this study was to understand of the effect of the mesh elements on the results of Nusselt number, friction, and performance evaluation factor. The typical twisted tape was meshed in two different ways, triangular and polygonal. Then, results of the study were compared each other and the experimental data of Bas and Ozceyhan [43].

4.3 PHYSICAL MODEL OF TYPICAL TWISTED TAPE

Table 4.1 and Figure 4.1 show boundary condition, physical model, and the mesh of the typical twisted tape.

Table 4.1 Geometrical parameters and boundary condition of typical twisted tape case

PARAMETERS / UNITS	VALUE
Diameter of tube / m	0.0508
Length of whole tube / m	1.25
Length of the twist tape / m	1.25
Twist ratio	3 and 4
Thick of twist tape / m	0.0008
Twist lengths / m	0.1524 and 0.2032
Inlet temperature / K	298.15
Heat flux / W/m^2	3
Working fluid	Air
Range of Reynolds numbers	5800-33100

Table 4.2 Codes of twisted tape having different twist ratio and mesh element

Twisted tape code	Twist Ratio (TR)	Mesh Type
TTTR3-T	3.0	Triangular
TTTR4-T	4.0	Triangular
TTTR3-P	3.0	Polygonal
TTTR4-P	4.0	Polygonal

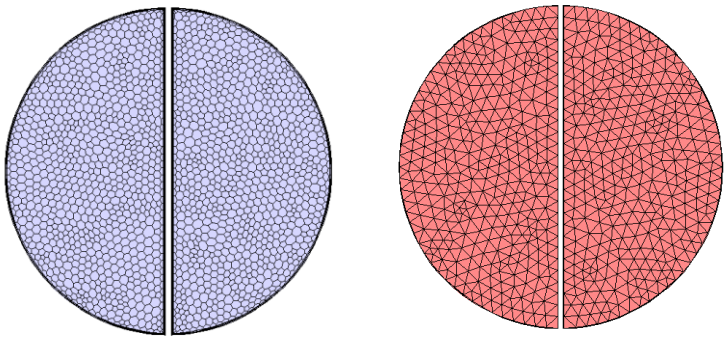

a) Polygonal b) Triangular

Figure 4.1 Triangular and polygonal mesh of typical twisted tape

Table 4.2 shows the codes of twisted tape having different twist ratio and mesh element. Two different mesh models were studied to compare their results. The 4084267 mesh size was used for triangular model, 3677139 for polynomial model. Inflation layers were also used for both models.

The fluid temperature at inlet was 298.15 K. The turbulence intensity was calculated by

$$I = 0.16 * Re^{(-1/8)} \qquad (4.4)$$

Turbulence intensity was found between 4 and 5% in the present study, and constant heat flux was applied on the wall, 3 W/m^2.

Air was used as the working fluid that thermophysical properties was calculated at the mean temperature by empiric equation, which was same at the validation. The mean temperature was used in the calculation because of the temperature variation observing along the pipe as shown in Figure 4.2.

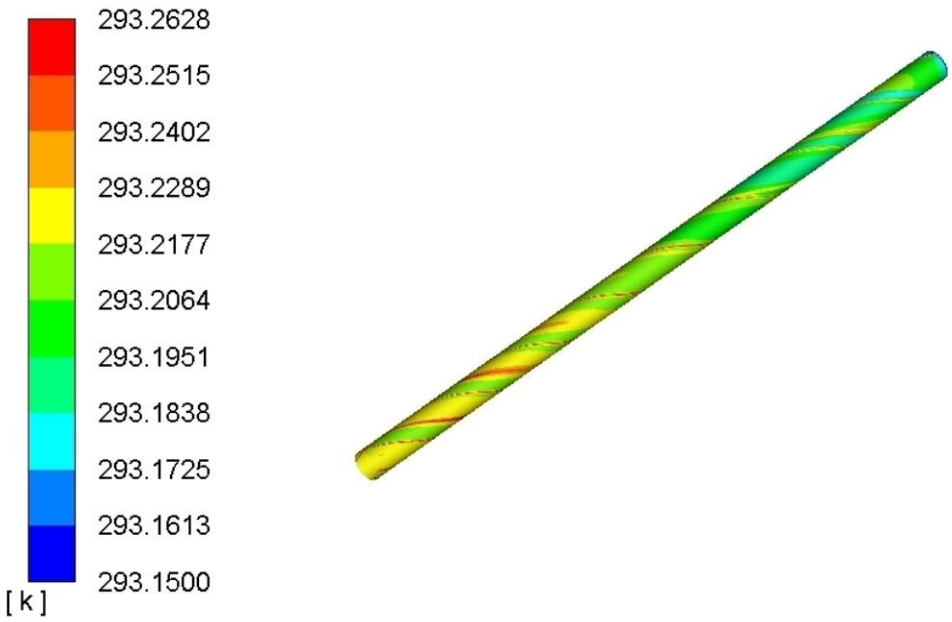

Figure 4.2 Variation of temperature along the pipe

Results were obtained using ANSYS v18.1. All needed parameters for using calculation were taken from twenty-four locations on the tested tube. Figure 4.3 shows locations where data were taken in axial direction. Then, Nusselt number, friction factor, and heat transfer coefficient were calculated by given equations in previous chapter.

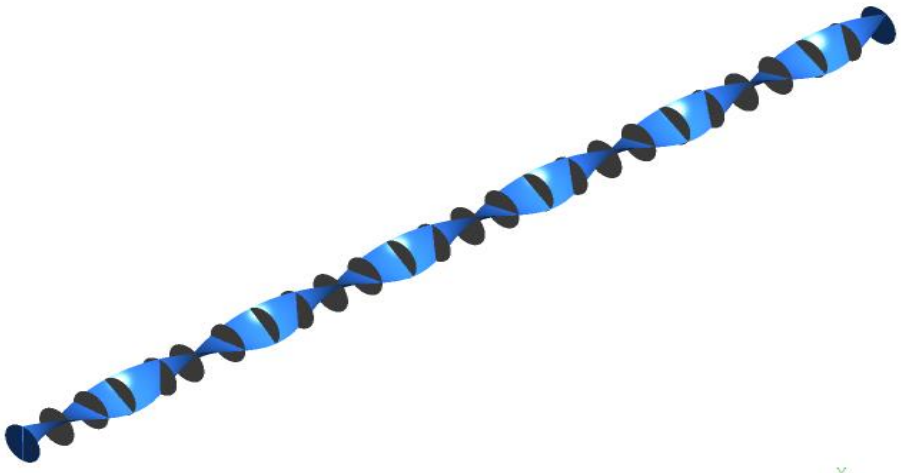

a)

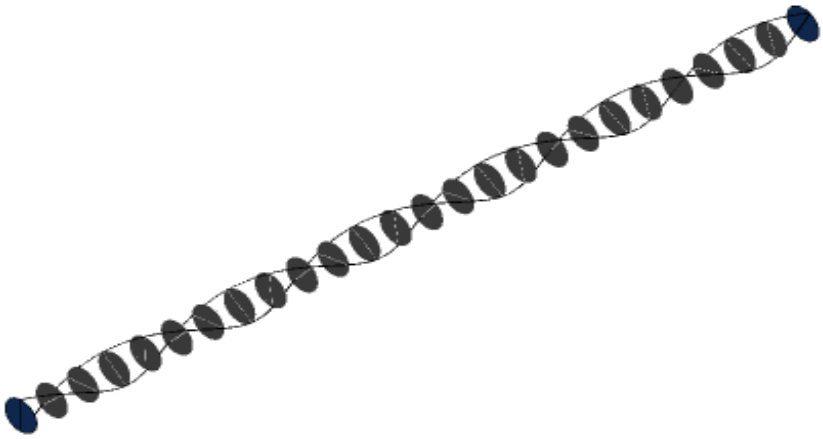

b)

Figure 4.3 Locations of calculated axial data along the tube A) Typical twisted tape with data locations B) Data locations in fluid domain

Figure 4.4 and Figure 4.5 show the numerical result of typical twisted tapes with two different twist ratios and two different mesh element (polygonal and triangular) in addition to the experimental results of Bas and Ozceyhan [43]. As seen from the Figure 4.4, Nusselt number deviation between results with polygonal and Bas and Ozceyhan [43] was much closer than the triangular mesh model. Deviation of polygonal model mesh was in the range of 4.23 and 8.29 % for 3.0 twist ratio, 11.06 and 1.58% for 4.0 twist ratio. Besides, it was observed that the deviation of the triangular mesh elements was major than the polygonal mesh elements. The polygonal model was found better than the triangular model for mesh according to the Graph of Nusselt Number versus Reynolds number. Also, for all cases, the Nusselt number increases with the increasing Reynolds number. According to the Figure 4.5, it was observed that the deviation between twisted tape results with polygonal mesh result and Bas and Ozceyhan [43] was so compatible than twisted tape results obtained by triangular mesh elements. The friction factor deviation was seen in the range of 0.66 and 10.79 % for 3.0 twist ratio, 0.32 and 8.29 % for 4.0 twist ratio. These results suggested that polygonal mesh model was better than triangular mesh models. It is decided to use a polygonal mesh model for the new cases for heat transfer enhancement.

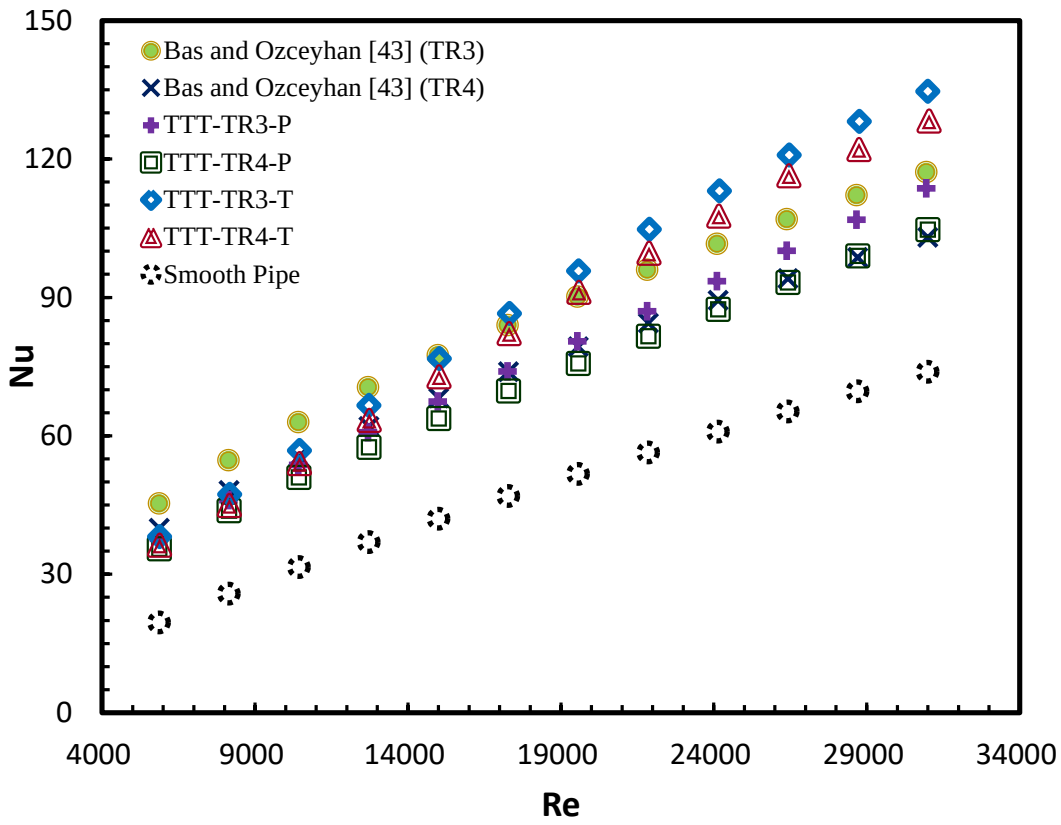

Figure 4.4 Graph of Nusselt number versus Reynolds number

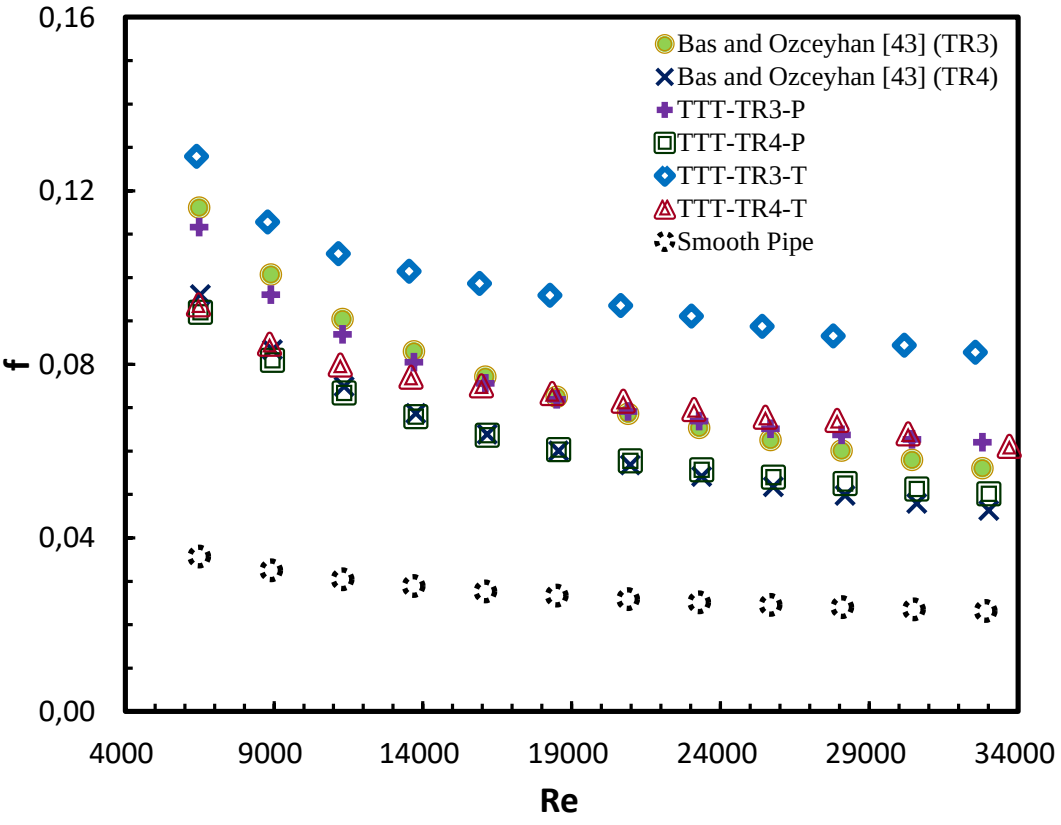

Figure 4.5 Graph of friction factor versus Reynolds number

The results of Nusselt number and friction factor of Bas and Ozceyhan [43] were given by below equations.

$$Nu = 0.6 * (Re^{0.57}) * (TR^{-0.45}) * (Pr^{0.4}) \quad (4.5)$$

$$f = 12.32 * (Re^{-0.45}) * (TR^{-0.65}) \quad (4.6)$$

To obtain the PEC, friction factor and Nusselt number for smooth pipe must be calculated. The friction factor correlations of Petukhov [48] and Nusselt number correlation of Gnielinski [49] were used for this purpose.

$$f_P = (0.79 * \ln Re - 1.64)^{-2} \quad (4.7)$$

$$Nu = \frac{\left(\frac{f}{8}\right)(Re-1000)Pr}{1+\left(12.7\sqrt{\frac{f}{8}}\right)*\left(Pr^{\frac{2}{3}}-1\right)} \quad (4.8)$$

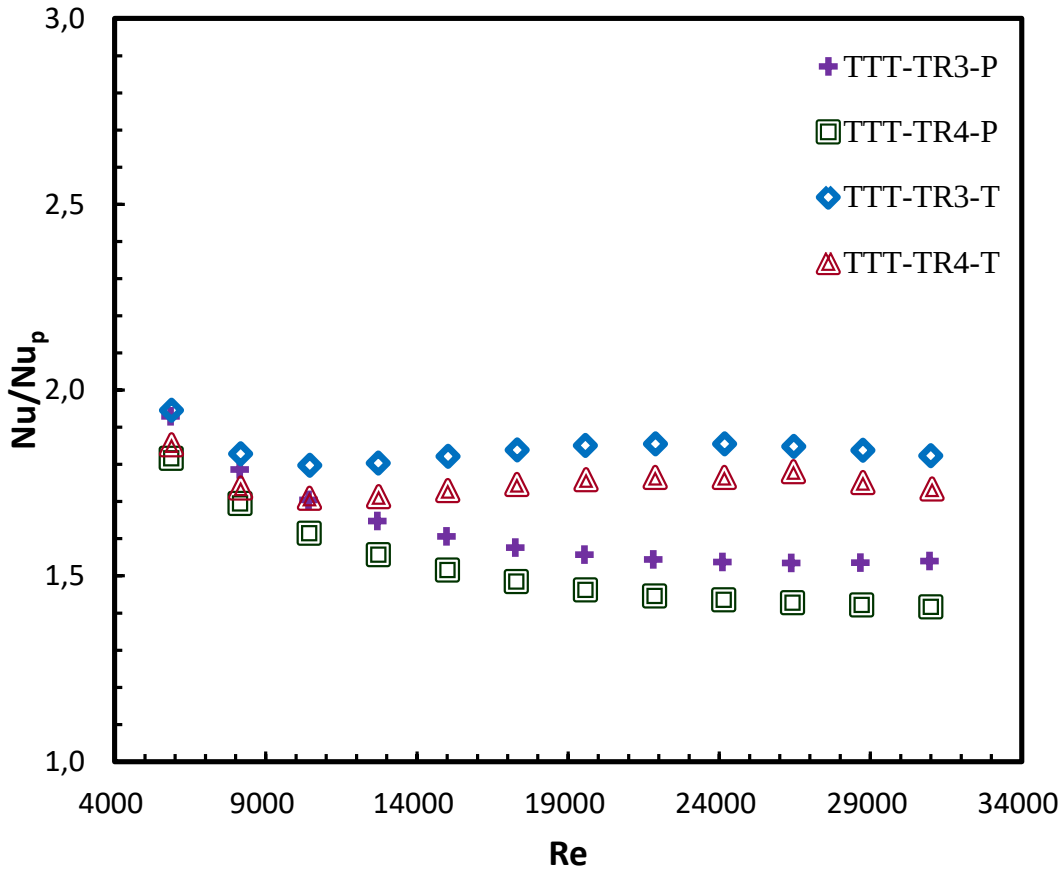

Figure 4.6 Graph of Nu / Nup versus Reynolds numbe

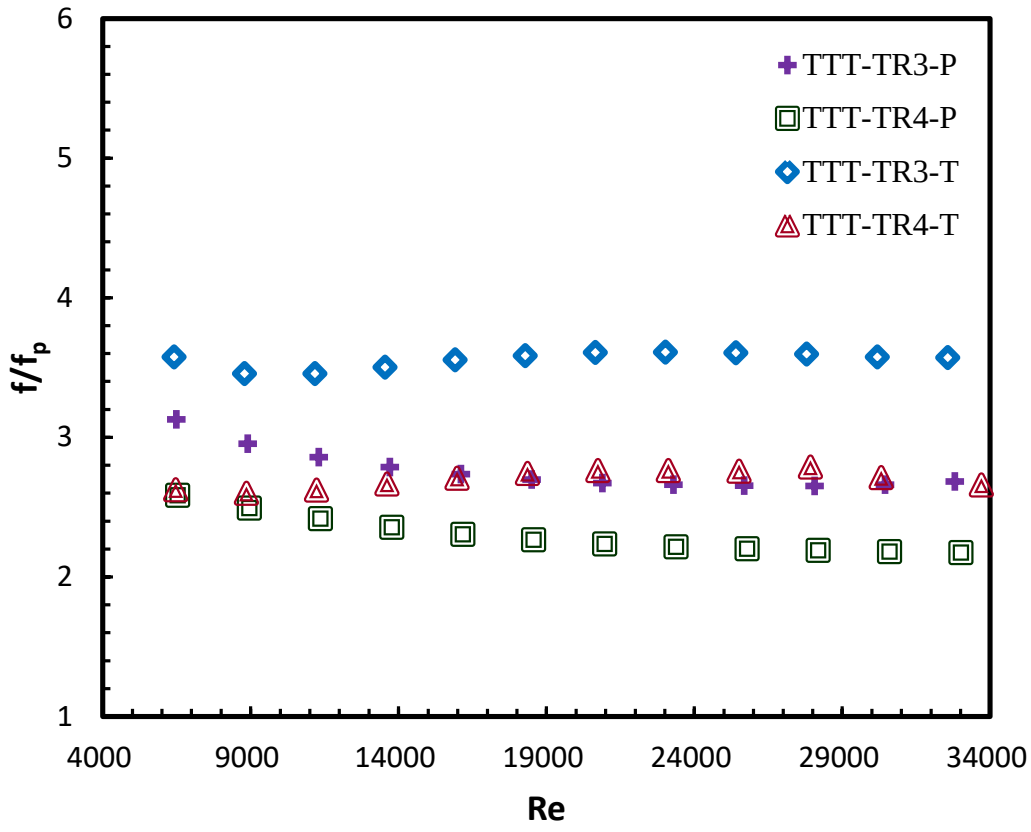

Figure 4.7 Graph of f /fp versus Reynolds number

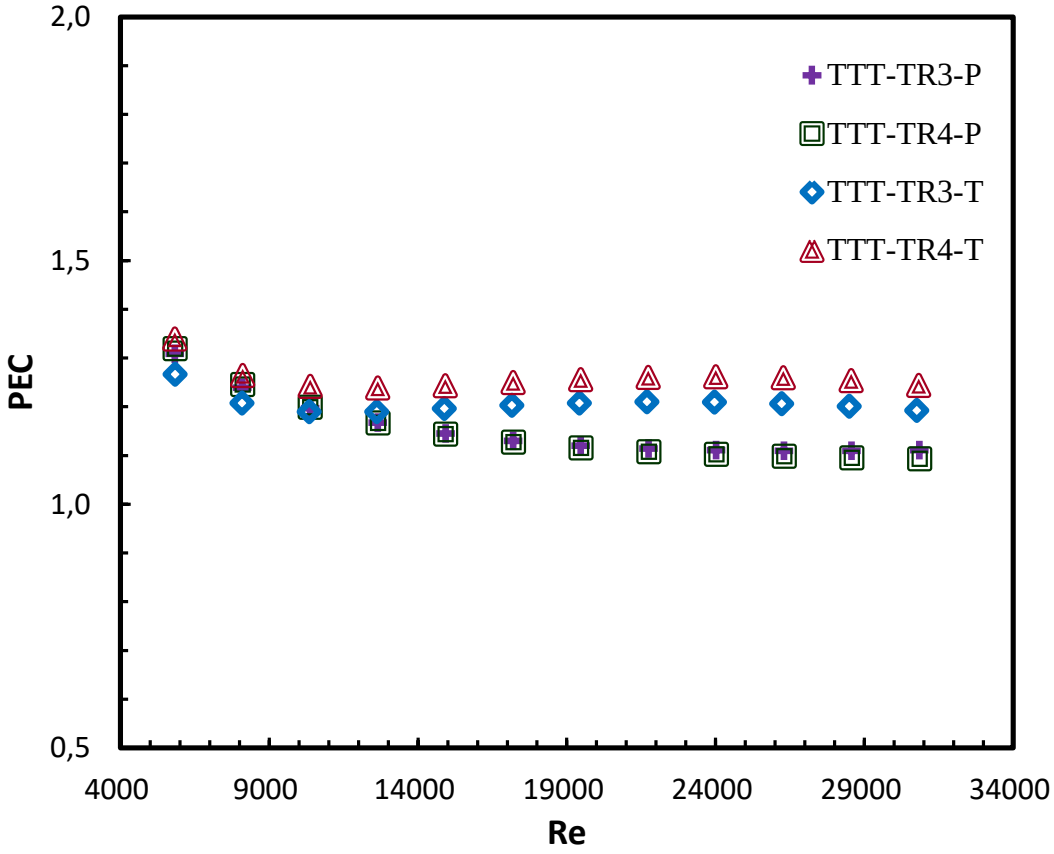

Figure 4.8 Performance of evaluation criteria versus Reynolds number

Figure 4.6 and Figure 4.7 show the heat transfer rate and friction ratios of twisted tapes for different mesh types. As Figure 4.8, performance of evaluation criteria for all twisted tapes were greater than unity.

4.4 NUMERICAL SIMULATION OF THE CURVED CROSS SECTIONAL TWISTED TAPE

Efficiency results of the curved cross sectional twisted tape in turbulent flow regimes using CFD simulation was declared in this section. The analysis of the new geometry began with the decision of the mesh model and number of elements. The best result was seen in the previous chapter in the polygonal mesh model and numbers of element used in the study in the region of 4200000-4500000. Polygonal mesh was used with minimum three-layer inflation. Inflation was most important due to the wall temperature distribution and turbulence between wall and tape inserts. Mesh was completed considering quality values such as Y+, skewness, and orthogonal quality. That was kept on maximum skewness < 0.95 and minimum orthogonal> 0.1. Moreover, the calculation method used in validation and smooth twisted tape was also used in analysis of new geometries.

4.4.1 PHYSICAL MODEL OF THE CURVED CROSS SECTIONAL TWISTED TAPE

The geometry and mesh of the curved cross sectional twisted tape inserts can be seen in Figure 4.9.

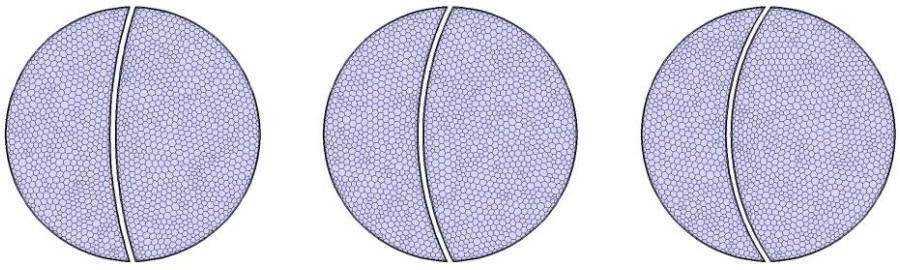

$\frac{D_c}{D_p}$ = 3.271 $\frac{D_c}{D_p}$ = 2.252 $\frac{D_c}{D_p}$ = 1.761

(a)

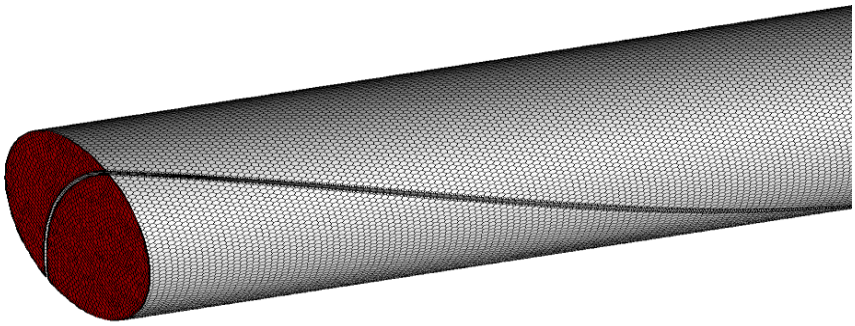

(b)

Figure 4.9 Mesh of curved cross sectional twisted tape a) inlet b) fluid domain

Thickness of twisted tape was 0.0008 m and diameter and length of the tube was 0.0504 m and 1.250 m. The curves radius (R_{CTT} = 83.09, 57.19, and 44.72 mm) were used for twisted tape with 152.4 and 203.2 pitches, which are the distance along the tape's axis that is covered by half rotation of the tape (180°). In addition to these, twist ratios (TR) was described the ratio between the pitch and the diameter of the pipe and, in the study, are equal to 3.0 and 4.0.

$$TR = y/D_{\text{Pipe}} \qquad (4.9)$$

Table 4.3 Physical model dimensions of curved cross sectional twisted tape insert

Table 0.1Diameter of tube / m	0.0508
Length of whole tube / m	1.25
Length of the twist tape / m	1.25
Twist ratio	3.0 and 4.0
Thick of twist tape / m	0.0008
Twist lengths / m	0.1524 and 0.2032
Inlet temperature / K	298.15
Heat flux / W/m^2	3
Working fluid	Air
Range of Reynolds numbers	5800-31000

Table 4.4 Codes of curved cross sectional twisted tape

Twisted tape name	Curve radius (r)	Twist Ratio(TR)	Curve ratio ($\frac{D_c}{D_p}$)
C1TR3	83.09	3.0	3.271
C2TR3	57.19	3.0	2.252
C3TR3	44.72	3.0	1.761
C1TR4	83.09	4.0	3.271
C2TR4	57.19	4.0	2.252
C3TR4	44.72	4.0	1.761

4.4.2 BOUNDARY CONDITIONS OF THE ANALYSIS

Air was selected as the working fluid that thermophysical properties were calculated at the mean temperatures by using empiric equations, which were same at the validation. The fluid temperature at the inlet was 298.15 K.

The turbulence intensities were calculated by

$$I = 0.16 * Re^{(-1/8)} \qquad (4.10)$$

Turbulence intensity was between 4 and 5% in the present study as shown in Table 4.5, and constant heat flux was applied on the wall, 3 W/m^2.

Table 4.5 Using values of velocity and turbulent intensity for curved cross sectional twisted tape

Inlet velocity	Intensity (at inlet)
1.8	5.32445
2.5	5.11024
3.2	4.95496
3.9	4.83393
4.6	4.73521
5.3	4.65210
6.0	4.58052
6.7	4.51777
7.4	4.46200
8.1	4.41187
8.8	4.36640
9.5	4.32482

4.4.3 RESULTS OF THE ANALYSIS

Results were obtained using ANSYS v18.1. All needed parameters for using calculation were taken from twenty four locations on the tested tube. Figure 4.10 shows these locations where data were taken in axial direction. Then, Nusselt number, friction factor, and heat transfer coefficient were calculated by given equations in previous chapter.

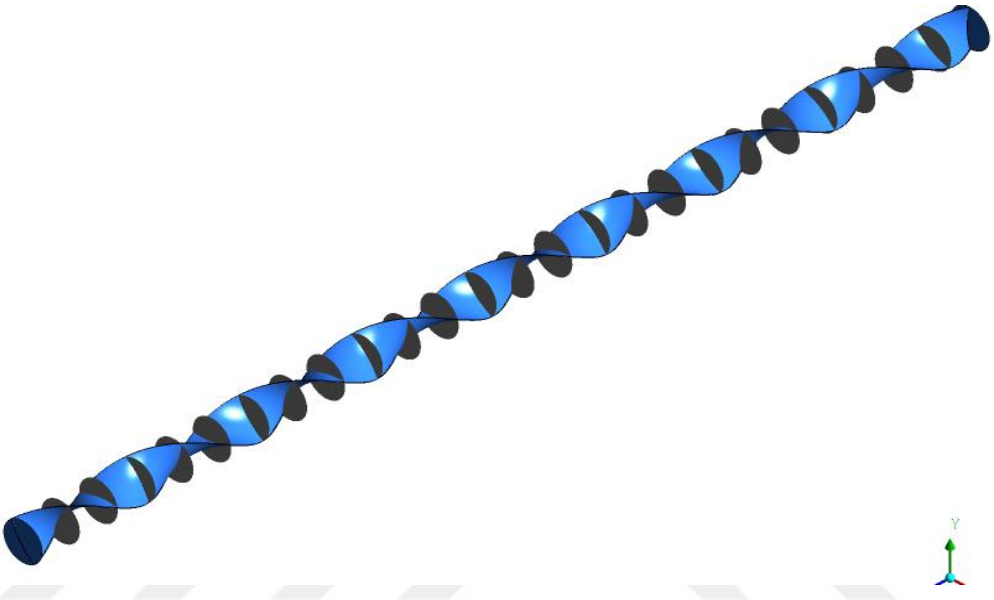

a) Curved cross sectional twisted tape with data locations

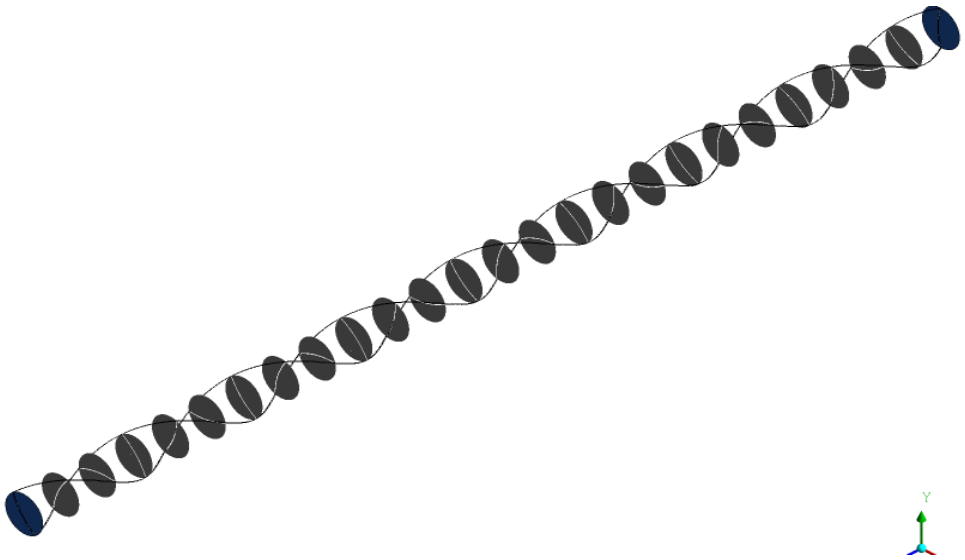

b) Data locations in fluid domain

Figure 4.10 Locations of calculated axial data along the tube a) curved cross sectional twisted tape with data locations b) data locations in fluid domain

The mean temperature was used in the calculation because of the temperature variation observing along the pipe .

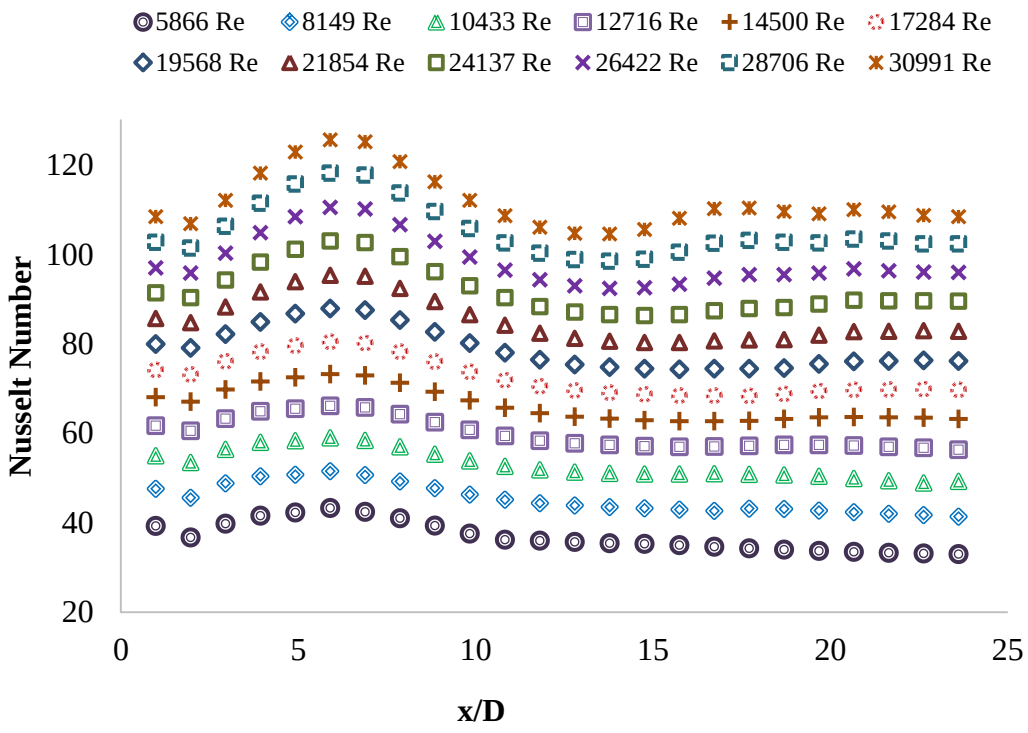

a) C1TR3

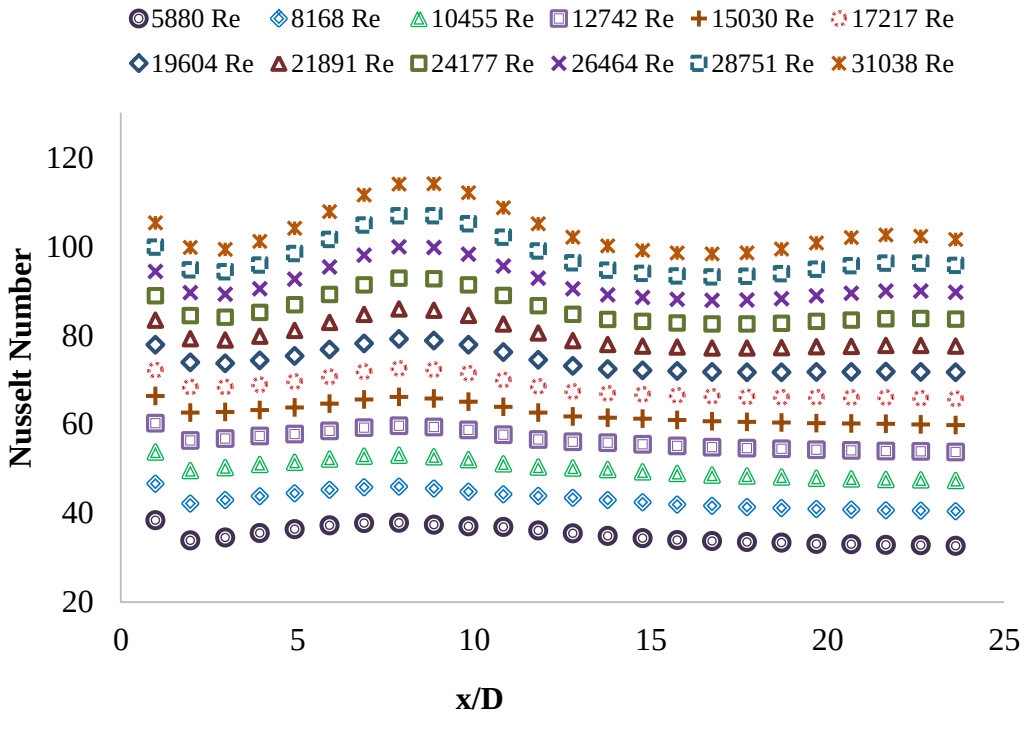

b) C1TR4

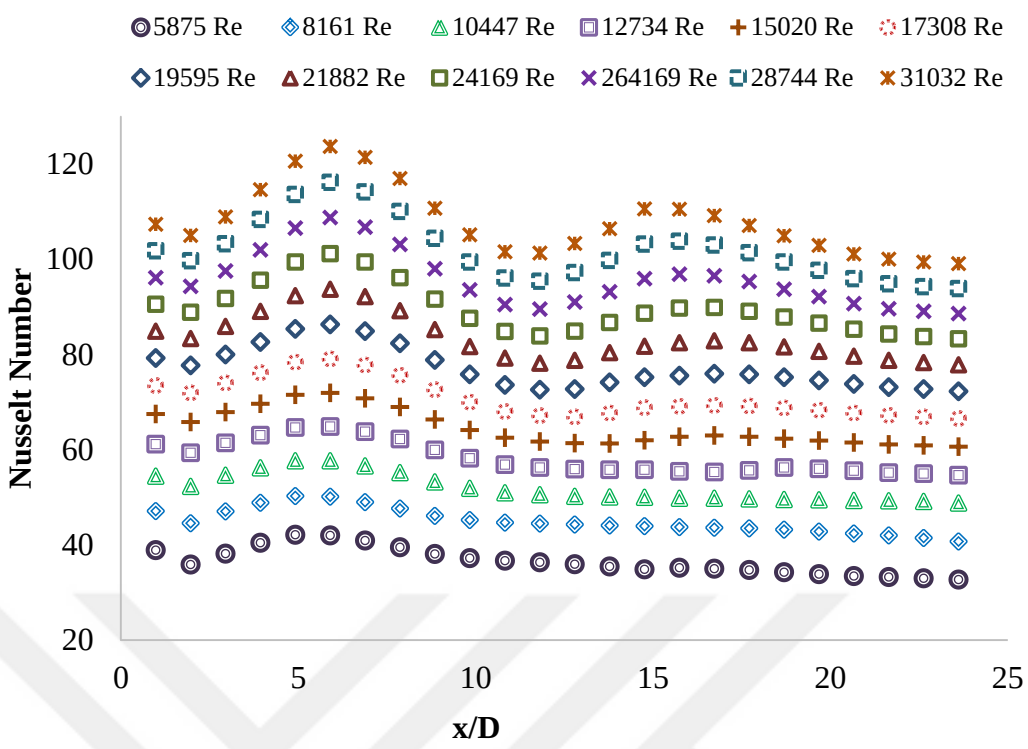

c) C2TR3

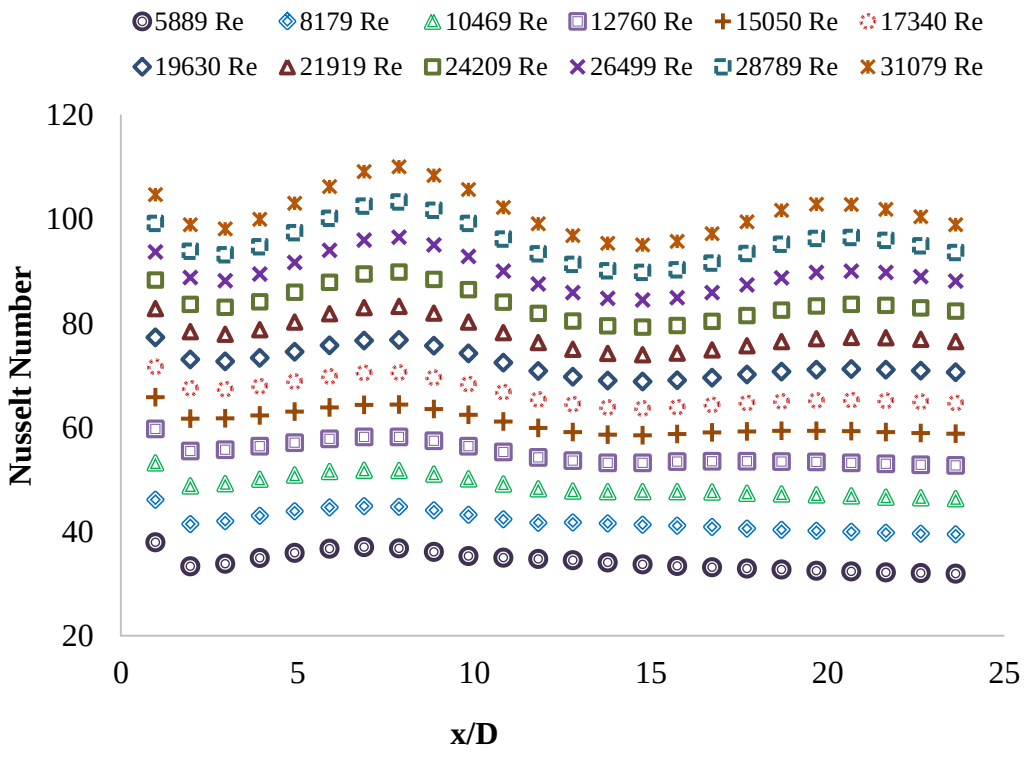

d) C2TR4

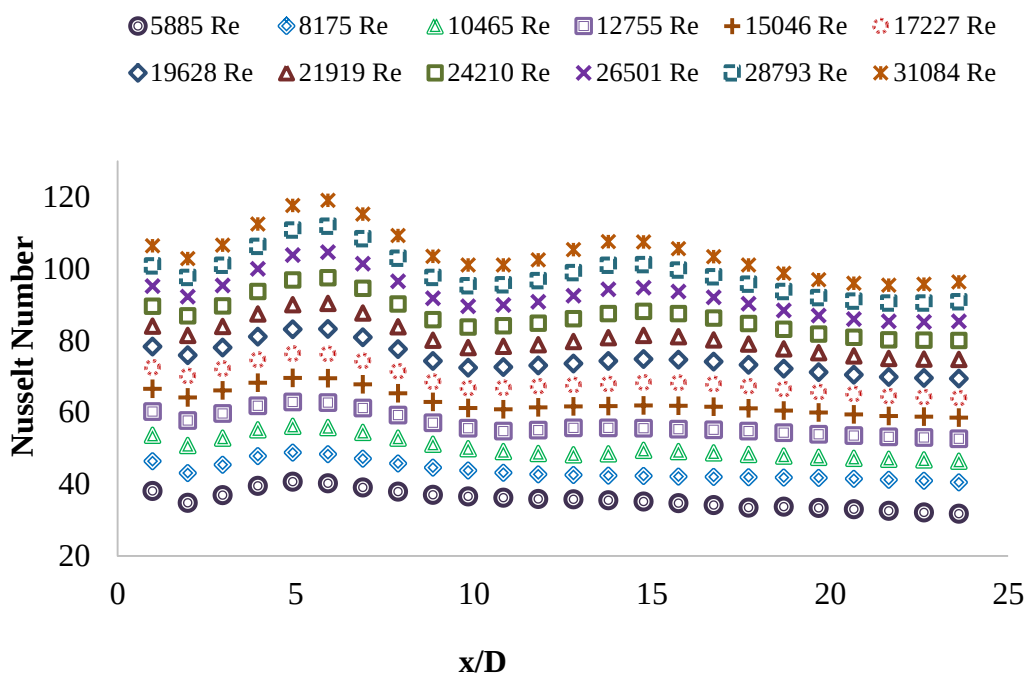

e) C3TR3

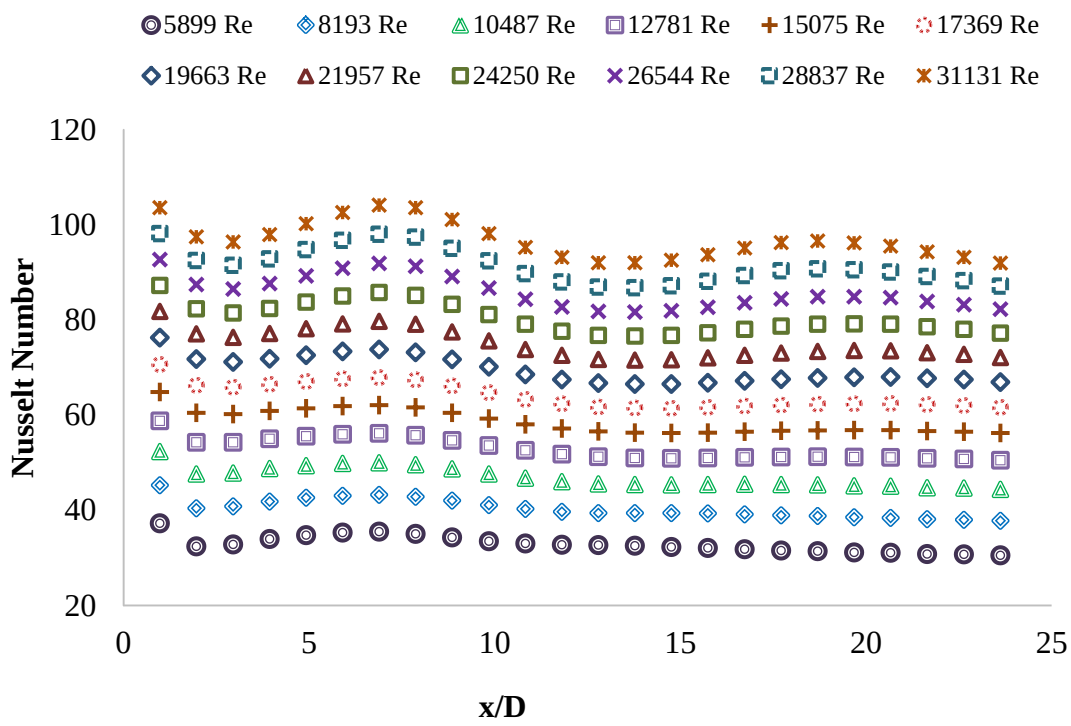

f) C3TR4

Figure 4.11 Axial distributions of Nusselt number along the tube for all curved cross sectional twisted tape models

Figures 4.11(a)-(f) shows the axial distributions of Nusselt number along the tube fitted with a curved cross sectional twisted tape at twelve different Reynolds numbers. Calculations were obtained twenty-four locations at the end of the analyses. While all the regional Nusselt numbers increase consistently as Re increases, Reynolds number regulated Nusselt number alteration in the pipe equipped with the curved cross sectional twisted tape insert illustrates the familiar characteristics of flow effort to establish hydraulically and thermally fully developed flow after the sudden entrance of the tape [28, 50, 51]. The wavy local Nusselt number profiles are noticed in the tube fitted with curved cross sectional twisted tape. By way of increasing Re from 5800 to 31000 as seen from Figures 4.11(a)-(f), the wavy profiles are correspondingly amplified.

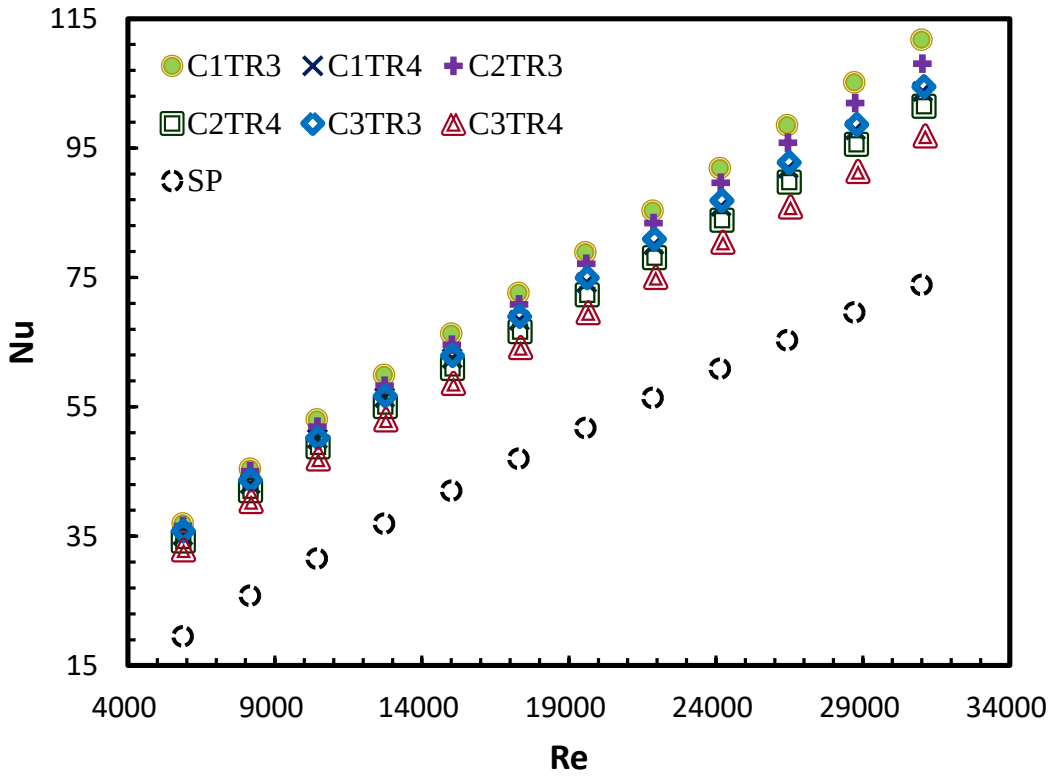

Figure 4.12 Nusselt number dependence on Reynolds number for curved cross sectional twisted tape

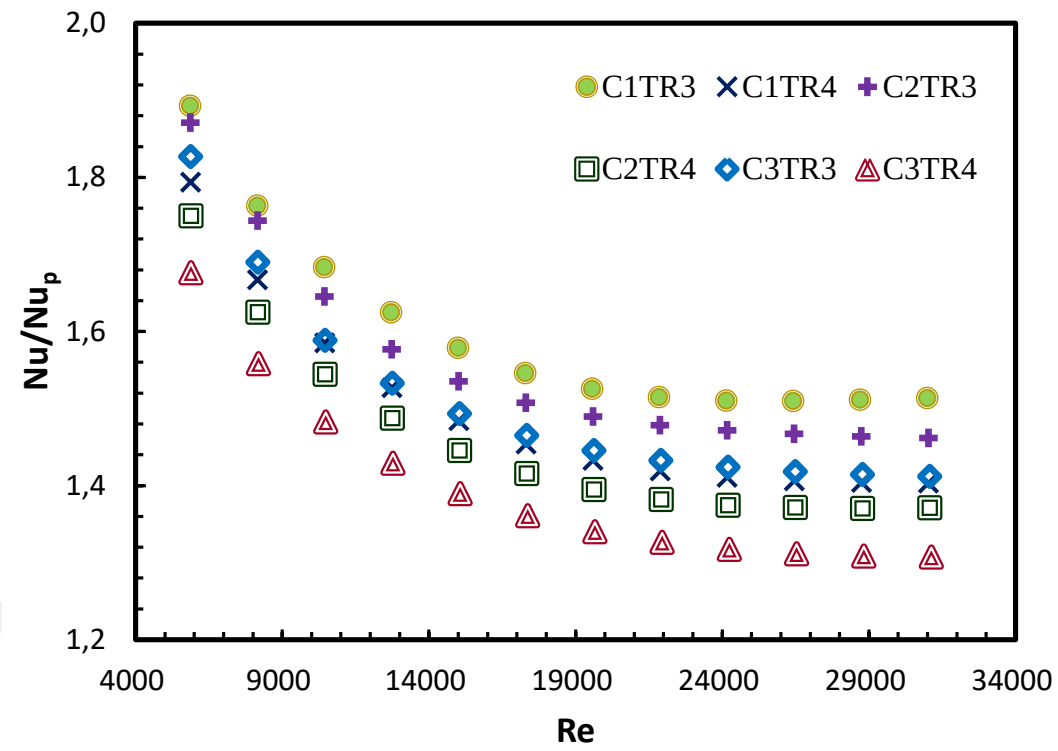

Figure 4.13 Nu/Nu$_p$ variations versus Reynolds number

Figure 4.12 and Figure 4.13 show the mean Nusselt number and the variation of Nu/Nu$_p$ of the curved cross sectional twisted tape in the plain tube with Reynolds number. Nusselt number increased with the increasing Reynolds number for all cases and was in the range of 32.9 to 112. Curved cross sectional twisted tapes improved the heat transfer according to the smooth pipe for all Reynolds numbers. The Nusselt number ratios of the curve twisted tapes were within the range of 1.31 to 1.89. This means that the tapes generate the strength swirl flow in the pipe. As expected, strong turbulent flow conditions resulted from the geometry of the twisted tape.

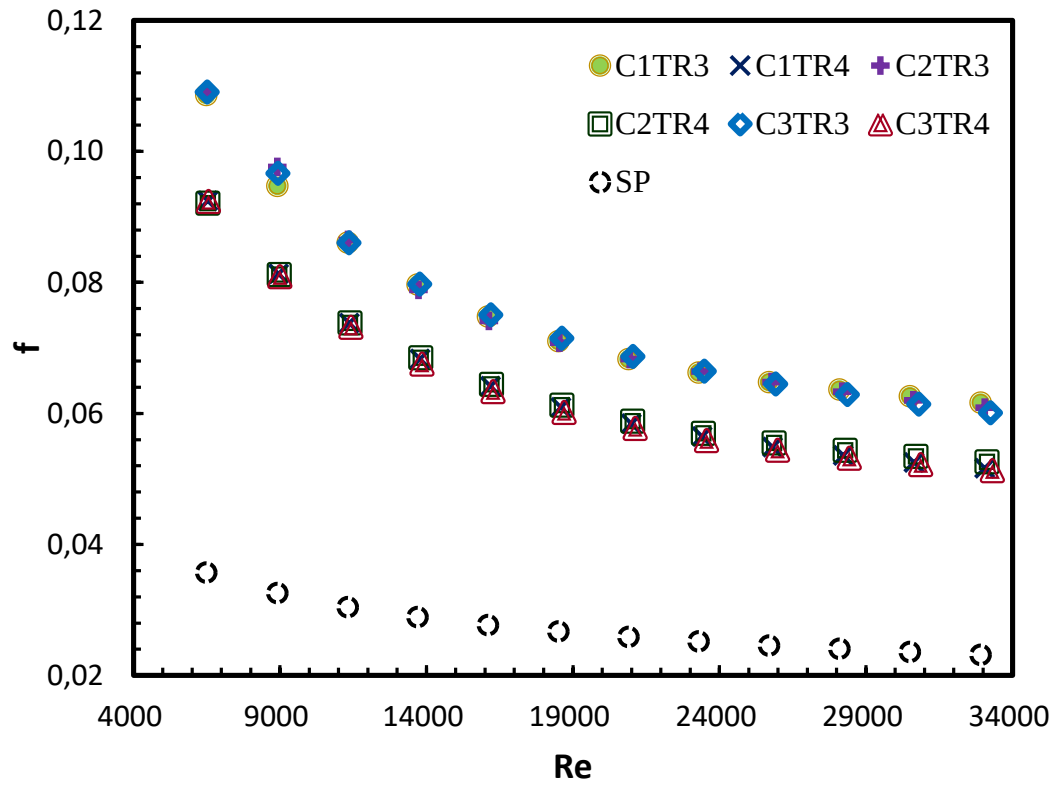

Figure 4.14 Friction factor dependence on Reynolds number for curved cross sectional twisted tape

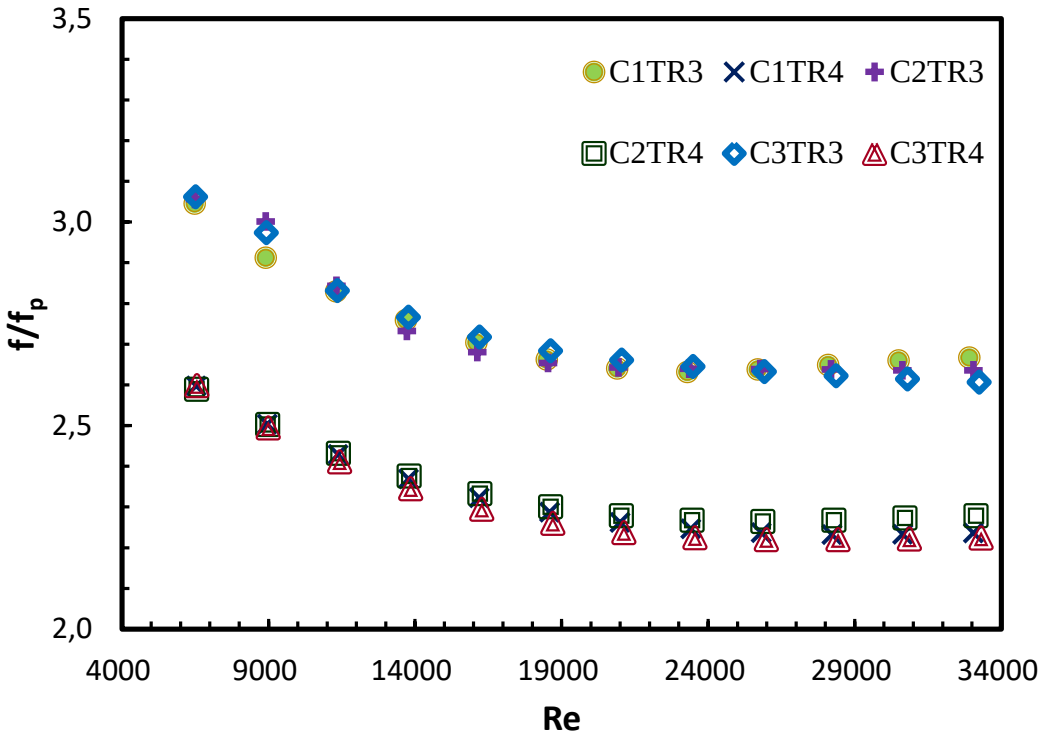

Figure 4.15 The f/f_p variation versus Reynolds number

The friction factor of the curved cross sectional twisted tape is presented in Figure 4.14. Friction factor decreases with the increasing the Reynolds number for all cases. As expected, curved cross sectional twisted tape gives a higher friction factor than the smooth pipe. As can been seen in the Figure 4.15, the ratio of f/f_p was in the range of 2.61 to 3.06 for 3 twist ratio, and 2.22-2.60 for 4 twist ratio. This means that the lower twist ratio gives more friction.

Figure 4.16 shows the calculated PEC values versus Reynolds number for curved cross sectional twisted tapes.

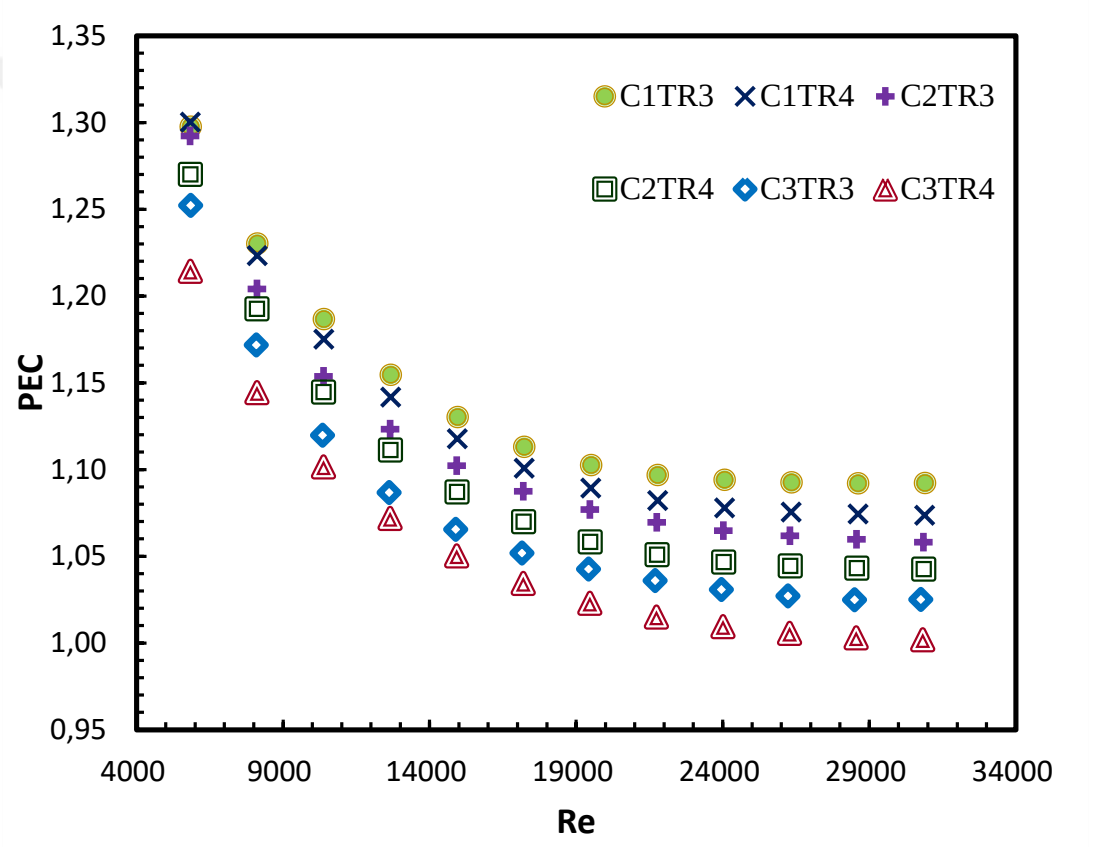

Figure 4.16 Performance evaluation criteria versus Reynolds number for curved cross sectional twisted tape

As can be seen from Figure 4.16, the performance evaluation factors are greater than unity for all runs. The performance evaluation value decreases with increasing the Reynolds number. The maximum PEC of C1TR3, C1TR4, C2TR3, C2TR4, C3TR3 and C2TR4 cases were calculated 1.297, 1.300, 1.292, 1.270, 1.252 and 1.214, respectively at the lower Reynolds number. The PEC of the twisted tape with the

radius of 83.09 mm ($\frac{D_c}{D_p}$ = 3.271) and 3.0 twist ratio is the highest, whereas for 44.72 mm ($\frac{D_c}{D_p}$ = 1.761) and 4.0 twist ratio, it is the lowest. The analyses results show that new twisted tape geometries have advantages according to the smooth pipe. The decreasing PEC with the increasing the Reynolds numbers indicates that curved twisted tape is actually suitable for low turbulent flow conditions.

Consequently, the results of Nusselt number, friction factor, and PEC for the curved cross sectional twisted tapes are correlated with regression rates of R^2 = 0.998, 0.993, and 0.999 as given by equations 4.12 to 4.14, respectively.

$$Nu = 0.1089 * Re^{0.6671} * Pr^{0.4} * TR^{-0.00002376} * \frac{D_c}{D_p}^{0.09972} \quad (4.12)$$

$$f = 2.568 * Re^{-0.3704} * TR^{-0.1135} * \frac{D_c}{D_p}^{0.001491} \quad (4.13)$$

$$\text{PEC} = 3.13 * Re^{-0.1155} * Tr^{0.00009194} * \frac{D_c}{D_p}^{0.09434} \quad (4.14)$$

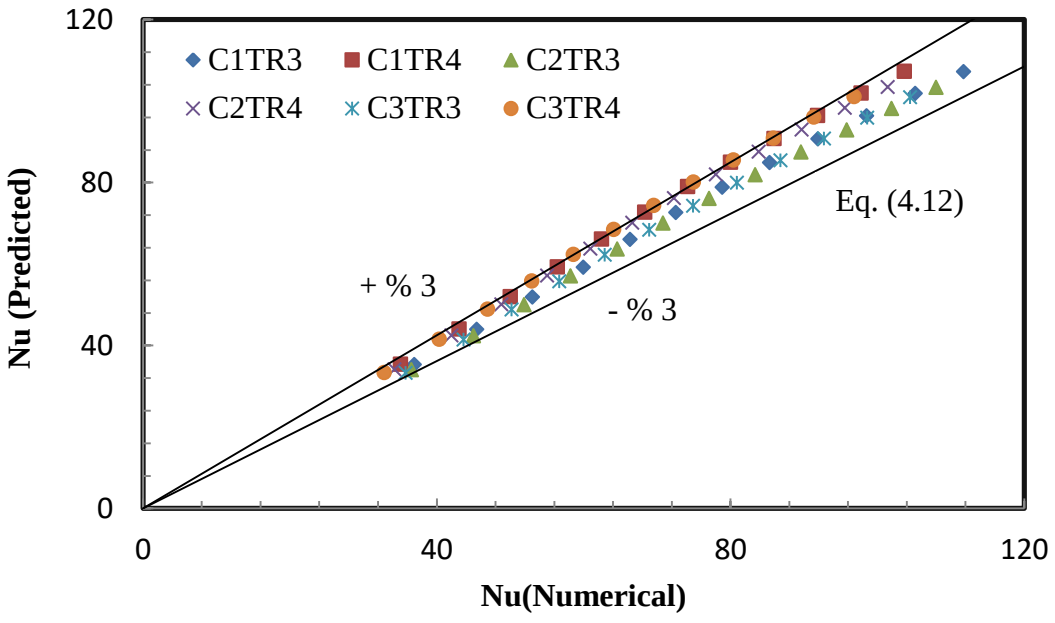

Figure 4.17 Comparison of Nusselt number between predicted and numerical results

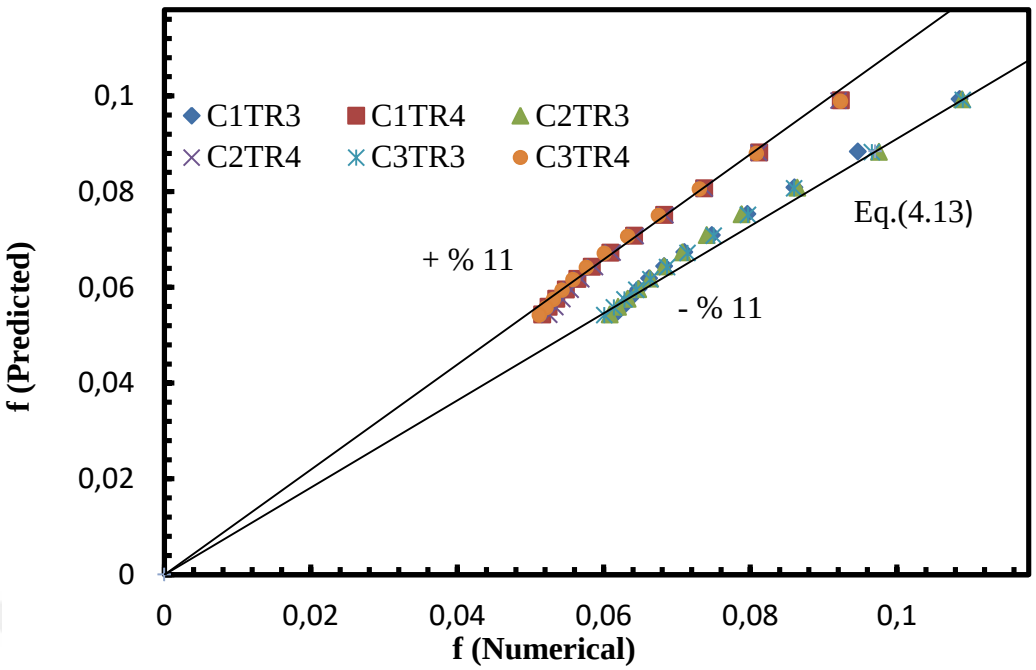

Figure 4.18 Comparison of friction factor between predicted and numerical results

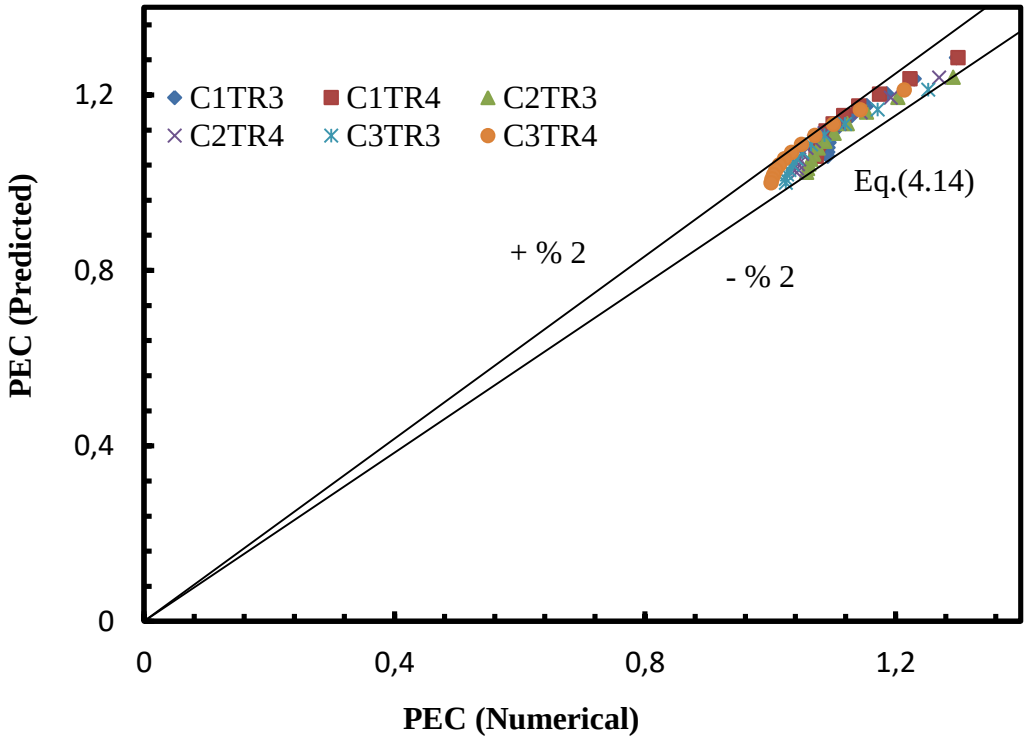

Figure 4.19 Comparsion of performance evaluation criteria between predicted and numerical results

As seen in Figure 4.17, 4.18, and 4.19, the deviation of Nusselt number,friction factor and PEC between numerical and predicted results depend on equation 4.12, 4.13 , and 4.14 were within ∓ 3%, ∓ %11, and ∓%2, respectivelly. The calculated

results from the correlated equations were well suitable with the numerical results of the new inserts which can be used to predict the heat transfer, pressure drop and performance of air flow in pipe with the reverse curved cross sectional twisted tapes. These equations were valid at the turbulent flow regime in the range of Reynolds number between 5800 and 31000.

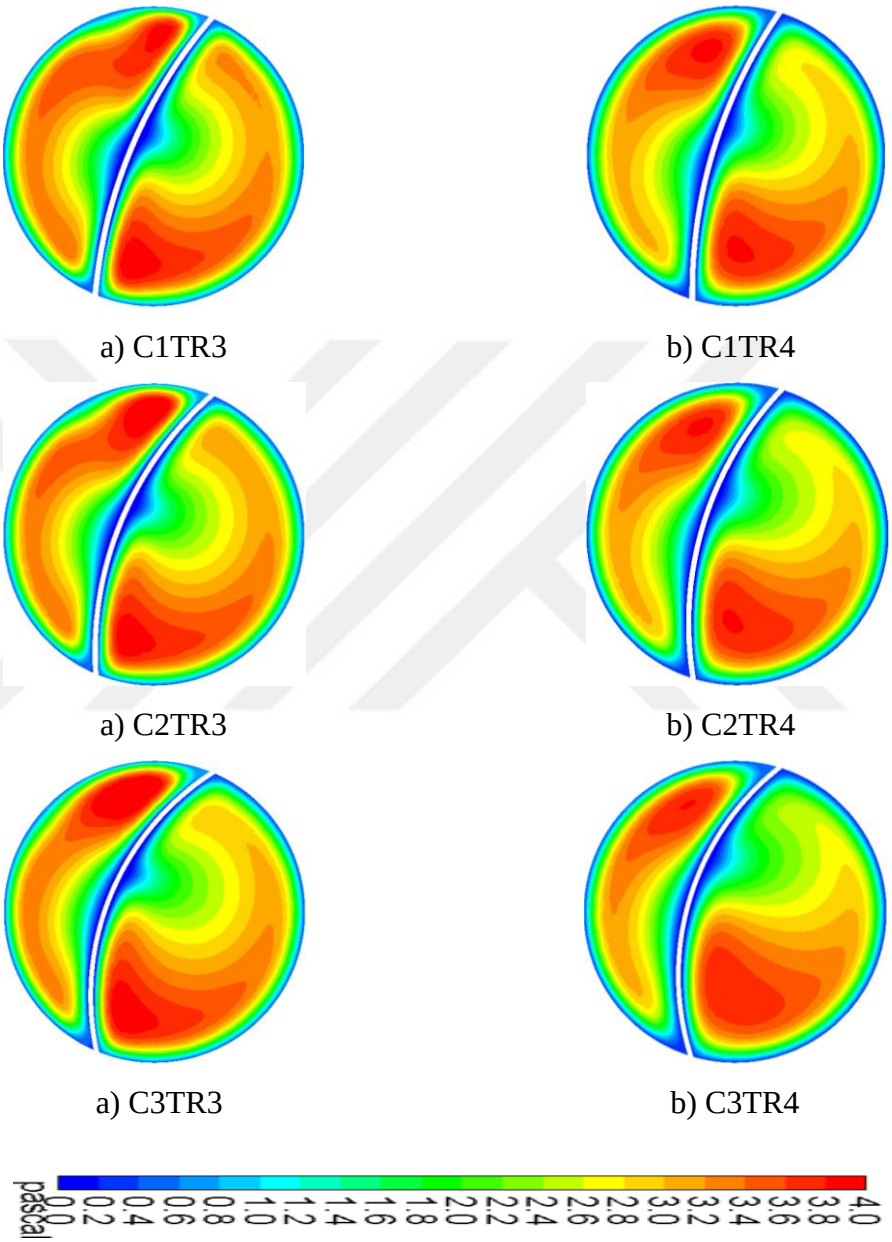

a) C1TR3 b) C1TR4

a) C2TR3 b) C2TR4

a) C3TR3 b) C3TR4

Figure 4.20 Pressure contours for velocity=1.8 m/s at the length of 1.2 m (x/d=23.62)

Figure 4.20 demonstrated the pressure contours for curved cross sectional twisted tapes with different diameter ratios ($\frac{D_c}{D_p}$ =3.271, 2.252, and 1.761) with 3 and 4 twist ratio at the length of 1.2 m. According to the Figure 4.20, as the curve ratio increases,

the pressure increases. The smallest pressure is also formed near the tube and insert wall.

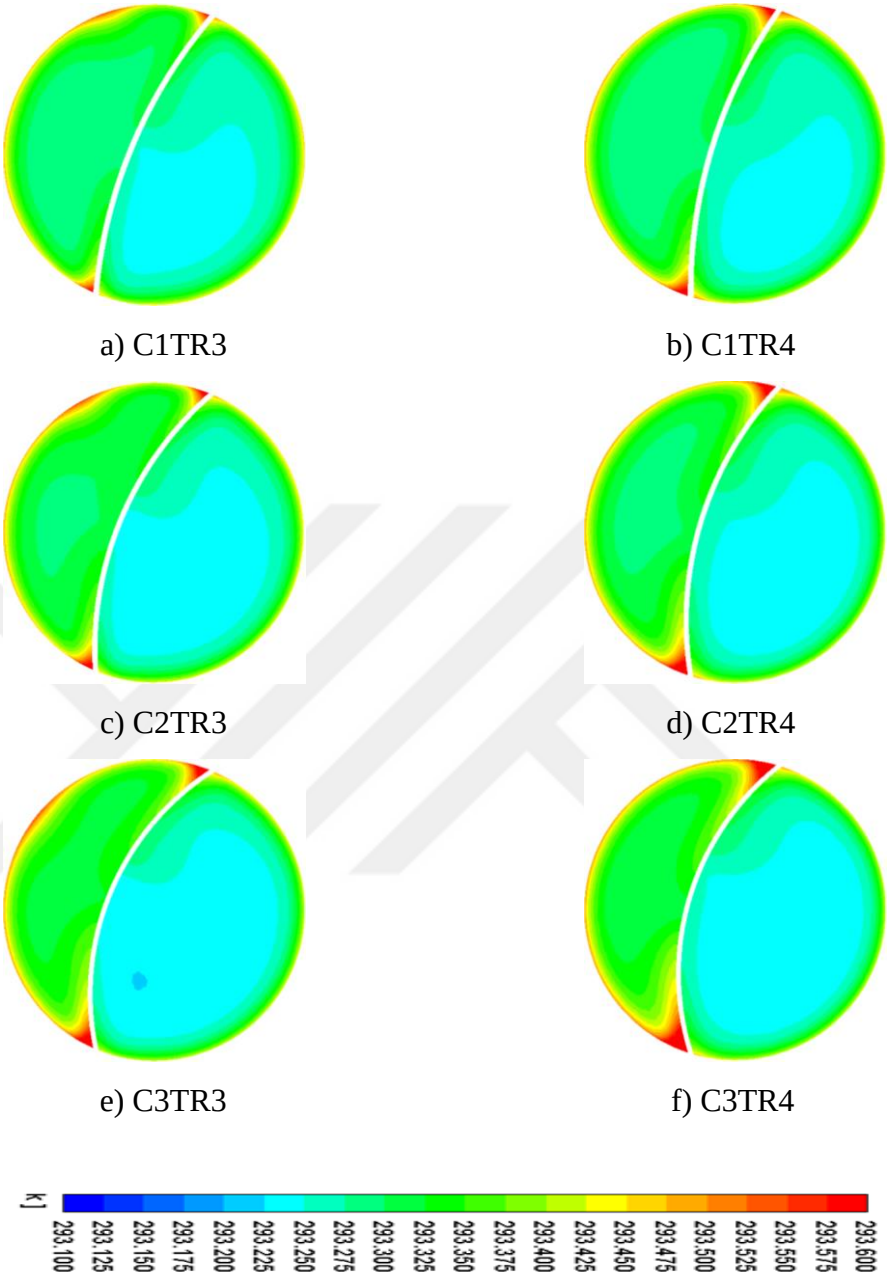

Figure 4.21 Temperature plots for velocity=1.8 m/s at the length of 1.2 m (x/d =23.62)

Figure 4.21 demonstrate the temperature variation contours for curved cross sectional twisted tapes with different diameter ratios ($\frac{D_c}{D_p}$ = 3.271, 2.252, and 1.761) and twist ratios at the length of 1.2 m. According to the Figure 4.21, a high-temperature field appears with the large diameter of curve and the smallest twist ratio due to the best

mixing and making strength turbulence. There is an observably thin thermal boundary layer near the tube wall as pressure plots images. Also, the high temperature of the fluid is observed at the sharp edges of the inserts.

These images show that the twist ratio is more effective on the heat transfer and pressure drop than the curve ratio.

CHAPTER 5

NUMERICAL SIMULATION OF REVERSE CURVED CROSS SECTIONAL TWISTED TAPE

5.1 PHYSICAL MODEL OF REVERSE CURVED CROSS SECTIONAL TWISTED TAPE

Reverse curved cross sectional twisted tape were created for three different curve radius (22.161, 16.441, and 14.081 mm) and two different twist ratios (3 and 4). The lengths of the pipe and insert were 1250 mm. Polyhedral mesh was used with acceptable quality values. As can be seen in Table 5.1, six kind of reverse curved cross sectional twisted tape were coded according to twist ratio and curve radius. Figure 5.1 shows the inlet mesh of reverse curved cross sectional twisted tapes for three different radii.

Table 5.1 Reverse curved twisted tape cases

Twisted tape code	Curve radius (r)	Twist Ratio (TR)	Curve ratio ($\frac{D_c}{D_p}$)
R1TR3	22.161	3.0	0.872
R2TR3	16.441	3.0	0.647
R3TR3	14.081	3.0	0.554
R1TR4	22.161	4.0	0.872
R2TR4	16.441	4.0	0.647
R3TR4	14.081	4.0	0.554

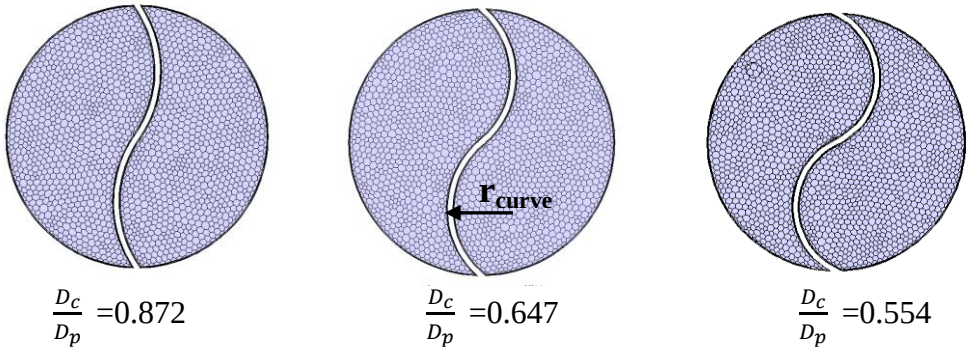

Figure 5.1 Inlet mesh of reverse curved cross sectional twisted tapes for three different radiuses

The same computational fluid dynamics method of curved cross sectional twisted tape was used to reverse curved cross sectional twisted tapes. The governing equations were solved with a pressure-based solver under steady condition. Viscous model, k-epsilon turbulence model, and enhanced wall treatment were used. Moreover, the convergence absolute criteria of 10^{-3} for k and ε, and energy, and 10^{-6} for momentum, continuity, energy, x-y-z velocities were set. Momentum and energy equations solved with second order, and kinetic energy and turbulent dissipation rate were solved with first order.

Same boundary condition at section 4.3 was applied on all geometries. All needed parameters for using calculation were taken from twenty four locations on the tested tube.

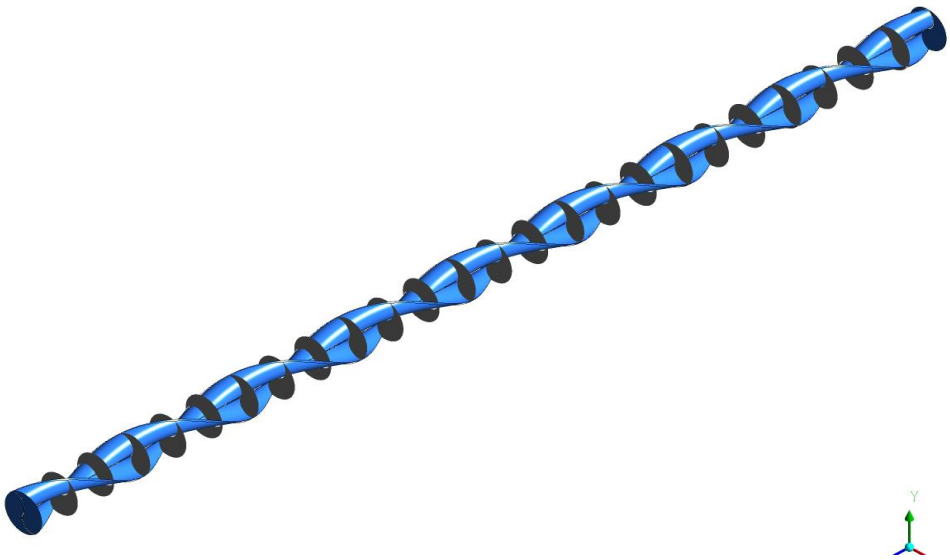

a) Reverse curved cross sectional twisted tape with data locations

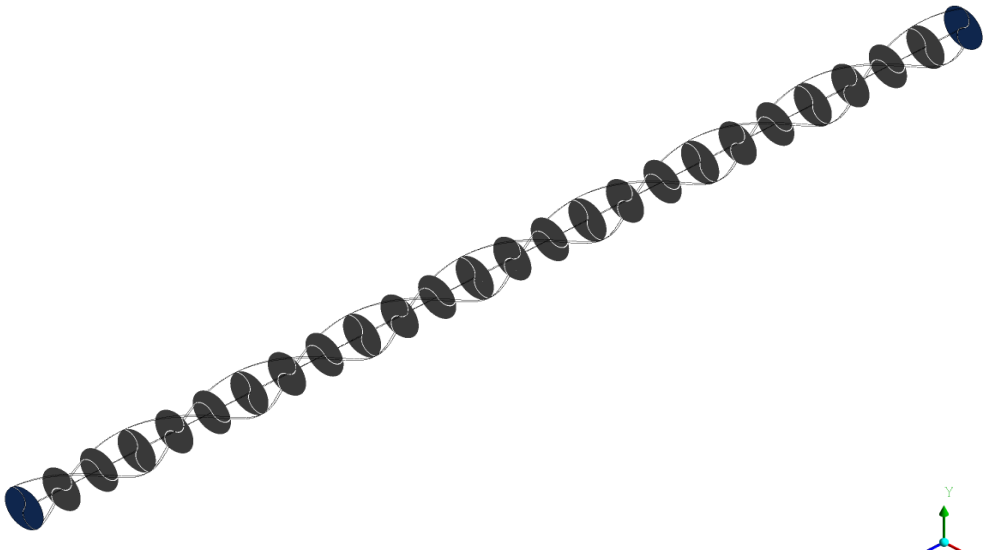

b) Data locations in fluid domain

Figure 5.2 Locations of calculated axial data along the tube a) reverse curve cross sectional twisted tape with data locations b) data locations in fluid domain

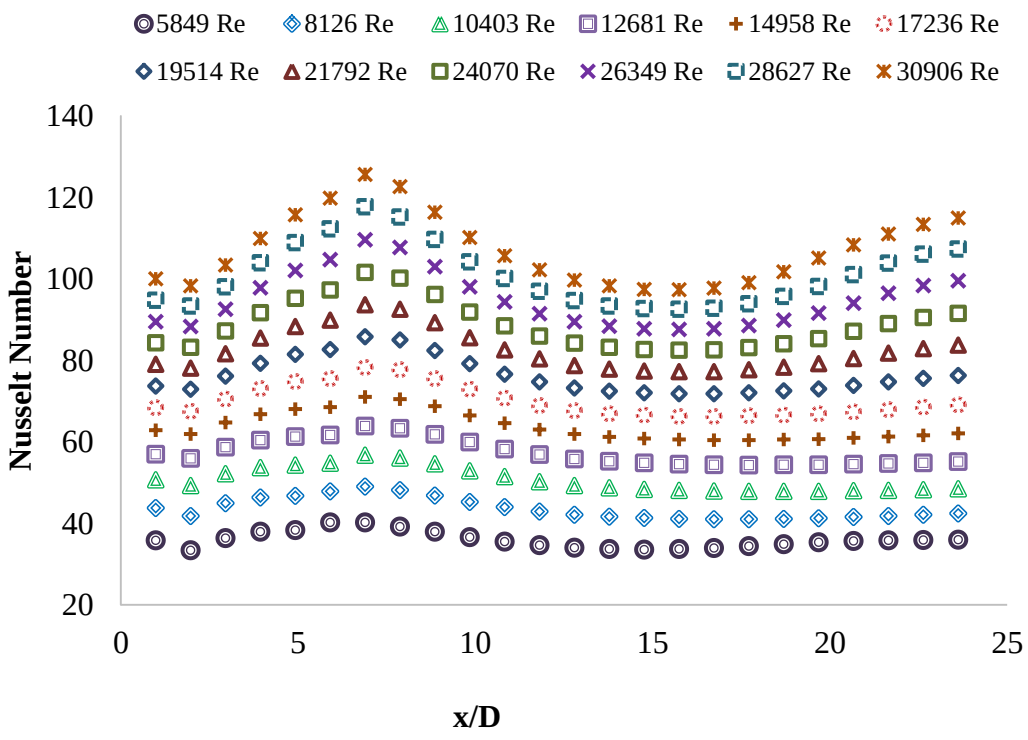

a) R1TR3

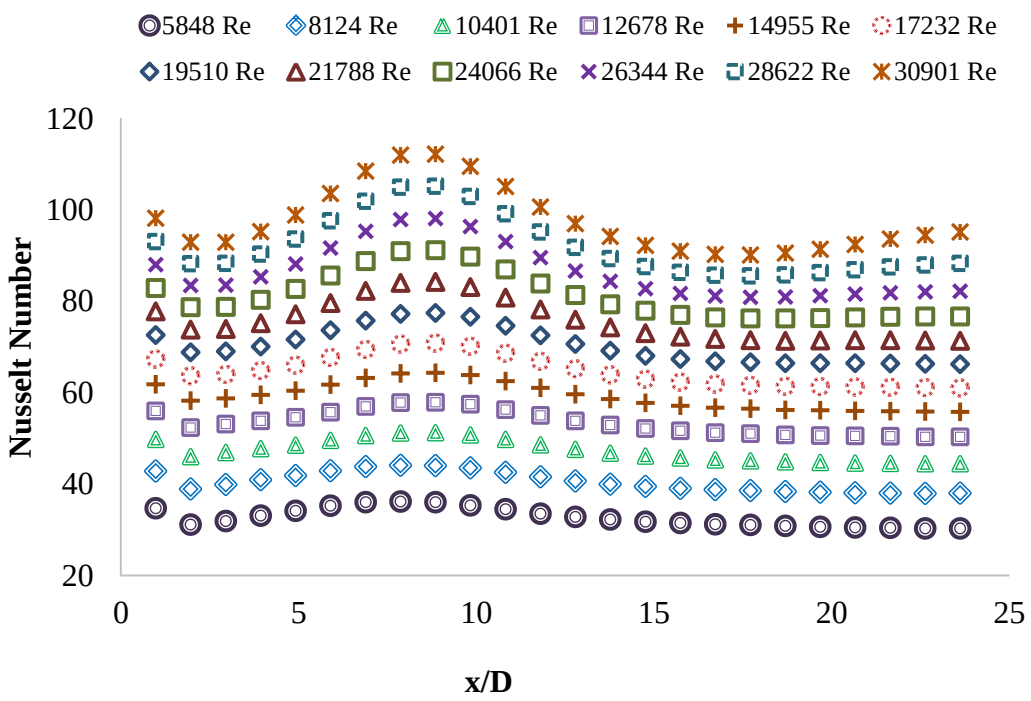

b) R1TR4

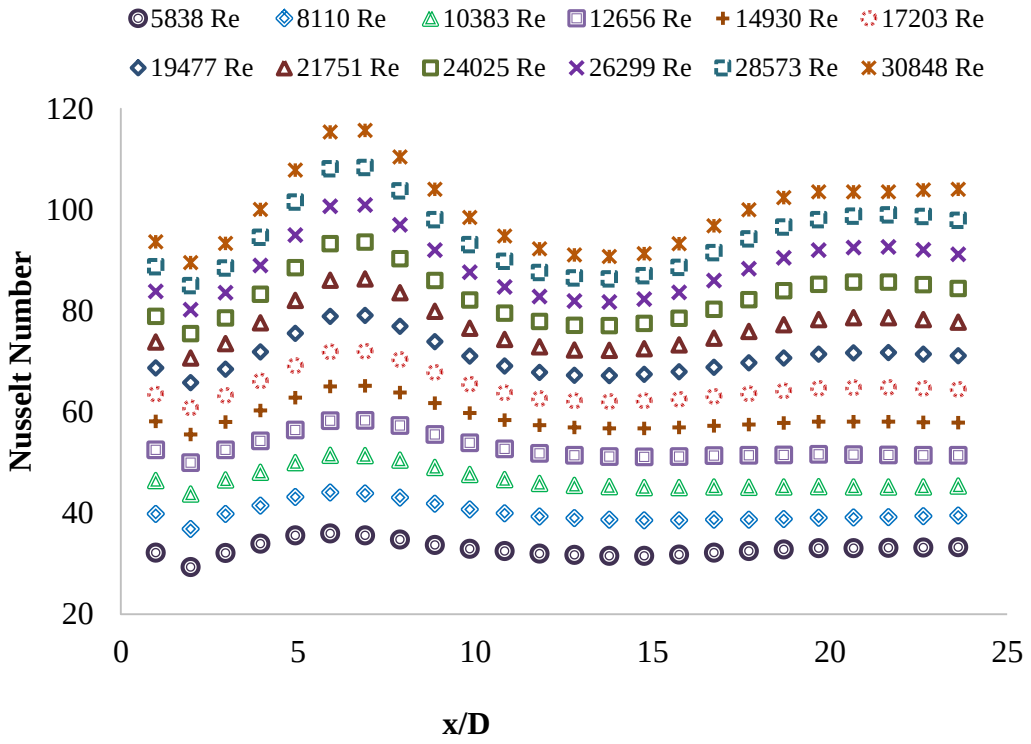

c) R2TR3

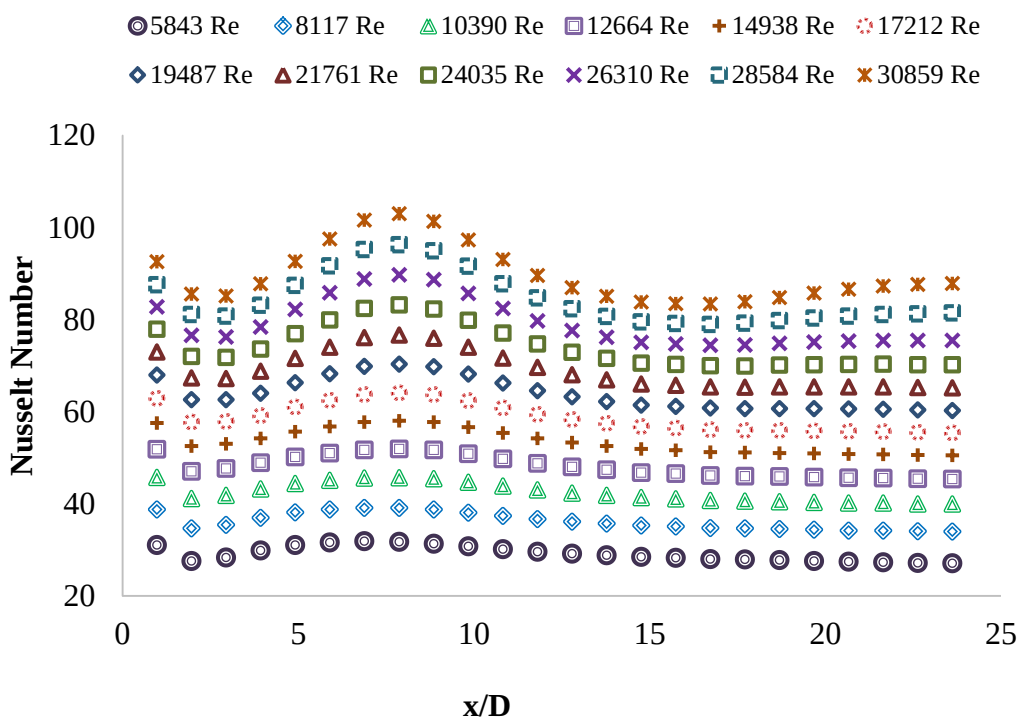

d) R2TR4

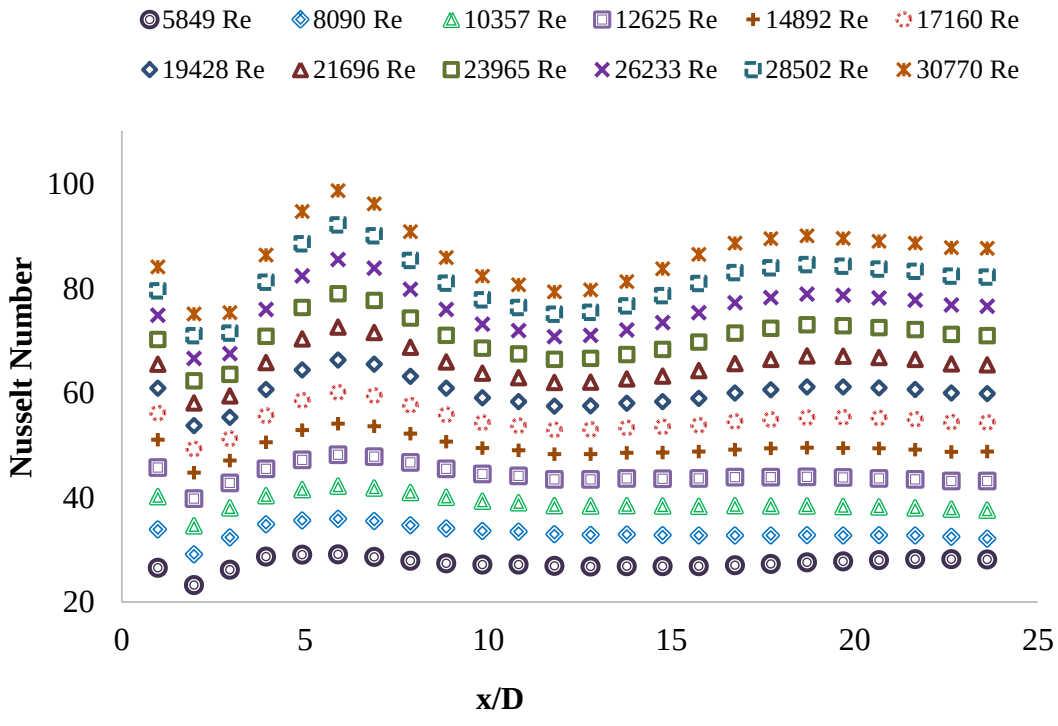

e) R3TR3

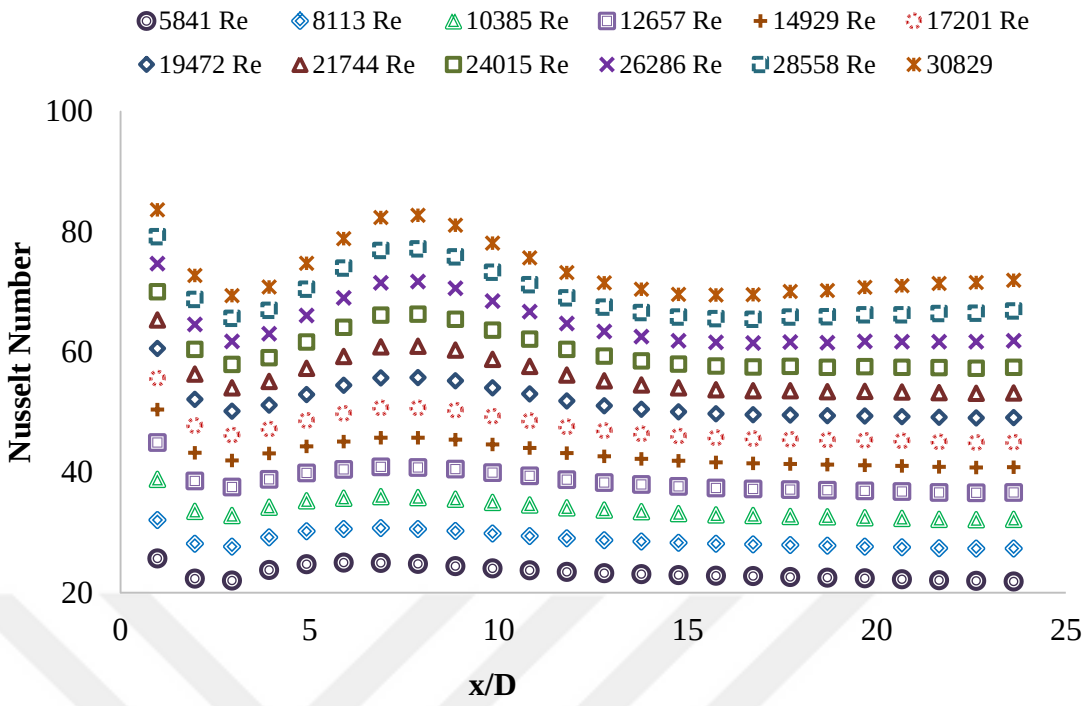

f) R3TR4

Figure 5.3 Axial distributions of Nusselt number along the tube for the reverse curved cross sectional twisted tape

Figures 5.3(a)-(f) shows the axial distributions of Nusselt number along the tube fitted with a reverse curved cross sectional twisted tape at twelve different Reynolds numbers. Calculations were obtained twenty-four locations at the end of the analyses. While all the regional Nusselt numbers increase consistently as Re increases, Reynolds number regulated Nusselt number alteration in the pipe equipped with the reverse curved cross sectional twisted tape insert illustrates the familiar characteristics of flow effort to establish hydraulically and thermally fully developed flow after the sudden entrance of the tape [28, 50, 51]. The wavy local Nusselt number profiles are noticed in the tube fitted with curved cross sectional twisted tape. By way of increasing Re from 5800 to 31000 as seen from Figures 5.3(a)-(f), the wavy profiles are correspondingly amplified. Furthermore, in the end of the tube, local Nusselt numbers gradually rise in the downstream direction due to the common effect of exit loss.

The results of the analysis between Figure 5.4 and 5.8 are presented in terms of the heat transfer, friction factor, and performance of evaluation criteria. Figure 5.4 and Figure 5.5 show the mean Nusselt number and the variation of Nu/Nu_p of the reverse

curved cross sectional twisted tape in the plain tube versus Reynolds number. Nusselt number increased with the increasing Reynolds number for all cases and was in the range of 23.29 to 107.29. The reverse curved cross sectional twisted tapes improved the heat transfer according to the smooth pipe for all Reynolds numbers. The Nusselt number ratios of the reverse curved cross sectional twisted tape were within the range of 1.00 to 1.85. This means that the tapes generate the strength swirl flow in the pipe. As expected, strong swirl flow conditions resulted from the geometry of the twisted tap

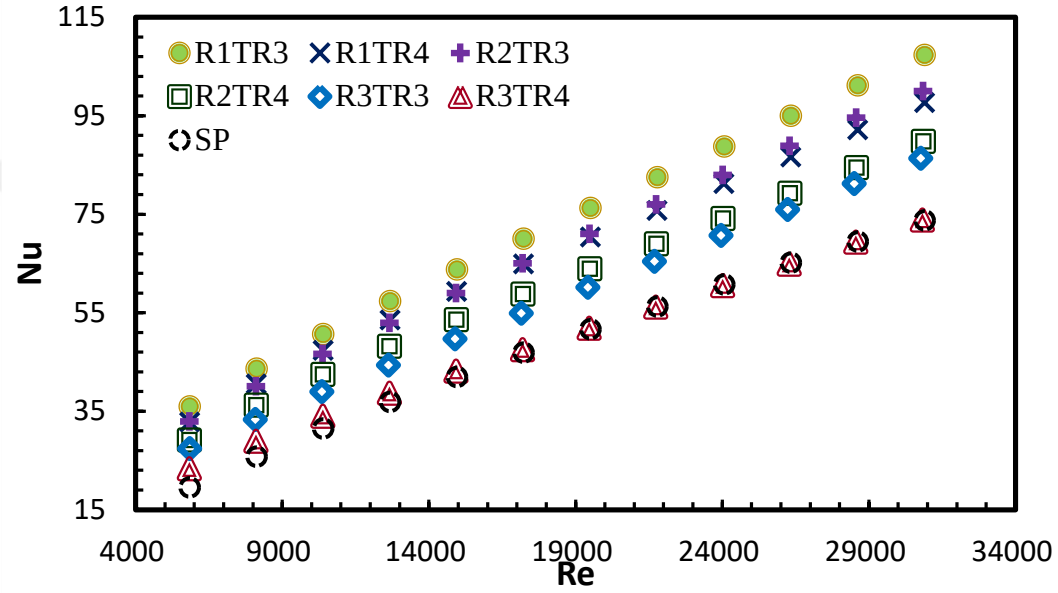

Figure 5.4 Nusselt number dependence on Reynolds number for the reverse curved cross sectional twisted tape

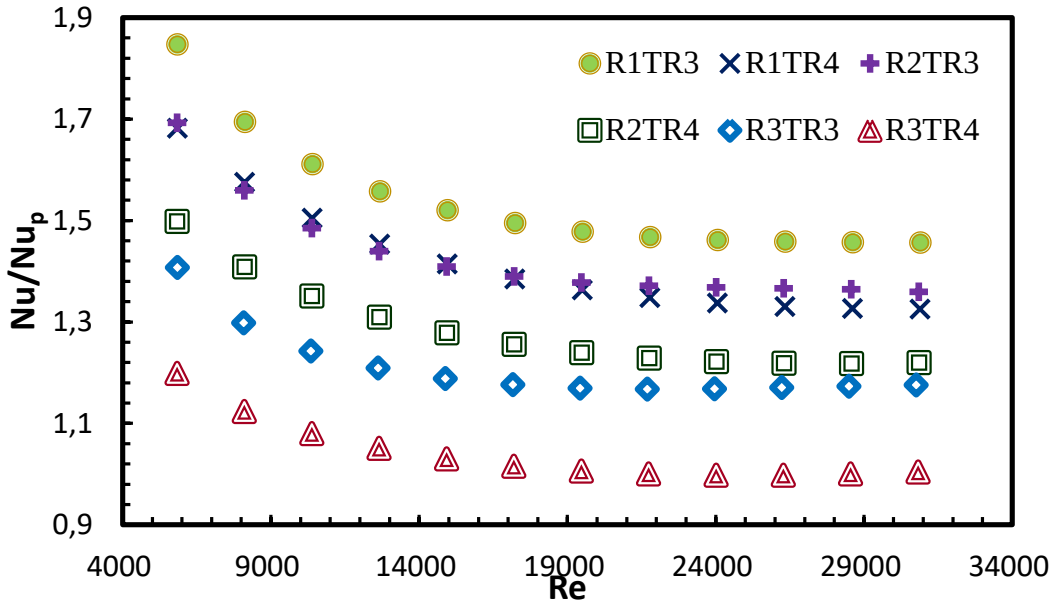

Figure 5.5 Nu/Nu_p variation versus Reynolds number for the reverse curved cross sectional twisted tape

At testing of each reverse curved cross sectional twisted tape, local Nusselt numbers were standardized by plain tube Nusselt number. The relationships between heat transfer and Reynolds number for R1TR3, R1TR4, R2TR3, R2TR4, R3TR3 and R1TR4 of the twist ratio 3 and 4 are displayed in Figure 5.4 and Figure 5.5. The Reynolds number varies from 5849 and 30828. It can be seen in the figures that Nu is increased with the increasing the diameter of the curve. Nusselt number is bigger than the smooth pipe due to the better flow mix and disturbance of the thermal boundary layer near the wall.

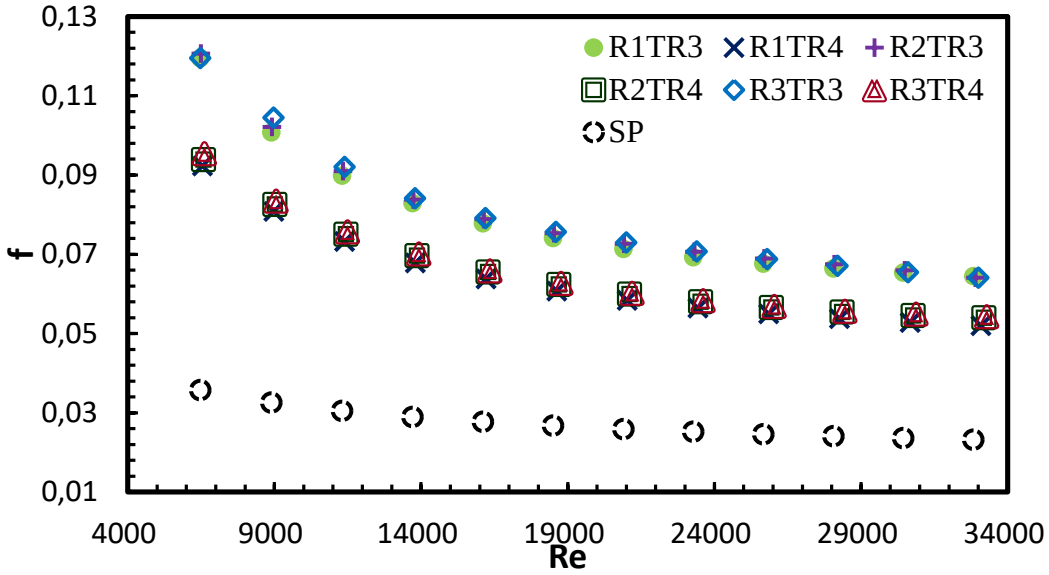

Figure 5.6 Friction factor dependence on Reynolds number for the reverse curved cross sectional twisted tape

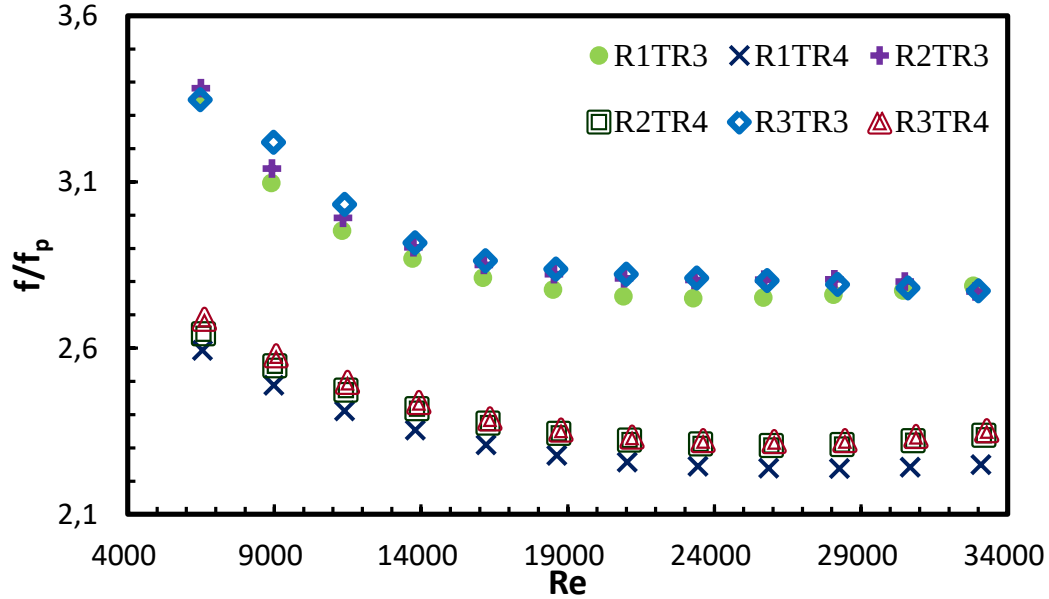

Figure 5.7 The f/f_p variation versus Reynolds number for the reverse curved cross sectional twisted tape

The friction factor of the reverse curved cross sectional twisted tape is presented in Figure 5.6. Friction factor decreases with the increasing the Reynolds number for all cases. As expected, reverse curved cross sectional twisted tape gives a higher friction factor than the smooth pipe.

It can be seen in the Figure 5.7, f/f_p curve of twist ratio 3 or 4 shows similar characteristics. The ratio of f/f_p was in the range of 2.75 to 3.38 for 3 twist ratio, and 2.24-2.69 for 4 twist ratio. The increasing of the twist ratio causes the decreasing of the f/f_p due to the decreasing surface, resistance, and pressure drop. This means that the lower twist ratio gives more friction ratio values.

The thermal performance factor was calculated by using equation 3.6. According to the Figure 5.8, the thermal performance factor is higher at lower Reynolds number. Furthermore, PEC tends to increase with the increasing the curve ratio. The numerical results show that the thermal performance factor varied between 0.75 and 1.22 for the three diameter curves with 3 or 4 twist ratios. PECs of R1TR3 and R1TR4 are higher than other reverse curved cross sectional twisted tapes. The maximum value of PEC is obtained for 1.22 at Reynolds number 5849 for R1TR3.

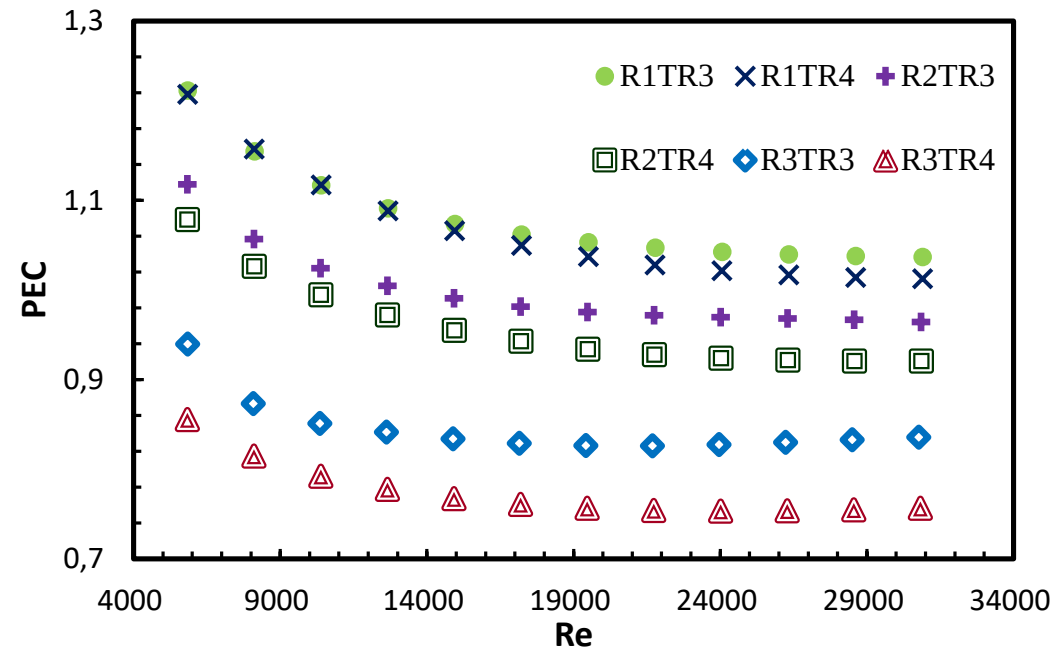

Figure 5.8 Performance evaluation criteria versus Reynolds number for the reverse curved cross sectional twisted tape

Consequently, the results of Nusselt number, friction factor, and PEC for the reverse curved cross sectional twisted tapes are correlated with regression rates of R^2= 0.949, 0.761, and 0.827 as given below equations 5.1 to 5.3, respectively.

$$Nu = 0.1013 * Re^{0.6884} * Pr^{0.4} * TR^{0.0003392} * \frac{D_c}{D_p}^{0.5089} \quad (5.1)$$

$$f = 2.921 * Re^{-0.3819} * TR^{-0.0001757} * \frac{D_c}{D_p}^{-0.05845} \quad (5.2)$$

$$\text{PEC} = 2.8 * Re^{-0.09043} * TR^{0.00009692} * \frac{D_c}{D_p}^{0.5546} \quad (5.3)$$

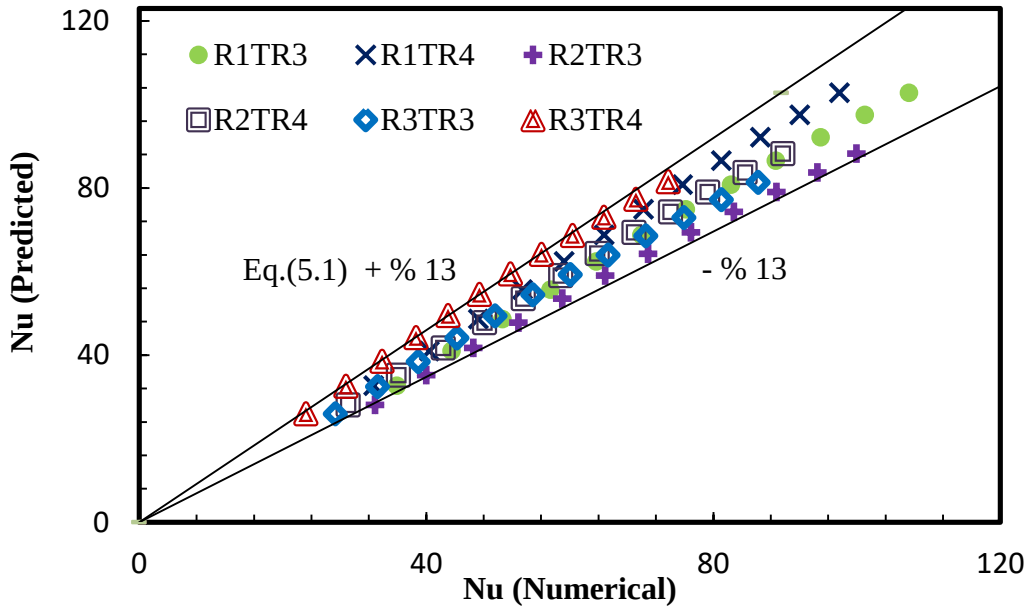

Figure 5.9 Comparison of Nusselt number between predicted and numerical results

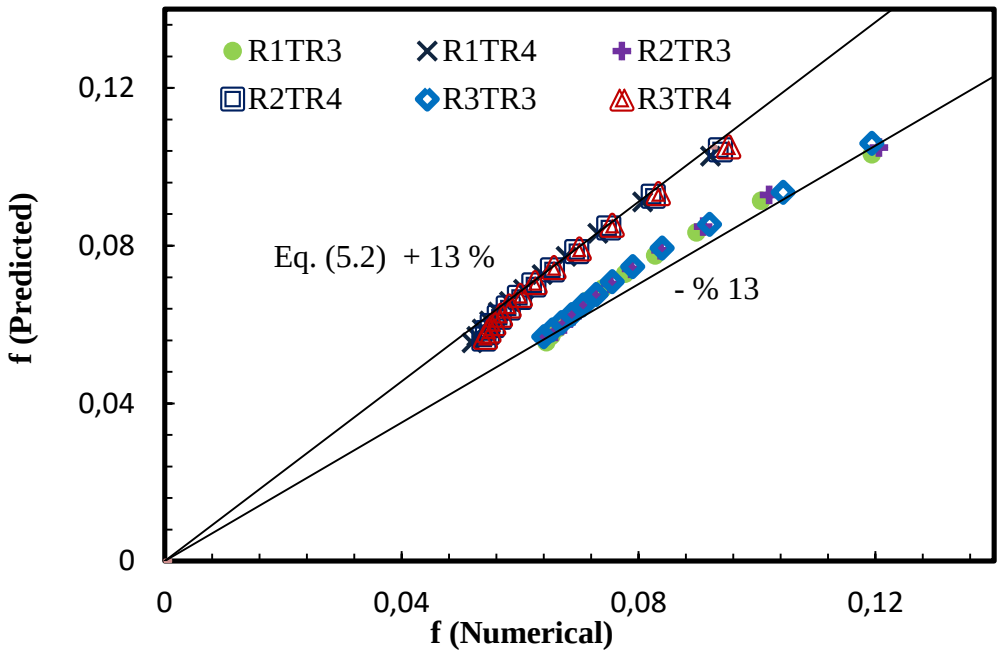

Figure 5.10 Comparison of friction factor between predicted and numerical results

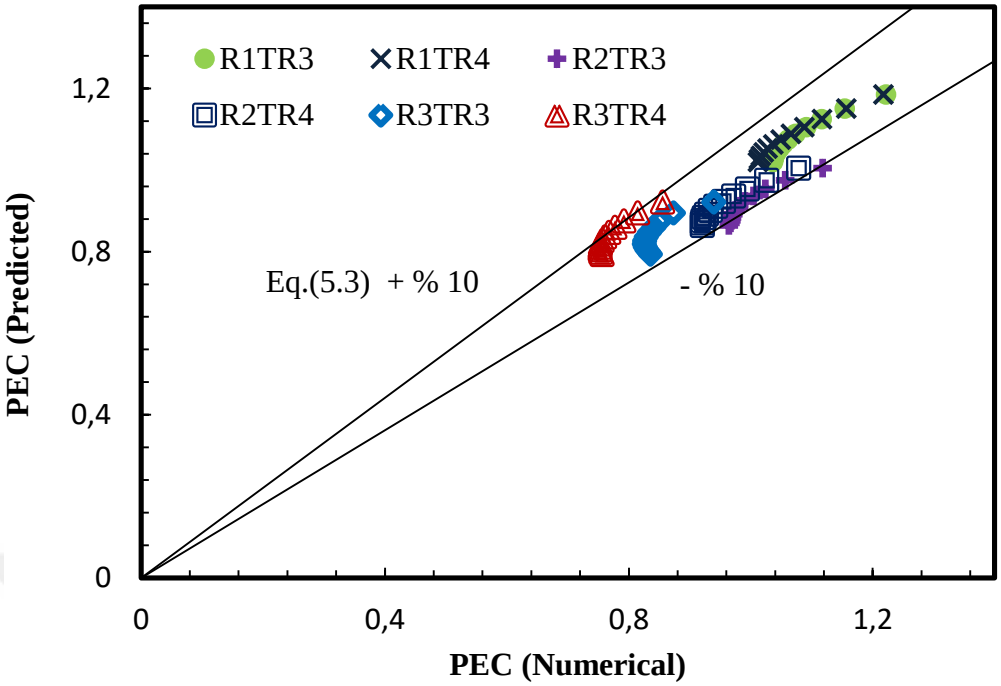

Figure 5.11 Comparision of performance evaluation criteria between predicted and numerical results

As seen in Figure 5.9, 5.10, and 5.11, the deviation of Nusselt number, friction factor and PEC between numerical and calculated results depend on equations 5.1, 5.2, and 5.3 within the range of ∓ 13%, ∓ %13, and ∓%10, respectivelly. Most of data was within the deviation of ∓ 6% for Nusselt number and performance, ∓ 10% for friction factor, ∓ 7% for performance evaluation criteria. The calculated results from the correlated equations which were well suitable with the numerical results of the new inserts can be used to predict the heat transfer, pressure drop and performance of air flow in pipe with the reverse curved cross sectional twisted tapes. These equation were valid at the turbulent flow regime in the range of Reynolds number between 5800 and 31000.

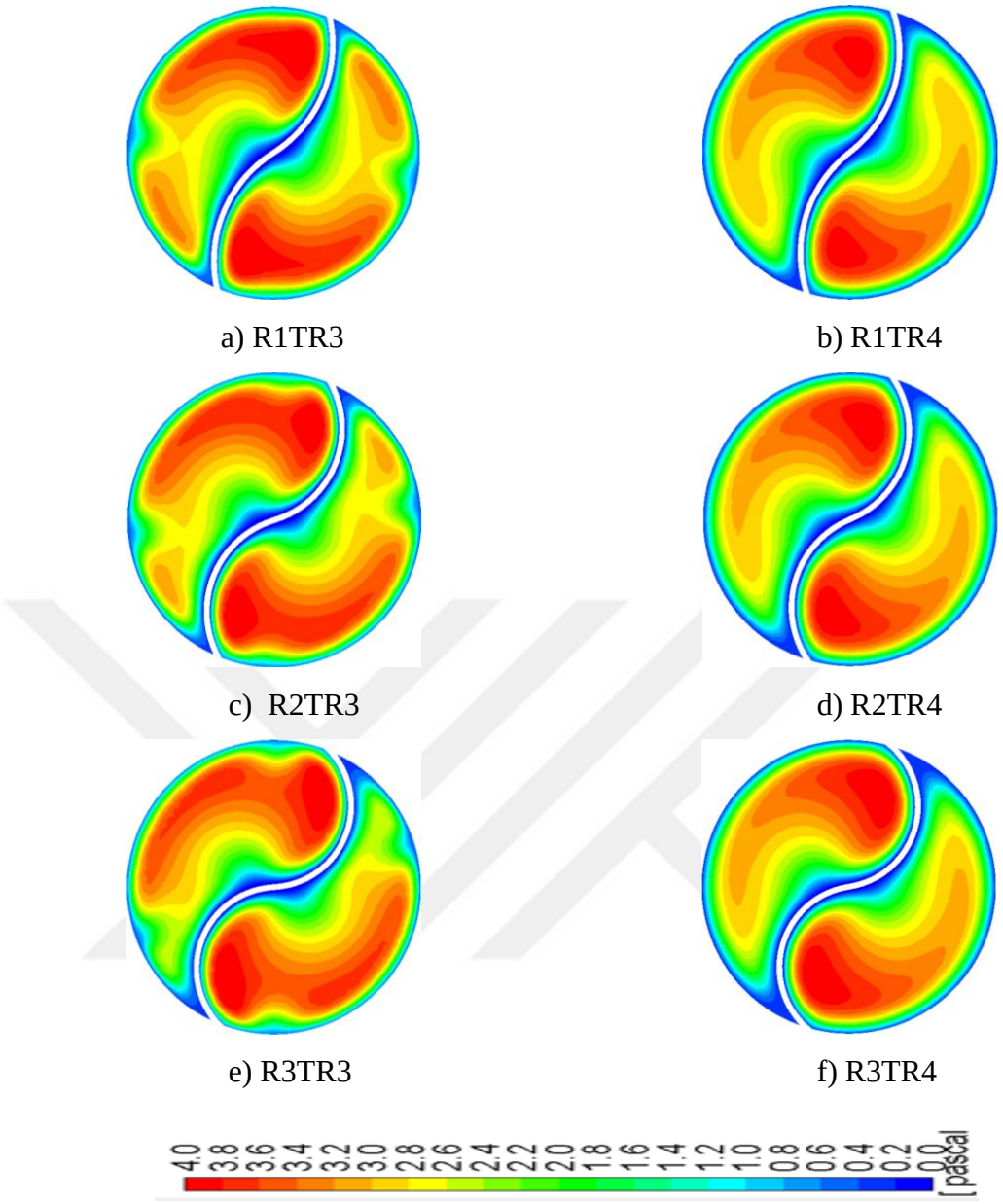

Figure 5.12 Pressure contours for velocity=1.8 m/s for the reverse curved cross sectional twisted tape at the length of 1.2 m

Figure 5.12 demonstrates the pressure contours for reverse curved cross sectional twisted tapes with different diameter ratios ($\frac{D_c}{D_p}$ = 0.872, 0.647 and 0.554) with 3 and 4 twist ratio at the length of 1.2 m. High pressure appears more clearly in Figure 5.12.a. for the insert having the highest curve ratio and the smallest twist ratio. The thin pressure boundary layer is formed near te tube wall.

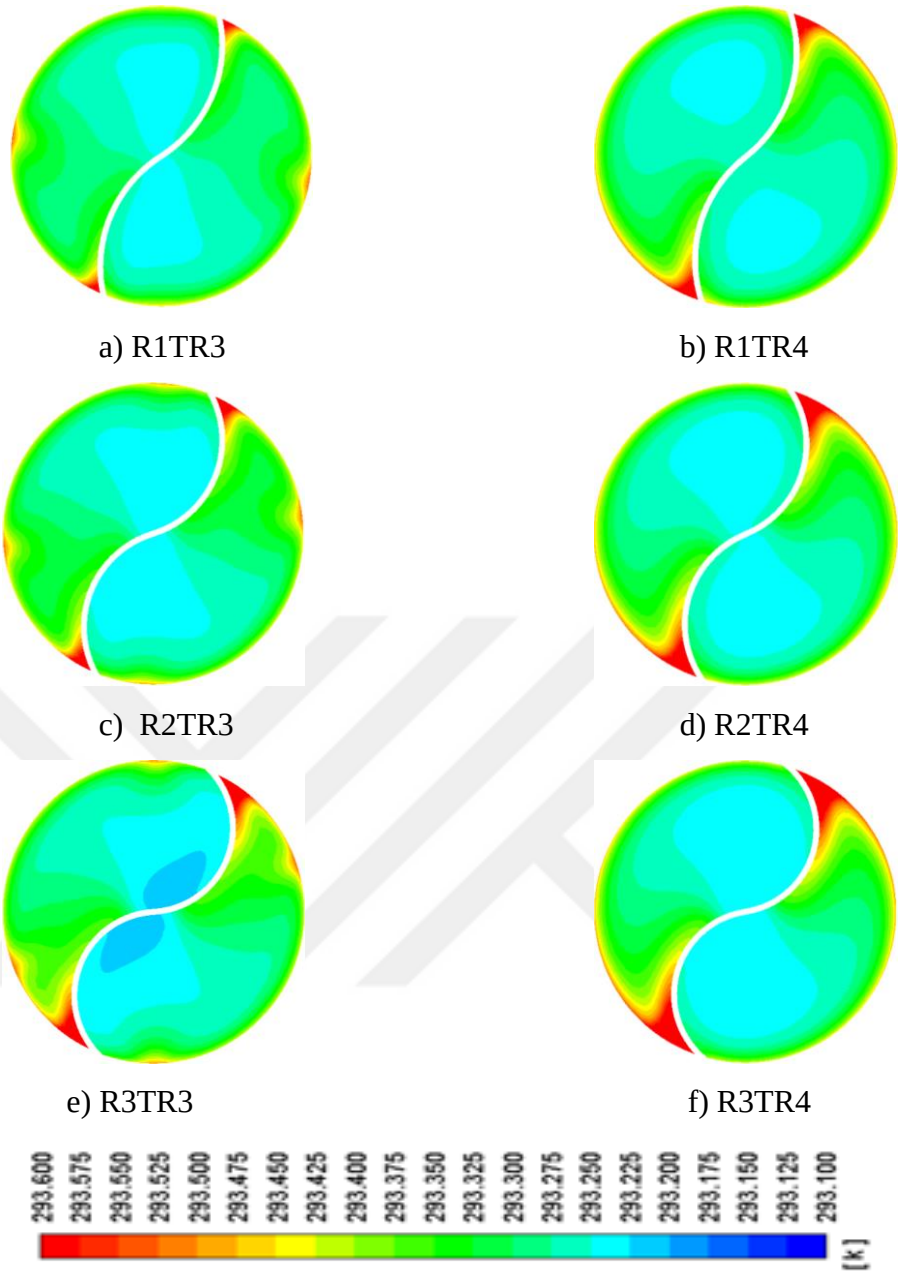

Figure 5.13 Temperature contours for velocity=1.8 m/s at the length of 1.2 m for the reverse curved cross sectional twisted tape

Figure 5.13 demonstrated temperature variation contours for reverse curved cross sectional twisted tapes with different diameter ratios ($\frac{D_c}{D_p}$ = 0.872, 0.647 and 0.554) and twist ratios at the length of 1.2 m. The high-temperature field appears in Figure 5.13.a. The twist ratio of the reverse curve cross sectional twisted tape is more effective than curve ratio on the heat transfer and pressure drop. The high temperature is observed near the sharp edge of the tape the same as curve twisted tape.

CHAPTER 6

CONCLUSION

6.1 RESULTS AND EVALUATION

This study is directed to determine the effects of the curved and reverse curved cross sectional twisted tapes on thermal and fluid fields in a circular pipe by using computational fluid dynamics.

The analyses made for twelve different geometries such as three curved and three reverse curved cross sectional twisted tapes with two different twist ratios. The diameter ratios of curve and pipe for curved twisted tape are 1.761, 2.252, and 3.271. The diameter ratios of reverse curve and pipe for reverse curved twisted tape are 0.554, 0.647 and 0.872. Both types of twisted tapes have two different twisted ratios (TR=3.0 and 4.0). Twelve different velocities were used in the analysis. The changes of the heat transfer, pressure drop, and performance of evaluation criteria were found out.

According to the analyses of curved cross sectional twisted tapes, the following conclusions can be drawn:

- The Nusselt number increased with increasing Reynolds number for all of curved cross sectional twisted tape types. The highest Nusselt number at the highest Re was around 112 and obtained from the C1TR3 model, which has the highest curve ratio and the lowest twist ratio. The Nusselt number of the C1TR3 was higher than C1TR4 generally 8%. The Nusselt number of curved cross sectional twisted tapes were higher than the smooth pipe approximately in the region of 31 to 89 % for all curved twisted types.

- The friction factor decreased with increasing Reynolds number. The maximum friction factor was obtained around 0.11 at the lowest twisted ratio and Re. The curve ratio effect on friction is negligible. The friction factor of curved cross sectional twisted tapes were higher than the smooth pipe approximately 122 to 206%.

- The Performance evaluation factor decreased with the rising speed as expected the increasing number of Re. Also it decreased with the increasing twist ratio. The maximum value of the curve twisted tape was calculated around 1.3 at Reynolds number 5800 for C1TR3 and C1TR4 cases due to the best mixing and high swirl. Better performance evaluation factors were observed in the lower Reynolds number.

- The deviation of Nusselt number, friction factor and performance evaluation factor between numerical and predicted data were within $\mp 3\%$, $\mp 10\%$, and $\mp 3\%$,respectively. The calculated values are extremely in good harmony with the numerical data.

- According to the results of curve cross sectional twisted tapes, it is observed that Reynolds number has dominant effect on PEC in the low Re region, between 4800 and 20000. Between 20000 and 31000, the effect of Re number is negligible. Twist and curve ratios has moderate effect in this region. However, at the low Re region, twist ratios having highest curve ratio has less effect on PEC.

According to the analyses of reverse curved cross sectional twisted tapes, the following conclusions can be drawn:

- Exactly like the other twisted tapes types, the Nusselt number increase with increasing Reynolds number. The highest Nusselt number was calculated the lowest twist ratio and the highest curve ratio, R1TR3. The high Nusselt number refers to the high heat transfer. The Nusselt number of reverse twisted tapes are higher than smooth pipe approximately 0 to 85 %.

- Friction factor decreased with increasing Reynolds number. Maximum friction factor was calculated at the lowest Reynolds number. It has been observed that curve diameter is the less effective than twist ratio on friction factor. The friction factor of reverse curved cross sectional twisted tapes are higher than smooth pipe in the region of 124 to 238 %.

- The PEC values of the cases having 0.872 curve ratio were determined to be over one for the study. At low Reynolds number, it is greater than one and at high Reynolds number it is less than one for the cases having median curve ratio of 0.647. For the lowest curve ratio of 0.554, it was calculated under one. The maximum value of PEC for the reverse curved cross sectional twisted tape was calculated around 1.22 at Reynolds number 5849 for R1TR3 and R1TR4.

- The deviation of Nusselt number, friction factor, and performance evaluation factor between all the numerical and predicted data were within ∓13%, ∓13%, and ∓10%, respectively. The deviation were calculated within ∓6% for most of data for heat transfer and performance, ∓10% for friction factor. The calculated values are in good harmony with the numerical data.

- According to the results of the reverse curve cross sectional twisted tapes, it can be said that a change in the Reynolds number between 4800 and 17000 has remarkably effect on PEC. Between 17000 and 31000, PEC shows a stable behavior and this indicates Re has negligible effect on PEC. The change of the twist ratio having higher curve ratio is less effective on the PEC, and twist ratio having lowest curve ratio has a moderate effect on PEC. Curve ratio has also a moderate effect on PEC in study range of Re.

  All these results show that the geometry of the twisted tape plays an important role on the heat transfer performance. Significant increases in heat transfer and performance evaluation criteria were obtained in this study despite the pressure drop penalty.

6.2 FUTURE WORK

Although the study presents computational framework on the analyses of different type twisted tapes, there are several aspects where the present study can be improved to further extend. The future scope can involve;

- The effect of Reynolds number on thermal-hydraulic performance was presented in the study. The study Reynolds number region can be extended to the different flow regimes.
- The twist ratio was found effective on the heat transfer and pressure drop rather than the diameter of the curved and reverse curved cross sectional twisted tapes. The analysis should be repeated for the tapes having the lower twist ratios.
- The analyses can be extended to understand thermodynamic advantageous of the tapes by using thermodynamics laws.
- The modified geometries of the curved and reverse curved tapes can be investigated to understand the effect of different cut on the tapes, alternate axis, multi tapes, etc.
- Clearance effect between the tape and pipe wall can be investigated.

REFERENCES

[1] E. Koc, M. Senel. (2013). The State of Energy in World and Turkey-General Evaluation, *Engineer and Machinery*, **54** (639) ,32-44.

[2] Z. Yılmaz. (2017). Türkiye'nin Mevcut Enerji Durumu, In: 8. Enerji Verimliliği Forum ve Fuarı, İstanbul.

[3] O. Türkyılmaz. (2015). Türkiye'nin Enerji Görünümü Raporu, In Bülten-TMMOB Makine Mühendisleri Odası.

[4] Tedaş (2015). Net Elektrik Tüketiminin Sektörlere Göre Dağılımı.

[5] M. Garg, H. Nautiyal, S. Khurana, M. Shukla.(2016). Heat transfer augmentation using twisted tape inserts: A review, *Renewable and Sustainable Energy Reviews*, **63**, 193-225.

[6] M. Sheikholeslami, M. Gorji-Bandpy, D.D. Ganji. (2015). Review of heat transfer enhancement methods: Focus on passive methods using swirl flow devices, *Renewable and Sustainable Energy Reviews*, **49**, 444-469.

[7] A. Dewan, P. Mahanta, K.S. Raju, P.S. Kumar. (2004). Review of passive heat transfer augmentation techniques, *Proceedings of the Institution of Mechanical Engineers, Part A: Journal of Power and Energy*, **218**(7), 509-527.

[8] S. Liu, M. Sakr. (2013). A comprehensive review on passive heat transfer enhancements in pipe exchangers, *Renewable and Sustainable Energy Reviews*,**19**, 64-81.

[9] A. Hasanpour, M. Farhadi, K. Sedighi. (2014). A review study on twisted tape inserts on turbulent flow heat exchangers: The overall enhancement ratio criteria, *International Communications In Heat and Mass Transfer*, **55**, 53-62.

[10] M. Hojjat, S.G. Etemad, R. Bagheri, J. Thibault. (2011). Turbulent forced convection heat transfer of non-Newtonian nanofluids, *Experimental Thermal and Fluid Science*, **35**(7),1351-1356.

[11] Q. Liao, M. Xin. (2000). Augmentation of convective heat transfer inside tubes with three-dimensional internal extended surfaces and twisted-tape inserts, *Chemical Engineering Journal*, **78**(2-3), 95-105.

[12] S. Saha, A. Dutta, S. Dhal (2001). Friction and heat transfer characteristics of laminar swirl flow through a circular tube fitted with regularly spaced twisted-tape elements, *International Journal of Heat and Mass Transfer*, **44**(22), 4211-4223.

[13] M. Rahimi, S.R. Shabanian, A.A. Alsairafi. (2009). Experimental and CFD studies on heat transfer and friction factor characteristics of a tube equipped with modified twisted tape inserts, *Chemical Engineering and Processing: Process Intensification*, **48**(3), 762-770.

[14] S. Eiamsa-ard, C. Thianpong, P. Promvonge. (2006). Experimental investigation of heat transfer and flow friction in a circular tube fitted with regularly spaced twisted tape elements, *International Communications in Heat and Mass Transfer*, **33**(10), 1225-1233.

[15] Y.-W. Chiu, J.-Y. Jang. (2009). 3D numerical and experimental analysis for thermal–hydraulic characteristics of air flow inside a circular tube with different tube inserts, *Applied Thermal Engineering*, **29**(2-3), 250-258.

[16] N. Piriyarungrod, S. Eiamsa-Ard, C. Thianpong, M. Pimsarn, K. Nanan. (2015). Heat transfer enhancement by tapered twisted tape inserts, *Chemical Engineering and Processing: Process Intensification*, **96**, 62-71.

[17] S. Eiamsa-Ard, P. Somkleang, C. Nuntadusit, C. Thianpong. (2013). Heat transfer enhancement in tube by inserting uniform/non-uniform twisted-tapes with alternate axes: Effect of rotated-axis length, *Applied Thermal Engineering*, **54**, 289-309.

[18] S. Eiamsa-Ard, V. Kongkaitpaiboon, K. Nanan. (2013). Thermohydraulics of turbulent flow through heat exchanger tubes fitted with circular-rings and twisted tapes, *Chinese Journal of Chemical Engineering*, **21**(6), 585-593.

[19] M. Bhuiya, M. Chowdhury, M. Saha, M. Islam. (2013). Heat transfer and friction factor characteristics in turbulent flow through a tube fitted with perforated twisted tape inserts, *International Communications in Heat and Mass Transfer*, **46**, 49-57.

[20] P. Bharadwaj, A. Khondge, A. Date. (2009). Heat transfer and pressure drop in a spirally grooved tube with twisted tape insert, *International Journal of Heat and Mass Transfer*, **52**(7-8), 1938-1944.

[21] A. Garcia, P.G. Vicente, A. Viedma. (2005). Experimental study of heat transfer enhancement with wire coil inserts in laminar-transition-turbulent regimes at different Prandtl numbers, *International Journal of Heat and Mass Transfer*, **48**(21-22), 4640-4651.

[22] C. Man, J. Yao, C. Wang. (2016). The experimental study on the heat transfer and friction factor characteristics in tube with a new kind of twisted tape insert, *International Communications in Heat and Mass Transfer*, **75**, 124-129.

[23] S. Al-Fahed, W. Chakroun. (1996). Effect of tube-tape clearance on heat transfer for fully developed turbulent flow in a horizontal isothermal tube, *International journal of heat and fluid flow*, **17**(2),173-178.

[24] A. Ujhidy, J. Nemeth, J. Szépvölgyi. (2003). Fluid flow in tubes with helical elements, *Chemical Engineering and Processing: Process Intensification*, **42**(1), 1-7.

[25] M. Yilmaz, O. Comakli, S. Yapici, O.N. Sara. (2003). Heat transfer and friction characteristics in decaying swirl flow generated by different radial guide vane swirl generators, *Energy Conversion and Management*, **44**(2), 283-300.

[26] P. Naphon. (2006). Heat transfer and pressure drop in the horizontal double pipes with and without twisted tape insert, *International Communications in Heat and Mass Transfer*, **33**(2), 166-175.

[27] P. Sivashanmugam, S. Suresh. (2006). Experimental studies on heat transfer and friction factor characteristics of laminar flow through a circular tube fitted with helical screw-tape inserts, *Applied Thermal Engineering*, **26**(16), 1990-1997.

[28] S.W. Chang, T.L. Yang, J.S. Liou. (2007). Heat transfer and pressure drop in tube with broken twisted tape insert, *Experimental Thermal and Fluid Science*, **32**(2), 489-501.

[29] S. Eiamsa-ard, P. Seemawute, K. Wongcharee. (2010). Influences of peripherally-cut twisted tape insert on heat transfer and thermal performance characteristics in laminar and turbulent tube flows, *Experimental Thermal and Fluid Science*, **34**(6), 711-719.

[30] P. Promvonge, S. Eiamsa-Ard. (2007). Heat transfer behaviors in a tube with combined conical-ring and twisted-tape insert, *International Communications in Heat and Mass Transfer*, **34**(7), 849-859.

[31] H. Gül, D. Evin. (2007). Heat transfer enhancement in circular tubes using helical swirl generator insert at the entrance, *International Journal of Thermal Sciences*, **46**(12), 1297-1303.

[32] A. Savekar, D. Jangid, M. Gurjar, V. Patil, C. Sewatkar. 2015. Analysis of Heat Transfer in Pipe With Twisted Tape Inserts, In: Second International Conference on Fluid Flow, Heat and Mass Transfer, Ottawa, ON, Canada.

[33] S. Shabanian, M. Rahimi, M. Shahhosseini, A. Alsairafi. (2011). CFD and experimental studies on heat transfer enhancement in an air cooler equipped with different tube inserts, *International communications in heat and mass transfer*, **38,** 383-390.

[34] R. Yadav, A. Padalkar,. (2007). CFD analysis for heat transfer enhancement inside a circular tube with half-length upstream and half-length downstream twisted tape, *Journal of Thermodynamics*, 2012.

[35] P.E. Geyer, D.F. Fletcher, B.S. Haynes. (2007). Laminar flow and heat transfer in a periodic trapezoidal channel with semi-circular cross-section, *International Journal of Heat and Mass Transfer*, **50**(17-18), 3471-3480.

[36] S.D. Salman, A.A.H. Kadhum, M.S. Takriff, A.B. Mohamad. (2013). CFD analysis of heat transfer and friction factor characteristics in a circular tube fitted with quadrant-cut twisted tape inserts, *Mathematical Problems in Engineering*, 2013.

[37] S.D. Salman, A.A.H. Kadhum, M.S. Takriff, A.B. Mohamad. (2013). Numerical Investigation of Heat transfer and friction factor characteristics in a circular tube fitted with V-cut twisted tape inserts, *The Scientific World Journal*, 2013

[38] H. Yuxiang, D. Xianhe, L. Zhang. (2012). 3D numerical study on compound heat transfer enhancement of converging-diverging tubes equipped with twin twisted tapes, *Chinese Journal of Chemical Engineering*, **20**(3), 589-601.

[39] K.P. Deshmukh, M.J. Dhanokar, N.S. Varkute, T.S. Kumar. (2014). Numerical simulation of enhancement of heat transfer in a tube with and without rod helical tape swirl generators, *International Journal of Mechanical Engineering and Technology*, **5**(6), 1-13.

[40] S. Eiamsa-Ard, K. Wongcharee, S. Sripattanapipat. (2009). 3-D Numerical simulation of swirling flow and convective heat transfer in a circular tube induced

by means of loose-fit twisted tapes, *International Communications in Heat and Mass Transfer,* **36**(9), 947-955.

[41] Y. Wang, M. Hou, X. Deng, L. Li, C. Huang, H. Huang, G. Zhang, C. Chen, W. Huang. (2011). Configuration optimization of regularly spaced short-length twisted tape in a circular tube to enhance turbulent heat transfer using CFD modeling, *Applied Thermal Engineering*, **31**(6-7), 1141-1149.

[42] P.S. Rao, K.K. Kumar. (2014). Numerical and experimental investigation of heat transfer augmentation in double pipe heat exchanger with helical and twisted tape inserts, *International Journal of Emerging Technology and Advanced Engineering*, **4**(9), 180-192.

[43] H. Bas, V. Ozceyhan. (2012). Heat transfer enhancement in a tube with twisted tape inserts placed separately from the tube wall, *Experimental Thermal and Fluid Science,* **41**, 51-58.

[44] J.F. Fan,W.K. Ding, J.F.Zhang, Y.L. He, W.Q. Tao. (2009). A performance evaluation plot of enhanced heat transfer tachniques oriented for energy-saving, *International Journal of Heat and Mass Transfer*,**52**, 33-44.

[45] R. Webb. (2009). Performance evaluation criteria for use of enhanced heat transfer surfaces in heat exchanger design, *International Journal Heat Mass Transfer,* **52**, 33-44

[46] S. Eiamsa-Ard, P. Promvonge. (2010). Thermal characteristics in round tube fitted with serrated twisted tape, *Applied Thermal Engineering*, **30**(13), 1673-1682.

[47] S. Chokphoemphun, M. Pimsarn, C. Thianpong, P. Promvonge. (2015). Thermal performance of tubular heat exchanger with multiple twisted-tape inserts, *Chinese Journal of Chemical Engineering*, **23**(5), 755-762.

[48] B. Petukhov. (1970). Heat transfer and friction in turbulent pipe flow with variable physical properties, *Advances in heat transfer*, 503-564.

[49] V. Gnielinski. (1976). New equations for heat and mass transfer in turbulent pipe and channel flow, *International Chemical Engineering*, **16**(2), 359-368.

[50] S.W. Chang, T.-M. Liou, J.S. Liou, K.-T. Chen. (2008). Turbulent heat transfer in a tube fitted with serrated twist tape under rolling and pitching environments with applications to shipping machineries, *Ocean Engineering*, **35**(16), 1569-1577.

[51] S.W. Chang, W.L. Cai, R.S. Syu. (2016). Heat transfer and pressure drop measurements for tubes fitted with twin and four twisted fins on rod, *Experimental Thermal and Fluid Science*, **74**, 220-234.